**SYNTHESIS OF WELL-DEFINED SINGLE AND MULTIPHASE POLYMERS
USING VARIOUS LIVING POLYMERIZATION METHODS**

by

Joseph M. DeSimone

Dissertation submitted to the Faculty of the
Virginia Polytechnic Institute and State University
in partial fulfillment of the requirements for the degree of

DOCTOR OF PHILOSOPHY

in

Chemistry

Approved by:

J. E. McGrath, Chairman

H. W. Gibson   L. T. Taylor

T. C. Ward   G. L. Wilkes

March, 1990
Blacksburg, Virginia

SYNTHESIS OF WELL-DEFINED SINGLE AND MULTIPHASE POLYMERS
USING VARIOUS LIVING POLYMERIZATION METHODS

by

Joseph M. DeSimone

Committee Chairman: James E. McGrath
Department of Chemistry

(ABSTRACT)

Hexenyl functionalized poly(dimethylsiloxane) and methacryloyloxy functionalized poly(methyl methacrylate) (PMMA) and poly(dimethylsiloxane) (PDMS) macromonomers were synthesized using living polymerization techniques. The PDMS macromonomers were prepared by the anionic ring-opening polymerization of hexamethylcyclotrisiloxane followed by termination with a functionalized chlorosilane derivative. The methacryloyloxy functionalized PMMA macromonomers were prepared using group transfer polymerization with a protected hydroxyl functional initiator. The molar masses of the macromonomers ranged from 1000 g/mol up to 20000 g/mol with narrow molar mass distributions, less than 1.1, and high percent functionalities. The hexenyl functionalized PDMS macromonomers, having a range of molar masses, were statistically terpolymerized with 1-butene and sulfur dioxide to yield poly(1-butene sulfone)-g-PDMS copolymers of various chemical compositions up to 20 wt% PDMS. The bulk and surface phase morphologies were investigated using DSC, TEM, XPS, and water contact angle

measurements. The graft copolymer was shown to be an excellent resist for electron beam lithography with a $4\mu C/cm^2$ sensitivity and a 33:1 etch ratio relative to a cross linked novolac resin. The 7000 g/mol methacryloyloxy functionalized PMMA macromonomers were copolymerized anionically with MMA to yield PMMA-g-PMMA polymers having absolute molar mass distributions less than 1.1 containing from 5 wt% to 40 wt% of the macromonomer at constant overall molar mass of 250000 g/mol. The graft polymers were utilized as model homopolymers exhibiting long chain branching. The methacryloyloxy functionalized PDMS macromonomers were free radically and anionically copolymerized with MMA to yield PMMA-g-PDMS copolymers. The graft copolymers were fractionated and their chemical composition distributions were determined as a function of copolymerization mechanism.

In addition, preliminary studies were started using aluminum-27 NMR to study several different aluminum porphyrins based on (5,10,15,20-tetraphenyl)porphine (TPPH$_2$). The aluminum porphyrins were formed by reacting trimethylaluminum with TPPH$_2$ to yield TPPAlMe. The resulting aluminum porphyrin was modified by adding a stoichiometric amount of various carboxylic acids to form aluminum porphyrin carboxylates that had varying steric and electronic effects on the macrocycle.

Dedicated to

My family, Philip and Arlene DeSimone, my brother David, my
sister Laura, my lovely wife Suzanne, and my little son
Philip, your support, encouragement, and love through the
years has made this, and the future, all possible.

ACKNOWLEDGEMENTS

necessary for resist evaluation, Professor Pavel Kratochvil and his colleague Professor Stejskal, who tediously evaluated many of our materials by light scattering and fractionation. Also, I want to thank Dr. Mia Siochi, who was involved in the solution characterization of several of our materials, and Dr. Michael Staengle, who taught me much about multinuclear magnetic resonance spectroscopy.

There are many whom I am indebted to for creating a forum for discussions, these include Dr. Guru Sinai-Zingde, Professor Judy Riffle, Professor Herve Marand, Mr. Tom Glass, and Dr. Guy Wilson, to name a few. I wish to acknowledge my advisory committee, Professor Ward, Professor Wilkes, Professor Gibson, and Professor Taylor, who gave their support, technical insight and encouragement over the years and recently during my transition from Virginia Tech to UNC-CH.

Finally, I want to thank my advisor and friend, Professor James E. McGrath, for providing me the opportunity to study under his auspices. He has given me the latitude to explore several different areas while still guiding me, in his subtle way, to realize the directions to proceed. His approach and enthusiasm towards research is greatly appreciated as was his encouragement to pursue a position in academics.

Table of Contents

List of Figures

xii

List of Schemes

List of Tables

SCOPE OF DISSERTATION

The research presented here has been divided into two parts for clarity and conciseness. Part 1, entitled "Synthesis, Characterization, and Microlithographic Evaluation of Well-Defined Graft Polymers", is devoted primarily to polymer synthesis using the macromonomer methodology. It begins with the literature review which was focussed on the appropriate topics necessary for an in-depth discussion to follow. It does not, however, begin with the fundamentals but rather it assumes a certain level of expertise and knowledge of the literature. This has allowed for a strong dependence of the Results and Discussions Section on the pertinent sections of the Literature Review.

Part 2 is entitled "Investigations of Aluminum Porphyrins as Initiators in Living Polymerizations". It is concerned with the utilization of aluminum porphyrins as living polymerization catalysts and initiators for the polymerization of alkylene oxides and their characterization by multinuclear magnetic resonance spectroscopy. It begins with a Literature Review Section that assumes a firm understanding of living polymerization processes and their relative kinetic constraints. It is primarily concerned with the most recent appropriate literature out of the laboratories of the leading authorities in this field. The

1

aluminum porphyrin section of this dissertation is an on going area of research for our laboratories and therefore is presented in a manner which reflects the directions we are currently pursuing.

PART 1

SYNTHESIS, CHARACTERIZATION, AND MICROLITHOGRAPHIC EVALUATION OF WELL-DEFINED GRAFT POLYMERS

Introduction and Literature Review

The research presented here is the culmination of our work involving the synthesis of well-defined single and multiphase polymers. Our goal throughout has been to obtain the polymers with the desired characteristics and hence we were not bound by using certain polymerization processes. We have made extensive use of the macromonomer method to synthesize well-defined graft polymers. Three different macromonomers were synthesized and incorporated into systems to create the selected materials. Methacryloyloxy functionalized PMMA and PDMS macromonomers were synthesized having controlled molar masses and narrow molar mass distributions. The PMMA and PDMS macromonomers were copolymerized with MMA to afford PMMA-g-PMMA and PMMA-g-PDMS systems, respectively. The grafted homopolymer was designed to be a model for materials exhibiting long chain branching. The PMMA-g-PDMS system was made using free radical and anionic copolymerization mechanisms. We were interested in the distribution of chemical composition as a function of the copolymerization mechanism. The third macromonomer synthesized was again a PDMS material; however, it was functionalized to have an olefinic end group. The olefinic end group allowed it to be terpolymerized in a statistical fashion with olefins and sulfur dioxide to afford a graft copolymer having a poly(olefin sulfone) backbone and PDMS

grafts. The bulk and surface properties of these graft copolymers were evaluated and correlated to their performance as electron beam resists in microlithography.

The literature review will now follow. It was directed towards three different areas. The first section will review what a macromonomer is and how others have taken advantage of this methodology. The second section is primarily concerned with one of the most often overlooked polymer parameters, namely chemical composition distribution (CCD). The CCD as it arises from statistical and conversional heterogeneity will be discussed along with the methods used to experimentally elucidate the CCD for block and graft copolymers. The third section will address the lithographic process and will briefly discuss the prior art involving the use of silicon containing polymers as resists in microlithography.

THE MACROMONOMER TECHNIQUE

In 1974, Dr. Ralph Milkovich[1] was granted a patent on functional macromolecular monomers under the trade name MACROMERS. A macromer, or more precisely, a macromonomer, is an oligomer or polymer that contains a polymerizable functional end group that can be incorporated into a polymeric system to form a graft copolymer. The most commonly used copolymerization process for incorporation is that of chain growth mechanisms. As shown in Scheme 1.1, when a macromonomer is statistically copolymerized with conventional small monomers, such as styrene or methyl methacrylate, it results in a graft copolymer where the backbone is comprised of the small monomer and the grafts are the result of the macromonomer.
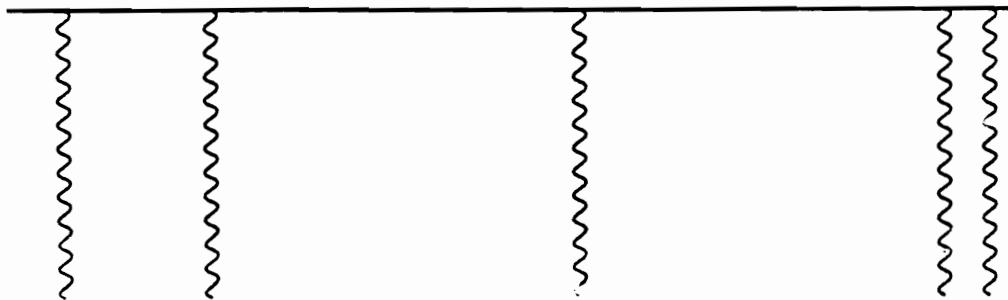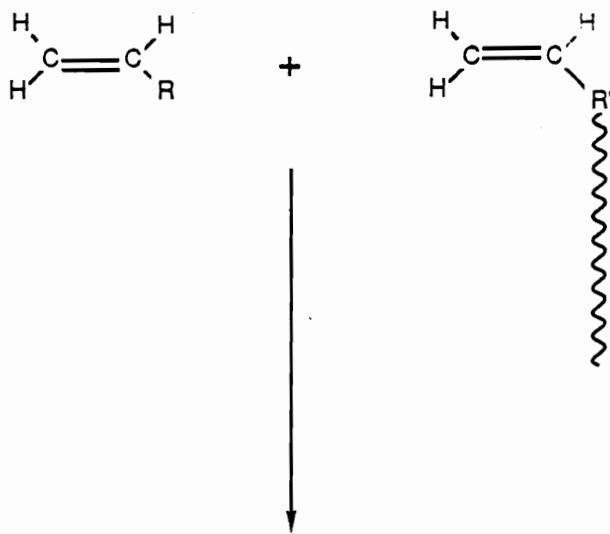
Many different synthetic schemes have been devised for the synthesis of macromonomers. Several excellent reviews have been written but none have been as comprehensive on the synthetic variations as the overview written on the subject by Smith.[2] A few examples will be given here to give the reader an appreciation for the synthetic utility of this technique.

Researchers have published on the synthesis of macromonomers using free radical, anionic, cationic, coordination, GTP, and condensation type processes. Often
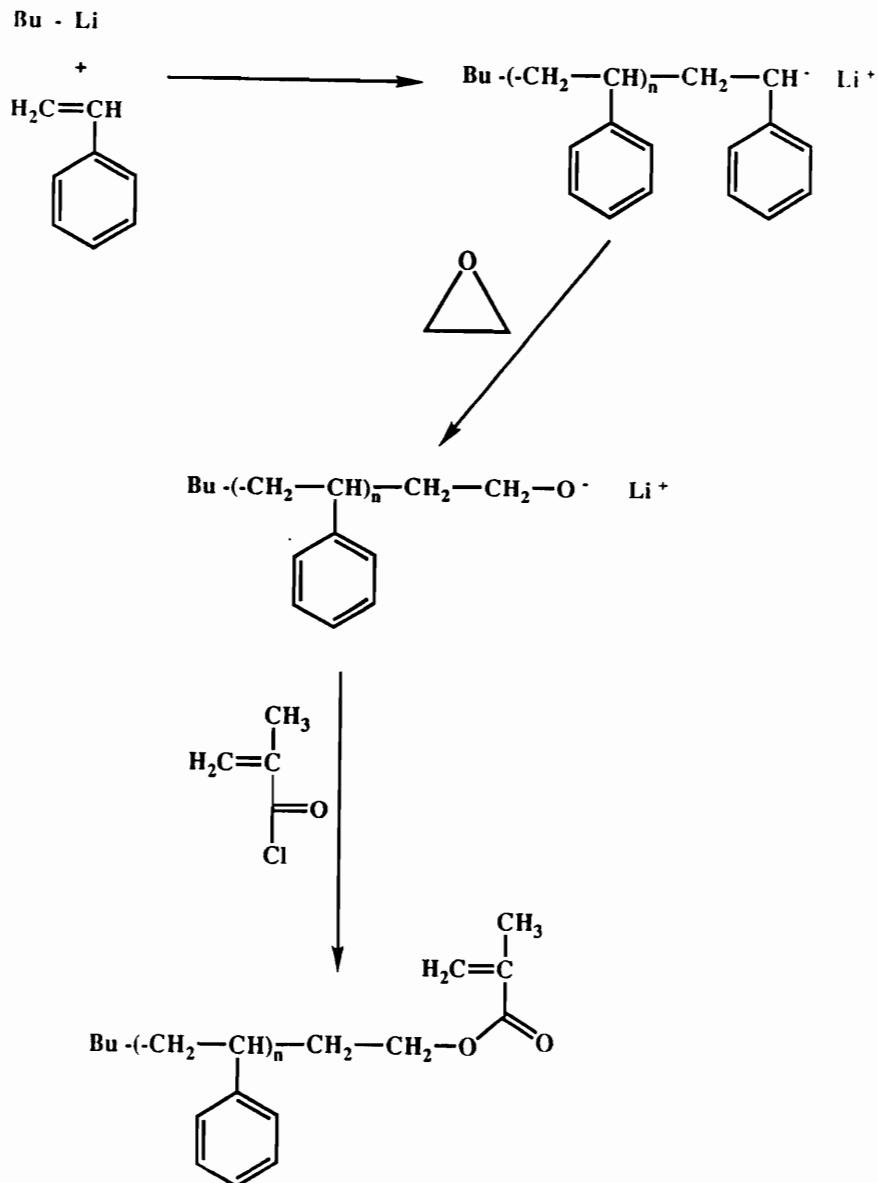
Scheme 1.1   Definition of a macromonomer and
~~~~ ~~~tion of synthetic utility.

MACROMONOMER ≡ Macromer^R

An oligomer or polymer that contains a polymerizable endgroup that can be incorporated into a system in a chain growth manner.

the free radical methods involved the use of appropriately functionalized chain transfer agents[3,4], or functionalized initiators (Fe/H_2O_2)[5] that would result in hydroxyl terminated oligomers that could be converted to polymerizable end groups. A unique approach has been the exploitation of inherent termination processes[6] to yield polymerizable endgroups. The dominate termination process during the free radical polymerization of MMA is disproportionation which yields one saturated end group and one unsaturated end group. It is this unsaturated end group that was shown to free radically copolymerize with other monomers to yield ill-defined copolymers with PMMA grafts.

Probably the most important method for synthesizing well-defined macromonomers involves the use of living polymerization techniques. In this way, the resultant graft copolymers will have grafts possessing narrow molar mass distributions. Many different examples can be found in the literature but most either use one of two methods. The most popular is the direct functionalization upon termination of the living polymerization, perhaps after deactivation of the chain end, to yield a polymerizable end group. The other most common method is to use protected functionalized initiators.

The use of the functionalized termination method was illustrated by Schulz and Milkovich[7], Scheme 1.2, when they polymerized styrene anionically with alkyllithiums and after complete conversion of the monomer they deactivated the carbanion with ethylene oxide. The lithium alkoxide was then added to methacryloyl chloride to form a methacryloyloxy functional poly(styrene) macromonomer. The preparation of macromonomers using functionalized initiators was demonstrated by Serre and Worsfold[8], Scheme 1.3. They used 4-lithiobutene-1 as an anionic initiator for the polymerization of styrene or hexamethylcyclotrisiloxane to yield macromonomers having a terminal ∝-olefin functional groups.

In principle, the methods used for the copolymerization of the macromonomer with conventional monomers are also just as varied. The easiest and hence the most common method of copolymerization employs a free radical mechanism. This method allows the most flexible choices for the type of end group on the macromonomer to copolymerize with the low molar mass monomers. Probably the most important constraint for this type of copolymerization is the reactivity ratio of each monomer. In addition, a living copolymerization method can be utilized to obtain a graft copolymer. This results in a material that not only has a narrow molar mass distribution for the graft part,

Scheme 1.2 Synthesis of poly(styrene) macromonomer using functional termination after chain deactivation.

 Bu - Li

$+$

$H_2C{=}CH$

$\longrightarrow$

Bu -(-CH$_2$—CH)$_n$—CH$_2$—CH$^{\cdot}$ Li$^+$

O (epoxide)

Bu -(-CH$_2$—CH)$_n$—CH$_2$—CH$_2$—O$^{\cdot}$ Li$^+$

CH$_3$

$H_2C{=}C$

$={=}O$

Cl

CH$_3$

$H_2C{=}C$

Bu -(-CH$_2$—CH)$_n$—CH$_2$—CH$_2$—O $=O$

Scheme 1.3 Synthesis of poly(styrene) macromonomer using functional anionic initiator.

$$H_2C{=}CH{-}CH_2{-}CH_2^{-} \quad Li^{+} \qquad H_2C{=}CH$$

$$H_2C{=}CH \cdot CH_2 \cdot CH_2 \cdot ({-}CH_2{-}CH)_{\overline{n}}{-}CH_2{-}CH^{-} \; Li^{+}$$

$$CH_3OH$$

$$H_2C{=}CH \cdot CH_2 \cdot CH_2 \cdot ({-}CH_2{-}CH)_{\overline{n}}{-}{-}H$$

which is relatively common, but also a narrow molar mass distribution for the backbone part as well. These highly uniform graft polymers will be a major focus of the work presented later.

Living copolymerizations of macromonomers and monomers typically use ionic mechanisms. Ionic polymerizations are mush less universal in their ability to make homopolymers let alone copolymers, especially for polar monomers. The most useful way to obtain a statistical ionic copolymerization of a macromonomer and a monomer would be to use a macromonomer whose end group closely emulates the low molar mass monomer. For instance, one could not anionically copolymerize a styrenic functionalized macromonomer with an alkyl methacrylate in a statistical fashion. A more appropriate choice would be to use a styrenic functionalized macromonomer with styrene or a methacryloyloxy functionalized macromonomer with an alkyl methacrylate.

The factors that affect the ability of a macromonomer to copolymerize with conventional small monomers are many and several that have been cited in the literature are listed in Table 1.1. The three major factors influencing the reactivity of a macromonomer in a particular system include: i) the copolymerization reactivity of the

Table 1.1   Parameters affecting the reactivity of macromonomers.

Influence of Substitution at the Terminal Unsaturated Unit.

$$CH_2={=}CH$$
R (benzene ring)

$$CH_2={=}C$$
with CH_3, $C{=}O$, O, R

$$CH_2={=}CH$$
with CH_2, CH_2, CH_2, CH_2, R

Kinetic Excluded Volume Effect.

$$f(\ ) = (Molecular\ weight)$$

Repulsive Interactions Between Growing Chain and the Graft.

Flory-Huggins X-interaction Parameter

Solvent.

polymerizable end group associated with the chemical structure of the end group, ii) the kinetic excluded volume effect related to the diffusion controlled reaction processes due to the large size of the macromonomer which can "shield" the end group from the reaction, and iii) the heterogeneous distribution of the polymerizable end group in the reaction system due to the thermodynamic repulsive interaction between the macromonomer and the propagating comonomer chain associated with the immiscibility between unlike polymers.

The most important of these parameters deals with the nature of the polymerizable end group. The type of end group will ultimately determine the efficiency of the functional oligomer to copolymerize with low molar mass monomers. Both Milkovich[9] and Rempp[10] showed that the classical copolymerization equation, equation 1,

$$\frac{d[M_1]}{d[M_2]} = \frac{[M_1]}{[M_2]} \frac{r_1[M_1] + [M_2]}{r_2[M_2] + [M_1]} \simeq \frac{[M_1]}{r_2[M_2]} \quad (1),$$

could be reduced as shown due to the low macromonomer concentration typically used. The reactivity ratio, r_2, can then be calculated, equation 2, simply from the ratio of the instantaneous conversions,

$$r_2 = M_2 \text{ conversion } / M_1 \text{ conversion} \qquad (2)$$

They both showed good agreement for experimental results, such as copolymerization between a methacryloyloxy functionalized macromonomer and styrene, yielding an r_2 value of 0.6, which is the same as the literature value for MMA and styrene.

Cameron and Chisholm[11] have discussed the effect of molar mass on the reactivity of macromonomers. They free radically copolymerized methacryloyloxy functional PDMS macromonomers having molar masses of 500 g/mol, 1000 g/mol, and 10000 g/mol, with styrene. They pointed out that the calculation of r_1 values was not valid due to the large errors associated with the experiments at these low concentration levels. They also concluded that the assumptions used by Milkovich and Rempp above to simplify the copolymerization equation are valid only when the molar mass of the macromonomer is greater than 10000 g/mol. Their data showed a strong dependence of the calculated r_2 values on the macromonomer molar mass. The r_2 values for their system, as well as a different system (methacryloyloxy functional poly(styrene) macromonomers with HEMA) reported by Ito[12], increased as the molar mass of the macromonomer increased. They attributed this reactivity dependence with molar mass on an excluded volume effect that occurs when the bulky side chain presents a barrier to the radical-

macromonomer reaction. They discussed that the radical-macromonomer reaction was activation controlled and the decrease in the rate of reaction with the length of the macromonomer was most likely due to the decreased probability of the growing radical finding the reactive site on the bulky macromonomer during the macromonomer-radical encounter. They also pointed out that the explanation for the decreased reactivity with molar mass given by Kennedy[13] was misleading. Kennedy and Lo suggested that the radical-macromonomer reaction was diffusion controlled like the termination step in free radical polymerizations. Cameron states that the radical-macromonomer reaction is not characterized by high rates and low energies of activation, which are necessary factors for diffusion controlled reactions.

The third parameter listed in Table 1.1 dealing with the factors affecting the reactivity of macromonomers was the thermodynamic repulsive interactions of unlike chains. Ito et al[14] suggested that the repulsion between dissimilar polymer chains is a factor responsible for reducing their reaction rates. They based their conclusions on the observation of a strong dependency of reactivity on the solvent used for the copolymerization. Even under theta conditions for the macromonomer, there was a significant rate reduction observed which decreased further as the

"goodness" of the solvent increased. They did not however suggest that the decrease in reactivity could be due to an excluded volume effect.

In 1987 Gnanou[15] reported the most conclusive evidence for thermodynamic reasons as opposed to excluded volume arguments for a decrease in macromonomer reactivity with an increase in molar mass. He synthesized a series of styrenic functionalized poly(styrene) macromonomers of various molar masses and free radically copolymerized them with p-methylstyrene and with styrene, Scheme 1.4. For the first series of materials, he polymerized the poly(styrene) macromonomers with p-methylstyrene. This system has the most structural similarities between the polymerizable group of the macromonomer and the monomer that anyone has combined. The second series of polymers was synthesized from the same poly(styrene) macromonomers, but with styrene instead of p-methylstyrene. He showed that there was a reactivity dependence related to the substitution of the low molar mass monomer but that it correlated well with the reactivity ratios of the copolymerization of styrene with p-methylstyrene. More importantly, he demonstrated that the reactivity of the macromonomer was not affected by its molar mass. The results indicated that one needs to consider the

Scheme 1.4 Synthesis of poly(styrene)-g-poly(styrene) and poly(p-methylstyrene)-g-poly(styrene) using styrenic functionalized poly(styrene) macromonomers.

Poly(styrene)-g-poly(styrene)

Poly(p-methylstyrene)-g-poly(styrene)

asymmetric nature of the solvent towards both the graft and the growing chain. The chi-interaction parameter between the graft and the growing backbone would be therefore be a function of the molar mass of each. In addition, for the copolymerization of a macromonomer with a monomer that is compositionally different, one should take into account the composition of the copolymer and its affect on the apparent reactivity of the macromonomer.

Despite the kinetic complexities involved during the copolymerization of a macromonomer, the macromonomer method allows for the study of structure/property relationships in an unprecedented fashion. This is because one can synthesize a series of graft polymers, all having the same weight percent of the macromonomer, but with the macromonomer having different molar masses. This is depicted in Figure 1.1, where all of the copolymers have the same composition, but vary in their architectures, ranging from materials that have very many short grafts to materials that have very few large grafts. As you might expect, as the graft molar mass is varied at constant composition, the physical properties of the copolymers can also be affected. Throughout this dissertation, the effect of branching on the bulk, surface, and solution properties will be addressed.

Figure 1.1 Illustration of different polymer architectures at constant composition.

CHEMICAL COMPOSITION DISTRIBUTION IN BLOCK AND GRAFT COPOLYMERS

A major effort in synthetic polymer chemistry involves the preparation of polymeric materials with control over the parameters that affect polymer properties. These parameters include chemical composition, chemical composition distribution (CCD), molar mass, molar mass distribution, microstructure, and topology. Of all of these recognized characteristics, the chemical composition distribution has received the least attention.

There are two different types of chemical heterogeneities found for statistical copolymers.[16] The first one, often referred to as conversional heterogeneity, results from the copolymerization of monomers with different reactivity ratios which significantly changes the feed ratio as a function of conversion, and hence affects the relative amounts of the comonomers incorporated. The other type of chemical heterogeneity is called statistical heterogeneity. This type of heterogeneity originates from the statistics of copolymerization. For the copolymerization of monomers with roughly the same molar mass, the statistical heterogeneity quickly approaches zero with increasing degree of polymerization.

The copolymerization of a macromonomer with conventional lower molar mass monomers, however, results in

a significantly broad chemical composition distribution as a result of the statistics of copolymerization, much broader than with conventional low molar mass monomers. Stejskal, Kratochvil, and Jenkins[17] have shown that the statistical copolymerization of a low molar mass monomer with 2 mol% of a macromonomer can result in a distribution of composition which may span several tens of weight percent. They developed a theoretical treatment for the determination of the CCD for graft copolymers prepared by the macromonomer method. Their approach handled macromonomers having both broad and narrow molar mass distributions. They graphically depicted their results by simulating the CCD that would arise for a graft copolymer prepared by the statistical copolymerization of a low molar mass monomer, 100 g/mol, with a macromonomer with a narrow molar mass distribution having a molar mass of 20000 g/mol. This corresponds to 80 wt% of the macromonomer units. The graph, Figure 1.2, shows the predicted CCD as a function of the degree of polymerization ranging from 50 to 5000. The data shows that as the degree of polymerization decreases, holding everything else constant, the CCD significantly increases asymmetrically.

Figure 1.2. Differential weight distribution function, W*(x), of chemical composition, x, of graft copolymers prepared by statistical copolymerization of a low molar mass monomer, 100 g/mol, with a macromonomer having a molar mass of 20000 g/mol. The copolymers contain 80 wt% graft component and differ in the degree of polymerization as curve 1 = 50, curve 2 = 500, curve 3 = 2000, and curve 4 = 5000.[17]

Stejskal and Kratochvil[18] have also evaluated the CCD that arises from conversional heterogeneity. They pointed out that both types of chemical heterogeneity, namely statistical and conversional, occur simultaneously and are superimposed in any practical experiment. Their calculations show that the molar mass and the molar mass distribution of the macromonomer is not a factor when considering the CCD developed as a result of conversional heterogeneity. The deciding parameter for the effect of conversional heterogeneity on the CCD is the product of the reactivity ratios between the macromonomer and the monomer. The model calculations show that the more the ratio differs from unity, the broader the CCD is, Figure 1.3. The values demonstrate, for example, for an initial feed ratio of 50 wt% of each comonomer at 50 wt% conversion, that there exist macromolecules differing by 25 wt% in graft content for r_A = 0.1, 21 wt% for r_A = 0.2, 11 wt% for r_A = 0.5, and only 2 wt% for r_A = 0.9. These values emphasize the necessity of choosing a system where the polymerizable end group of the macromonomer closely emulates the low molar mass comonomer. When the monomer and the macromonomer have similar reactivities, the conversional heterogeneity can therefore be neglected for statistical copolymerizations.

Figure 1.3. The cumulative CCD, Iw(x), for statistical copolymers of an ordinary monomer A with a macromonomer M for different monomer reactivity ratios. The value x is the chemical composition of the copolymers as expressed in weight fraction.[18]

One of the main reasons why living polymerization methods have been developed to such an extent has to do with their unique ability to synthesize polymers having controlled molar masses with narrow molar mass distributions. Due to their narrow molar mass distributions, the chemical heterogeneity has been regarded as negligible. In many cases, Stejskal and Kratochvil[19] point out that this assumption may not be justified. They calculated a two-dimensional weight distribution function for di- and triblock copolymers of fairly narrow molar mass distribution of 1.2. The results, Figure 1.4, show that at any given molar mass there exists a distribution of composition, even though the material has an overall narrow molar mass distribution. In addition, they calculated the distribution functions of chemical composition for a diblock and a triblock copolymer as a function of the molar mass distribution. The diblock case is shown in Figure 1.5 and the triblock calculations are shown in Figure 1.6. The calculated CCDs are relatively broad, even for fairly narrow molar mass distributions of 1.1. This indicates that the chemical heterogeneity of block copolymers can not be ignored. When the molar mass distribution is 2, the most probable distribution, the CCD of the diblock copolymer is uniform! That is, macromolecules with any and all possible

Figure 1.4. Two dimensional differential weight distribution function $W(M,x)$ of molar masses, M. and chemical composition, x, for a diblock copolymer (Mn = 100000 g/mol, Mw/Mn = 1.2.[19]

Figure 1.5. Differential weight distribution function W(x) of chemical composition, x, of a model diblock copolymer having the indicated molar mass distributions.[19]

Figure 1.6. Differential weight distribution function W(x) of chemical composition, x, of a model triblock copolymer having the indicated molar mass distributions.[19]

compositions are present in <u>identical relative amounts</u>. If the molar mass distributions exceed 2, then the CCDs are concave and the content of macromolecules having a composition close to that of the homopolymers increases. This can be easily visualized for a diblock copolymer. Since the precursors have broad molar mass distributions, the probability of joining two macromolecules with the same molar mass, (where the composition is 50 wt%) is obviously low.

There are essentially three different methods for investigating the chemical heterogeneity in copolymers.[20] The first two, equilibrium sedimentation or centrifugation in a density gradient and fractional precipitation or dissolution techniques, can evaluate the entire distribution of chemical composition under appropriate experimental conditions. The third method, light scattering, can be applied more generally than the first two techniques; but, the method only allows for the determination of statistical moments of the CCD, referred to as the parameters P and Q.

The equilibrium sedimentation methods are only applicable for very high molar mass copolymers and are not used that often. The fractional precipitation methods and dissolution techniques are utilized more often. These

methods are numerous and include high performance precipitation liquid chromatography[16], cross fractionation[21], fractionation in demixing solvents[22], and supercritical fluid extraction fractionation.[23,24]

In the light scattering method, the parameter P is related to the mutual dependence of the chemical composition distribution and the molar mass distribution, while the parameter Q characterizes the width of the chemical composition distribution. Benoit and Bushuk[25] derived the relationship, equation 3,

$$M_{ap} = M_w + 2PR + QR^2 \qquad (3),$$

where $R = [[(dn/dc)_A - (dn/dc)_B]/(dn/dc)_C]$ and $(dn/dc)_J$ are the refractive index increments of the constituent homopolymers ($J = A,B$) and of the copolymer ($J = C$). Parameter P then refers to the first moment of the z distribution of composition and parameter Q refers to the second moment of the z distribution of composition. The above equation can be shown graphically, as in Figure 1.7. The moments, P and Q, can be calculated by fitting the curve with a parabolic function. In the case of chemically uniform copolymers, such as those obtained in an azeotropic copolymerization or an exactly alternating copolymerization, the first and second moments will be zero since there is no distribution in composition. Copolymers, therefore, with

Figure 1.7. Dependence of the apparent molar mass as a function of R in various solvents. The solid line is a parabola calculated from all points by quadratic regression.[17]

uniform compositions give molar masses that do not depend on the refractive index of the solvent when light scattering measurements are carried out in various solvents. An interesting extension of the light scattering method has been the hyphenation of LALLS and GPC. Dumelow and coworkers[26] defined the parameter H as the ratio of Q/Q_{max} which takes a value between 0 (for a compositional homogeneous sample) and 1 (for a homopolymer blend, i.e. maximum heterogeneity).

With the presentation of the above literature dealing with the distribution of composition, it is hoped that the reader will gain a deeper appreciation for this often overlooked polymer parameter. This concludes this section of the Literature Review - Part 1. The utilization of multiphase polymeric systems in microlithography will be discussed next.

c) **SILICON CONTAINING COPOLYMERS IN MICROELECTRONICS**

The microelectronics field has dramatically affected the way we live today. The tremendous growth in our dependence on microelectronics has been spurred by the advent of ultra-large scale integration of electronic circuits and sub-micron device patterns. Since 1959, the number of transistors on memory chips has doubled every year.[27] Improvements in lithographic systems, both from materials and process points of view, has allowed the routine fabrication of devices with dimensions of 2 to 3 micron sized features, while the state of the art 4 megabyte DRAM memory chips have 1 micron sized features. It is believed that in order to fabricate 16 and 64 megabyte DRAM memory chips that the technology will need to utilize 0.7 micron sized features.[28] In order to fabricate device geometries with these dimensions, improvements in lithographic resist materials are a necessity.

The principle of lithography is based on the structural degradation or alteration of highly specialized polymeric films induced by some form of radiation such as mid UV, deep UV, X-ray, or electron beam irradiation. Traditionally, photolithography is most often used in high volume production of electronic devices. However, the ever demanding ability to fabricate smaller device geometries

continues to spark interest in other processes, such as the electron beam systems. High energy electrons have exceedingly short de Broglie wavelengths which allow the circumvention of the inherent resolution limits imposed by UV.

A particular problem facing the microelectronics industry is that as the device geometries and spacings, referred to as line pitch, become smaller, the film thickness overall has stayed relatively constant. This creates relatively high, nonuniform steps in multi-layered topographies. This becomes most apparent in the metallized conductor layers of the circuits which ussualy extend for many microns and are tightly packed together. One solution around this inherent problem is the use of planarizing layers of low dielectric polymeric materials. This approach has motivated the use of multi-level resist processes[29]. A typical multi-level resist is shown in Figure 1.8 for a bi-level resist. There are other processes based on tri-level resists, however the bi-level resists will be emphasized since that is how the polymers synthesized in this dissertation were evaluated. The bi-level resist system consists of a substrate, typically a semiconductor material, such as silicon or gallium arsenide, in wafer form. Upon the substrate lies a thick planarizing layer ussualy made of a polimide, a highly crosslinked novolac, or a highly

THE MICROLITHOGRAPHIC PROCESS

Figure 1.8 The microlithographic process for a
bilevel resist.[30]

cross linked material based on bis-benzocyclobutenes. On top of the planarizing layer lies a normally thin resist layer. The resist layer serves two functions. First, it is responsible for the imaging of the pattern after development. The secondly, the resist should be resistant to reactive ion etching plasmas (RIE). In that way, where the resist has been removed, the RIE will degrade and remove the organic planarizing layer. In the areas where the resist remains, it will act as a barrier and prevent the underlying organic substrate from being removed. This results in the transfering of the image from the resist through the planarizing layer to the semiconductor wafer.

The pattern is the result of the resist layer "interacting" with the applied radiation. This interaction usually takes one of two forms. Either the polymer in the exposed areas becomes more soluble or it becomes less soluble. If the polymer becomes more soluble and it is removed upon development, the resist is considered to act in a positive fashion, that is, the developed image is the positive image of the applied radiation. This increase in solubility usually occurs by a lowering of the molar mass of the polymer through random chain scission or a change in the chemical structure resulting in a dramatic change in the solubility characteristics of the polymer. The most elegant process for a change in chemical structure was developed by

Willson at IBM.   He coined the phrase "chemical amplification"[31] for the process by which an added sensitizer, such as an onium salt, upon photo absorption, generates a strong acid. The liberated acid attacks the existing poly(t-butoxycarbonyloxystyrene) in a catalytic manner and causes acidolysis of the carbonate group to produce poly(p-hydroxystyrene), carbon dioxide, and isobutylene. The hydroxylated polymer is now soluble in alkaline solutions, thus differentiating it from the unreacted polymer. In addition, a common theme in most positive resists is that besides the main reaction which changes the solubility of the polymer, there is also the generation of low molar mass, volatile components, such as carbon dioxide and isobutylene in the above example. These fragments cause microporosity in the exposed areas which also facilitates their dissolution due to increased surface area. The dissolution times are therefore shorter than what would have been expected for a change in chemical structure or molar mass alone.

If the polymer becomes less soluble in the exposed areas and is not removed during development it is considered a negative acting resist. The decrease in solublility is usually induced by crosslinking the polymer upon exposure to the applied radiation. One example of a polymer that behaves in this manner is the partially chloromethylated

polystyrenics when exposed to deep UV or X-rays. Another important example of a negative acting resist is poly(dimethylsiloxane) (PDMS). PDMS undergoes cross linking reactions under relatively low doses of e-beam.

As mentioned above, the second function of the resist is to be resistant to a RIE plasma. The possibility that an organic polymer could be resistant to an oxygen RIE plasma grew out of our nation's space exploration effort. In the early 1980s, researchers in the aerospace industry recognized the fact that the degradation and weight loss of organic polymers placed in low-earth orbit, where an abundance of atomic oxygen exists, could be dramatically reduced and improved by incorporating certain refractory elements into the polymer.[32,33,34] The state of the art has come a long way since then, and it is now well documented that the incorporation of polysiloxanes into high performance materials such as polyimides and polybenzimadazoles greatly extends the variety of specialty aerospace applications upon which these materials can be utilized.[35] In the early 1980s, the microelectronics industry expanded upon this idea of incorporating refractory elements into organic polymers. They showed that by incorporating elements such as silicon and titanium into organic polymers, that the materials exhibited enhanced resistance to oxygen RIE processes[36]. This resistance is a

result of the formation of silicon oxides at the top surface of the resist upon exposure to the reactive oxygen species present in the oxygen RIE. The resultant silicon oxide layer acts as a barrier to the plasma and therefore protects the underlying substrate.

Recent investigations have resulted in several resist materials that are based on organic polymers containing silicon moieties. In all cases, whether the materials were homogeneous or multiphase, the idea was that the majority of the material served the function of a resist, that is it interacted in an appropriate fashion with the applied radiation and that the silicon imparted oxygen RIE resistance. These materials include: poly(3-butenyltri-methylsilane sulfone),[37] poly(silylstyrene sulfone),[38] poly(methyl methacrylate)-g-poly(dimethylsiloxane),[39] poly(trimethylsilylstyrene-co-chloromethylstyrene)[40], pol(trimethylsilylstyrene-co-p-chlorostyrene)[41], poly(di-alkylsilane)[42], terpolymer of phenol-trimethylsilylphenol-formaldehyde with o-quinonediazide as a sensitizer[43], trimethylsilylmethylated resorcinol-formaldehyde with naphthoquinohediazide as a sensitizer[44], poly(phenylsilyl-sesquioxane)[45], and poly(p-methylstyrene)-b-poly(dimethyl-siloxane)[46], to name a few.

This concludes this section and the entire Literature Review Section - Part 1. The three topics covered in this section, macromonomers, CCD, and resists, will be referred to several times in the Results and Discussion Section - Part 1 which will follow immediately after the Experimental Section which is next.

EXPERIMENTAL

REAGENTS AND PURIFICATION

This section describes in detail the purification of the many reagents used throughout this work. Particular emphasis was placed not only on the purification of the reagents but also on their subsequent handling under anaerobic conditions when necessary; for example, use of syringe techniques, cannulas, and a dry glove box for air sensitive reagents.

Nitrogen

Prepurified nitrogen (99.99%) (Airco) was regulated through a 1 1/2 in steel drying column at ca. 50 psig (345 kPa). The drying column was packed with freshly activated 4 Å molecular sieves (Linde) and supported by glass wool at both ends. After passing through the drying column, the dried nitrogen was regulated to ca. 6-8 psig (42-56 kPa) and connected to a glass nitrogen/vacuum manifold fitted with five greaseless Teflon rotoflow stopcocks. The vacuum manifold was connected to a mechanical vacuum pump with an in-line electronic pressure transducer and an in-line liquid nitrogen cold trap. This system is capable of ca. 15 mtorr.

Glassware

Most polymerizations that proceed by living polymerization mechanisms, such as anionic and group transfer polymerization, require purity levels commonly associated with high vacuum line work and typically exceeds those levels associated with normal purification procedures. The preparation of all of the glassware and reactors that were used to handle the reagents for such tedious reactions involved the srupulous cleaning of the glassware with soap and water. Frequently, the glassware was rinsed with hydrofluoric acid (49 %), followed by rinses with dilute base, water, and acetone. This glassware was then dried in a forced air convection oven at 120 °C for ca. 12 h, followed by fitting the appropriate glassware with cleaned Teflon coated magnetic stir bars and rubber septa that were secured with two wraps of copper wire. The flasks were purged with purified nitrogen while they were thoroughly flamed to remove traces of adsorbed moisture from the surface of the glassware. When cool, the purge needles were removed from the flasks and the flasks were back filled with 6-8 psig (42-56 kPa) of nitrogen using the nitrogen/vacuum manifold. Once cool, these flasks were ready to be charged with various reagents using anaerobic techniques to assure minimal contamination.

Solvents

Tetrahydrofuran. Tetrahydrofuran (Fisher, Certified Grade) (THF) was placed in a 2000-mL, 1-neck, round bottom flask equipped with a Teflon coated stir bar. The THF was allowed to reflux under a nitrogen atmosphere in the presence of several grams of a sodium metal dispersion in paraffin wax. After complete dissolution of the parafin wax with heat and stirring, a fine dispersion of sodium, having a higher surface area compared to sodium metal balls, remains to efficiently dry the solvent. After refluxing for several hours, ca. 0.1-0.3 g of benzophenone (Aldrich) was charged to the mixture of THF and dispersed sodium and allowed to reflux under nitrogen. It is important to use an excess of sodium in order to prevent distillation of the benzophenone. The function of the benzophenone is not for purification, but rather for the indication of purity. Immediately upon the addition of benzophenone, one should see the formation of a blue color associated with the onset of the formation of the sodium/benzophenone ketyl, and after several hours the color should change from blue to deep purple, indicating the THF is ready for use. The formation of the ketyl is accomplished by the initial formation of a benzophenone radical anion which is blue in color. The deep purple color is associated with the conversion of the

radical anion over to the dianion, indicating that the solvent is completely dry and oxygen free.[47]

Prior to collection of the THF for polymerization, ca. 50 mL of distillate was removed and the middle fraction was collected in a previously cleaned, flamed, and nitrogen purged flask fitted with a rubber septum. The rubber septum was secured in place with copper wire in order that a positive pressure of nitrogen could be maintained. Despite these purification steps under inert conditions, it has been reported that ca. 0.5-1.0 mmole/1000 mL of impurities still exist.[48]

Cyclohexane. The major impurity present in commercial grades of cyclohexane is cyclohexene.[49] The allylic protons are fairly acidic and therefore this impurity would react with strong bases, such has living carbanions present in anionic polymerizations. In order to remove the unsaturated impurity, cyclohexane (Fisher, Reagent Grade) was stirred in the presence of concentrated sulfuric acid at room temperature for 5-7 days. This procedure sulfonates the cyclohexene, rendering it water soluble. After stirring, the two phases were allowed to separate, and the cyclohexane layer was decanted from the aqueous layer. The decanted cyclohexane was placed in a 1000-mL, one-neck, round bottom flask and 2-3 g of sodium dispersed in paraffin was slowly

added. The cyclohexane was refluxed for 24 hr under dry nitrogen. Prior to collection of the cyclohexane, ca 25 mL was distilled and the middle fraction was collected in a previously cleaned, flamed, and nitrogen purged round bottom flask. After the distillation was complete, the receiver was removed under a positive nitrogen purge and fitted with a rubber septum. The septum was secured in place with copper wire and stored under 6-8 psig (42-56 kPa) of purified nitrogen.

Toluene. Toluene (Fisher, Certified Grade) was purified for free radical reactions by thorough degassing and storage under nitrogen. Degassing was accomplished by pulling a vacuum on a round bottom flask containing toluene while stirring and cooling to avoid distillation.

Dichloromethane. Dichloromethane (Mallinckrodt, Analytical Grade) was stirred over calcium hydride for ca. 12 h followed by fractional distillation under nitrogen and the middle fraction was collected. The solvent was then thoroughly degassed and stored under nitrogen in the dark.

Cyclopentanone. The solvent used to spin coat the PBS-g-PDMS copolymers was cyclopentanone. Cyclopentanone (Aldrich) was passed through a column of neutral alumina to remove peroxides resulting in a colorless liquid.

Miscellaneous. Chloroform (Aldrich, Certified Grade), chloroform-d (Aldrich, 99.8% deuterated), hexanes (Fisher) and methanol (Fisher) were used in situations where oxygen and moisture were not a problem, such as in precipitations and routine NMR analysis, and therefore they were used as received.

Monomers

Hexamethylcyclotrisiloxane. The cyclic siloxane trimer, known as D_3 in the silicon literature, was kindly provided by General Electric Corporation (Dr. Bruce Frye: (518) 233-2545). D_3 was purified by vacuum sublimation from a heterogeneous calcium hydride mixture in an apparatus shown in Figure 1.9. The apparatus was thoroughly cleaned and flame dried under nitrogen. The apparatus was disassembled and the receiving flask was tared (including the stir bar) and its weight was recorded. Approximately 460 g of D_3 was added to the sublimation flask along with ca. 5 g of calcium hydride. The apparatus was reassembled and purged with nitrogen. The cyclic monomer was melted (70 °C) and was stirred over calcium hydride for ca. 12 h. The monomer was cooled back to room temperature and the glass cross path was covered with an electrical heating tape and heated to ca. 70 °C. The sublimation flask was cooled to -78 °C and after thermal equilibrium was reached, the

Figure 1.9 Vacuum sublimation apparatus.

apparatus was evacuated to 50 mtorr. At this time the apparatus was isolated from the vacuum manifold. The cold bath was moved from the sublimation flask to the receiving flask and the sublimation flask was heated with warm water to ca. 35 °C. At this time the monomer would sublime (takes ca. 4 h). After approximately 90% of the monomer had transferred, the apparatus was purged with nitrogen and the heating and cooling baths were removed. After sublimation, enough dry cyclohexane was added via cannula to the receiving flask to dissolve the purified monomer. Since the dissolution of the monomer was endothermic, in addition to the stirring, sometimes a warm water bath (40 °C) was placed under the receiving flask to expediate the dissolution. After the monomer had dissolved, the solution was transferred from the sublimation flask via cannula to a 1000-mL volumetric flask that had been cleaned, flamed, nitrogen purged, and fitted with a septum. Additional cyclohexane was added to the volumetric flask in order to dilute the solution to the appropriate mark. The sublimation apparatus was disassembled and the sublimation flask was reweighed to back calculate exactly the amount of D_3 that was transferred. This procedure typically results in a 40 w/w% solution of D_3 in cyclohexane that was stored under nitrogen until ready for use in polymerizations. This

solution was stable and could be handled by syringe techniques for monomer additions.

Methyl Methacrylate. Methyl methacrylate (Rohm and Haas) (MMA) was transferred to a cleaned and flamed round bottom flask equipped with a stir bar. Finely ground calcium hydride was added to the monomer and the evolution of hydrogen was immediately evident. The flask was fitted with a rubber septum and was purged with nitrogen until the evolution of hydrogen stopped. The monomer was allowed to stir over the heterogeneous drying agent for ca. 3 days. The flask was connected to a previously cleaned and flamed vacuum distillation apparatus and the monomer was degassed by three successive freeze/thaw cycles. The monomer was again cooled to -78 °C and a good vacuum was established (<100 mtorr) followed by flame drying the apparatus once again. The apparatus was isolated from the vacuum manifold and the monomer (b.p. = 100 °C) was allowed to distill while cooling the receiving flask to -78 °C with a dry ice/isopropanol bath. The monomer would typically distill at ca. 15 °C at the stated initial pressure. After distillation of approximately 95% of the monomer, the apparatus was back filled with nitrogen and the purified distillate was transferred via cannula to a clean, flamed, and nitrogen purged brown bottle fitted with a septum for storage. The uninhibited MMA monomer could be stored for

extended periods of time (many months) at -20 °C without appreciable polymer formation. The MMA monomer that was purified in this manner was adequate for use in free radical polymerizations since it was largely free of inhibitor and oxygen; however, the monomer was not sufficiently free of impurities to be successfully used in living anionic polymerizations with good molecular weight and molecular weight distribution control.

For use in anionic polymerizations, the MMA was further purified immediately prior to use with trialkyl aluminums.[50] The desired amount of conventionally purified MMA was transferred via cannula to a previously cleaned, flamed, and nitrogen purged vacuum distillation apparatus connected with 2-neck distilling and receiving flasks that were fitted with rubber septa. The monomer was first thoroughly degassed using three successive freeze/ thaw cycles. Triethylaluminum (25 wt% in heptane) (TEA) (Kindly provided by Dr. Tom Hanlon at Ethyl Corporation) was slowly syringed into the cold monomer. It was necessary to slowly add the TEA while stirring to avoid the undesirable exotherm that accompanies complexation. Once the yellow-green (chablis) colored complex formed, one was certain that the protonic impurities had been scavenged. A 50% excess of the TEA was added after a stable complex color persisted. The complexed monomer was allowed to stir under nitrogen for 1 h

prior to distillation. The monomer was subsequently distilled under vacuum in a similar manner to the method used when distilled from calcium hydride. The monomer was frozen with liquid nitrogen and stored under a positive nitrogen atmosphere and covered with black cloths preventing exposure to light until it was syringed directly from the distillation apparatus into the reaction vessels. It was imperative to thoroughly degas the monomer prior to the addition of the TEA since it would react with dissolved oxygen to form radical intermediates which would result in premature polymerization prior to distillation.

1-Butene. 1-Butene (Aldrich, 99.9%) was used as received to prepare poly(1-olefin sulfone)s with sulfur dioxide.

Norbornene. Norbornene (Aldrich) was purified by vacuum sublimation and was dissolved under nitrogen in purified and degassed dichloromethane to obtain stock solutions of ca. 45% solids.

5-Ethylidene-2-norbornene. 5-Ethylidene-2-norbornene (Aldrich, mixture of <u>exo</u> and <u>endo</u>) was fractionally distilled under nitrogen and the middle fraction was used.

Sulfur dioxide. Sulfur dioxide (Aldrich, anhydrous) was used as received to prepare many different poly(1-olefin)s with various olefins and diolefins.

Initiators, Terminating Agents and Catalysts

sec-Butyllithium. sec-Butyllithium (Lithco Division of FMC) was obtained as a 1.4 M solution in cyclohexane. In order to reduce the extent of contamination from insertion of syringe needles, small aliquotes of the solution were transferred to previously cleaned, flamed, and nitrogen purged serum bottles fitted with rubber septa. The molarity was then determined by titration using 2,5-dimethoxybenzyl alcohol, a self indicating standard.[51] The aliquots of sec-butyllithium were stored at -20 °C.

1,1-Diphenylethylene. 1,1-Diphenylethylene (Eastman Kodak Company) (DPE) was typically vacuum distilled from sec-butyllithium. This method of purification is possible due to the inability of 4-methyl-1,1-diphenylpentyllithium, the 1:1 reaction product of sec-butyllithium and DPE, to initiate the anionic polymerization of DPE. The crude, viscous liquid (b. p. = 270 °C) was characterized by a yellow color. The "as received" DPE was transferred via cannula to a previously cleaned, flamed, and nitrogen purged vacuum distillation apparatus fitted with 2-neck

distillation and receiving flasks that were fitted with rubber septa. The DPE was thoroughly degassed using three succesive freeze-thaw cycles (100 mtorr, -198 °C). sec-Butyllithium was added dropwise to the degassed DPE while stirring at room temperature. The DPE solution immediately turned dark green and after further additions of sec-butyllithium, the solution turned dark brown. Eventually the solution turned dark red indicating the formation of 4-methyl-1,1-diphenylpentyllithium. The color changes during the titration of DPE have been attributed to trace quantities of biphenyl and benzophenone.[52] The DPE was allowed to stir for ca. 30 min under nitrogen prior to distillation. Due to the high boiling point of DPE, constant vacuum was applied during distillation while cooling the receiving flask with liquid nitrogen and heating the distillation flask to ca. 60 °C. The distillate was colorless and was transferred via cannula to previously cleaned, flamed, and nitrogen purged brown bottles fitted with septa. The purified DPE was stored in a refrigerator, without degradation, under a positive nitrogen atmosphere for extended periods of time.

4-Methyl-1,1-diphenylpentyllithium. A more stable, less reactive anionic initiator was utilized for the anionic copolymerization of MMA with either methacryloyloxy functionalized PMMA or PDMS macromonomers. The initiator,

4-methyl-1,1-diphenylpentyllithium, also commonly known as 1,1-diphenyhexyllithium (DPHL), was prepared from 1,1-diphenylethylene and sec-butyllithium. To a previously cleaned, flamed, and nitrogen purged 100-mL round bottom flask fitted with a septum and a stir bar, was added 30 mL of purified THF via syringe. The solvent was brought down to -78 °C by a dry ice/isopropanol bath and after reaching thermal equilibrium 2.2 mL (0.012 mole) of purified DPE was added, followed by 7.5 mL of 1.4 M sec-butyllithium (0.010 mole). This produced a 0.25 M solution of DPHL which was then handled by syringe.

1,1'-Azobis(isobutyronitrile). 1,1'-Azobis(iso-butyronitrile) (DuPont) (AIBN) was recrystallized from acetone, dried under reduced pressure at room temperature, and stored in a dark brown bottle at -20 °C. Standard solutions of AIBN were routinely prepared by dissolving a known amount of purified AIBN in either degassed toluene or benzene. The solution was handled and stored under nitrogen.

t-Butylhydroperoxide. t-Butylhydroperoxide (Aldrich, 90 w/v% in isopropanol) was used as received and handled under nitrogen.

3-Methacryloyloxypropyldimethylchlorosilane. 3-Meth-acryloyloxypropyldimethylchlorosilane (Petrarch) was used as

received to terminate living D_3 polymerizations to form methacryloyloxy functionalized PDMS macromonomers.

5-Hexenyldimethylchlorosilane. 5-Hexenyldimethylchlorosilane (Petrarch) was used as received to terminate living D_3 polymerizations to form hexenyl terminated PDMS macromonomers.

Triethylamine. Triethylamine (Aldrich, Gold Label) was refluxed for 12 hrs over calcium hydride followed by fractional distillation under nitrogen and the middle fraction was collected.

Methacryloyl chloride. Methacryloyl chloride (Aldrich) was vacuum distilled and handled under nitrogen.

MACROMONOMER SYNTHESIS AND CHARACTERIZATION

The detailed synthesis of three different macromonomers is reported in the following section. All three of the macromonomers were prepared using living polymerization methods in order to control the molecular weight, molecular weight distribution, and to obtain highly functionalized oligomers.

Methacryloyloxy Functionalized PMMA Macromonomers

Poly(methyl methacrylate) Macromonomer Synthesis. The synthesis of methacryloyloxy functionalized PMMA macromonomers began with the synthesis of primary hydroxyl functionalized PMMA. The primary hydroxyl functionalized PMMA oligomers were synthesized by Dr. Ann Marie Hellstern and the detailed synthetic procedure can be found in her dissertation.[53] Group transfer polymerization methods were used to synthesize a PMMA oligomer with a molar mass of 6300 g/mol. The primary hydroxyl functionalization was realized by using a protected hydroxyl functional silylketene acetal as the initiator and tetrabutylammonium benzoate as the catalyst. The protected GTP initiator was synthesized by first protecting 2-hydroxyethyl methacrylate with trimethyl chlorosilane, followed by performing a selective 1,4-hydrosilylation using Wilkinson's catalyst with trimethylsilane.

Deprotection of the hydroxyl group involved hydrolysis of the trimethylsilyl group with dilute HCl in purified THF.[54] The hydroxyl functional polymer was precipitated in hexanes and dried under reduced pressure at ambient temperature until constant weight. The dried PMMA oligomer was dissolved in purified THF under a nitrogen atmosphere. A 20 mole % excess of purified triethylamine was added via syringe to act as an acid scavenger. A 5 mole % excess of

purified methacryloyl chloride was added. Immediately upon the addition of the acid chloride, the hydrochloride salt of triethylamine precipitated. The reaction was allowed to proceed for ca. 16 h after which the solution was filtered to remove the salts and the PMMA macromonomer was precipitated in hexanes.

Methacryloyloxy Functionalized PDMS Macromonomers

Anionic polymerizations of D_3 were carried out in rigorously cleaned and flame dried one-neck round bottom flasks each equipped with a Teflon coated magnetic stirring bar and a rubber septum secured with copper wire under a 6-8 psig (42-56 kPa) prepurified nitrogen atmosphere. The cyclohexane solution of D_3 was syringed into the reaction flask and a calculated amount of sec-butyllithium was added to initiate the ring-opening polymerization. The initiation reaction was allowed to proceed for ca. 2 h, followed by the addition of ca. 10 percent by volume purified THF to promote propagation of the living siloxanolate species. The polymerization was terminated after 48 h with 3-methacryloyloxypropyldimethylchlorosilane to afford the macromonomer which was then precipitated in methanol after 2 h and dried under reduced pressure at room temperature until constant weight.

Hexenyl Functionalized PDMS Macromonomers

The olefinic terminated PDMS macromonomers were used in terpolymerizations with olefins and sulfur dioxide. The synthesis of the hexenyl functionalized PDMS macromonomers was exactly the same as reported earlier for the methacryloyloxy functionalized PDMS macromonomers except that 5-hexenyldimethylchlorosilane was used as the terminating agent instead of 3-methacryloyloxypropyl-dimethylchlorosilane.

PMMA-g-PMMA BY ANIONIC COPOLYMERIZATION

In this next section, the detailed synthesis of a series of novel branched PMMA hompolymers will be presented. These well-defined materials were excellent models for the elucidation of structure/property relationships in both the solid and solution states for homopolymers exhibiting long chain branching.

Synthesis and Characterization

Copolymerization. The anionic copolymerizations of MMA with the methacryloyloxy functionalized PMMA macromonomers were performed in previously cleaned, flamed, and nitrogen purged one-neck round bottom flasks each equipped with a magnetic stir bar and a rubber septum under a 6-8 psig (42-56 kPa) prepurified nitrogen atmosphere. A

calculated amount of PMMA macromonomer was charged to the
reaction flasks prior to their final sealing with rubber
septa. The macromonomers were thoroughly degassed for 20
min under vacuum followed by backfilling and pressurization
of the flasks with nitrogen. The purified polymerization
solvent, THF, was added via cannula to the reaction flasks.
The amount of solvent charged yielded solutions of ca. 4
w/v% MMA monomer. A cleaned and flamed thermocouple was
passed through the septum on each reaction flask and
submerged into the solution in order to monitor the reaction
temperature. The reaction flasks were submerged into -78 °C
baths and allowed to reach thermal equilibrium. The MMA,
previously distilled from triethylaluminum, was syringed
into each flask in order to obtain the desired ratio of MMA
to PMMA macromonomer. The initiation of the anionic
copolymerization was achieved by adding 0.2 mL aliquots of a
0.25 M 4-methyl-1,1-diphenylpentyllithium (DPHL) solution to
the reaction vessels at one minute intervals until an
exotherm was noted. After the temperature reequilibrated to
-78 °C (approximately 10 min), the polymerization was
terminated with degassed methanol. The resulting graft
polymers were precipitated in hexanes.

Extraction of Unincorporated Macromonomer. The above
precipitated PMMA graft polymers all had residual
unincorporated PMMA macromonomer. It was desired to measure

the absolute number average molar mass of the graft polymers using a colligative property measurement and therefore it was necessary to remove the free macromonomer.

This procedure was performed by E. J. Siochi in Professor Tom Ward's laboratory at Virginia Tech. The most effective way of performing the fractionation involved making a 1 wt% solution of the reaction product in THF. Hexane was slowly added to this solution with agitation just before the turbidity point. At this point the solution was allowed to ripen for several hours. More hexane was added until precipitates, the high molar mass fraction, were visible and the solution was allowed to settle. The solution was filtered to isolate the graft polymer from the still dissolved and unincorporated PMMA macromonomer. The precipitate was dried under reduced pressure at room temperature until constant weight.

PMMA-g-PDMS BY FREE RADICAL AND ANIONIC COPOLYMERIZATION

This section deals with the synthesis of graft copolymers based on PDMS macromonomers and MMA. The copolymerization methods chosen were based on those used by Dr. Steven Smith[2] in Professor James E. McGrath's research laboratories. The purpose was to further establish the chemical composition distribution (CCD) of graft copolymers prepared by the macromonomer technique using different modes

of copolymerization, namely free radical and anionic copolymerization mechanisms.

Synthesis and Characterization

The following describes the different copolymerization methods used for a specific molar mass macromonomer. It was also desired, from a structure/property point of view, to use a broad molar mass distribution macromonomer. This was simulated by using a mixture of different molar mass macromonomers and following the same procedures as described below for the copolymerization of a single molar mass macromonomer with MMA.

Free Radical Copolymerization. The free radical copolymerizations of the methacryloyloxy functionalized PDMS macromonomer with MMA were performed in degassed toluene at 65 °C for ca. 50 h using 0.1 weight percent (based on MMA) AIBN. The copolymerizations were carried out at 20 weight percent solids under a nitrogen atmosphere. The graft copolymers were precipitated in methanol and dried under reduced pressure. The reaction product was thoroughly extracted with hexanes in a soxhlet extractor to remove any unincorporated PDMS macromonomer.

Anionic Copolymerization. The anionic copolymerizations of MMA with the methacryloyloxy functionalized PDMS macromonomers were performed in

previously cleaned, flamed, and nitrogen purged one-neck round bottom flasks each equipped with a magnetic stir bar and a rubber septum under a 6-8 psig (42-56 kPa) prepurified nitrogen atmosphere. A calculated amount of various molecular weight PDMS macromonomers was charged to the reaction flasks prior to their final sealing with rubber septa. The macromonomers were thoroughly degassed for 20 min under vacuum followed by backfilling and pressurization of the flasks with nitrogen. The purified polymerization solvent, THF was added via cannula to the reaction flasks. The amount of solvent charged yielded solutions of ca. 4 w/v% MMA monomer. A cleaned and flamed thermocouple was passed through the septum on each reaction flask and submerged into the solution in order to monitor the reaction temperature. The reaction flasks were submerged into -78 °C baths and allowed to reach thermal equilibrium. The MMA, previously distilled from triethylaluminum, was syringed into each flask in order to obtain the desired ratio of MMA to PDMS macromonomer. The initiation of the anionic copolymerization was achieved by adding 0.2 mL aliquots of a 0.25 M 4-methyl-1,1-diphenylpentyllithium (DPHL) solution to the reaction vessels at one minute intervals until an exotherm was noted. After the temperature reequilibrated to -78 °C (approximately 10 min), the polymerization was terminated

with degassed methanol. The resulting graft polymers were precipitated in methanol and thoroughly extracted with hexanes in a soxhlet extractor to remove any unicorporated PDMS macromonomer.

POLY(OLEFIN SULFONE)S BY FREE RADICAL ALTERNATING COPOLYMERIZATION

The free radical alternating co- and ter-polymerizations were carried out in a low-pressure polymerization reactor designed by the author. The reactor is based on the commercialy available Fisher-Porter glass bottles. The bottle cap was replaced with an in-house machined 316 stainless steel reactor cap assembly. The reactor cap contained a vacuum inlet, a nitrogen inlet, a septum port for reagent additions, a thermocouple, a cooling/heating coil, and an overhead motor driven Parr Magnetic Stirrer. The detailed machining specifications can be found in Appendix A along with the commericial suppliers list.

Synthesis of Poly(5-ethylidene-2- norbornene sulfone)s

Poly(5-ethylidene-2-norbornene sulfone) (PENS) was synthesized under a 6-8 psig (42-56 kPa) nitrogen atmosphere. The purified cyclic diene was charged to the polymerization reactor and diluted with purified dichloromethane to yield overall dilutions of ca. 5 wt/v% solids. High polymer was obtained by two methods. The

first method involved charging the sulfur dioxide to the diene solution via cannula at temperatures below -15 °C, followed by the addition of ca. 0.1 wt% t-butyl hydroperoxide (based on monomer). The second method was similar to the first method but the sulfur dioxide was added after the initiator. In both methods, the ratio of diene monomer to sulfur dioxide was varied from 1:1 to 1:2. Under these conditions, a redox type free radical copolymerization was initiated as soon as the hydroperoxide and sulfur dioxide are mixed. The copolymers were precipitated into hexanes and dried to constant weight under reduced pressure at room temperature.

Synthesis of PBS-g-PDMS

A calculated amount of the hexenyl terminated PDMS macromonomer was added to the modified Fisher-Porter polymerization reactor and the bottle was attached to the reactor cap. The PDMS macromonomer was then thoroughly degassed under vacuum at room temperature for 30 min. After degassing, the reactor was charged with prepurified nitrogen and the polymerization solvent, dichloromethane was added via syringe. The amount of solvent that was added corresponded to an amount that would result in a 20 w/v% solution of total polymer in dichloromethane. The reactor temperature was brought down to -20 °C by manually

controlling the amount of liquid nitrogen passing through the cooling coil. After attaining -20 °C, calculated volumes of 1-butene and sulfur dioxide were condensed into separate calibrated vessels and were transferred via cannula into the stirred polymerization reactor. The free radical initiator, t-butyl hydroperoxide, was added via syringe using four aliquots that resulted in 0.066 w/v% (based on 1-butene and sulfur dioxide) additions at 5 minute intervals. The resulting graft copolymers were immediately precipitated into a ten-fold excess of methanol containing 2 v/v% of triethylamine, filtered, and dried to constant weight under reduced pressure at room temperature. The polymers were then extensively extracted with hexanes to remove any unincorporated PDMS macromonomer in a soxhlet extractor that was modified to have a water-cooled solvent resevoir. The extracted polymers were routinely stored at -20 °C to avoid any possible thermo-oxidative degradation.

STRUCTURAL AND COMPOSITIONAL ANALYSIS OF MACROMONOMERS AND HIGH POLYMERS

Multinuclear Magnetic Resonance Spectroscopy

Multinuclear magnetic resonance spectroscopy has been used extensively throughout the different facets of this work. The technique was used to check the purity of reagents, to follow chemical reactions, to ascertain average chemical compositions of polymers, to perform end-group

analysis on oligomers and low molecular weight polymers, and to probe polymer microstructure. The exploitation of this technique for the aforementioned determinations will be addressed in the Results and Discussions section.

^{1}H NMR. ^{1}H NMR measurements were recorded on either a Bruker WP 270 spectrometer or a Bruker WP 200 spectrometer. The Bruker WP 270 spectrometer was operated at 270.132 MHz with a sweep width of 3000 Hz and a 45° pulse width of 4 us. The Bruker WP 200 spectrometer was operated at 200.135 MHz with a 2400 Hz sweep width and a 45° pulse width of 15 us. A total of either 16 or 32 transients were accumulated and were Fourier transformed with a line broadening equivelent to the Hz per point resolution.

^{13}C NMR. ^{13}C NMR spectra were recorded on a Bruker WP 200 spectrometer operating at 50.324 MHz. The NMR experiments were made using a 10 mm multinuclear broad band probe with a 12500 Hz sweep width. A powergated pulse sequence was used with a 45° pulse width of 8.0 us and a 0.328 s aquisition delay.

^{29}Si NMR. Quantitative ^{29}Si NMR spectra were recorded on a Bruker WP 200 spectrometer operating at 39.763 MHz. The NMR experiments were made using a 10 mm multinuclear broad band probe with a 16000 Hz sweep width. An inversegated pulse sequence was used to decouple the protons

and to eliminate the nuclear Overhauser effect (NOE). The sequence utilized a 45° pulse width of 25.0 us and a 0.508 s aquisition delay. A total of 2500 transients were collected and were Fourier transformed with a line broadening of 2. A relaxation agent, 0.4 M chromium(III)acetylacetonate solution in $CDCl_3$, was employed to shorten the relaxation time, T1, as well as to help suppress NOE.[55]

Ultraviolet Spectroscopy

UV spectroscopy was used to determine the molar mass of the methacyloyloxy functionalized PDMS macromonomers using end group analysis methods. UV spectra were recorded on a Perkin Elmer 552 spectrometer scanning from 350 nm to 190 nm at 20 nm/min. The molar mass of the macromonomers was determined using an end group analysis of the methacryloyloxy functional group. The wavelength maximum for the methacryloyloxy group was established to be 214 nm. MMA in cyclohexane was used as the standard to prepare a Beer-Lambert Law plot. From this plot, the extinction coefficient was determined to be 6863 L/mol in cyclohexane. PDMS macromonomer solutions of known concentrations were made in cyclohexane. The absorbance was then extrapolated back to the methyl methacrylate concentration and the functional molar mass was obtained.

Vapor Phase Osmometry

Vapor phase osmometry (VPO) was used to measure the molar mass of the methacryloyloxy and hexenyl functionalized PDMS macromonomers. The experiments were carried out on a Wescan model 233 vapor phase osmometer in toluene at 80 °C using a multistandard technique for calibration. The standards used were: squalene, 410 g/mol; sucrose octaacetate, 678 g/mol; polystyrene, 1800 g/mol; and poly(methyl methacrylate)s of 7800, 13000, and 19700 g/mol. Four concentrations were used for each standard with four readings for each concentration and the polymers being analyzed were handled in a similar manner. The data was handled in the usual manner to make the calibration plot of Mn^{-1} vs ŁV/C to obtain the slope and intercept which was used with the results from the polymer standards to obtain the molar mass of the analyte.

Membrane Osmometry

The number average molar mass of high polymers was measured by membrane osmometry (MO). MO was used to analyze many fractions of a selected PMMA-g-PDMS copolymer (prepared free radically) that was fractionated by supercritical fluid fraction methods. In addition, MO was used several other times by the author and our colleagues in Czechoslovakia for other PMMA-g-PDMS samples and for PBS-g-PDMS samples. Also,

MO was used by E. J. Siochi for analysis of the fractionated PMMA-g-PMMA materials.

The MO experiments performed at Virginia Tech were carried out on a Wescan Model 231 recording membrane osmometer. The measurements were done with RC 52 and RC 51 regenerated cellulose membranes which have low molar mass cut-off limits of 20000 g/mol and 10000 g/mol respectively. Experiments were conducted at 30 °C in HPLC grade toluene for both the PMMA-g-PDMS copolymers and the PMMA-g-PMMA materials. Seven solutions with concentrations ranging from 2 to 8 g/L were used (for the series of PMMA-g-PDMS copolymers resulting from supercritical fluid fraction, due to the limiting amount of several of the fractions, fewer concentrations were used, with a lower limit of four). The solutions were filtered through 0.5 um teflon GPC filters.

Gel Permeation Chromatography

The apparent molar masses and apparent molar mass distributions were analyzed by gel permeation chromatography (GPC) for the PMMA-g-PDMS copolymers and for the various poly(olefin sulfone)s. Absolute molar mass and molar mass distributions were able to be measured by GPC for the linear PMMA's and for the PDMS's since GPC standards were available for these polymers. The instrument was a Waters 150-C17 GPC

equipped with Ultra Styragel columns of 500, 10^3, 10^4, 10^5, and 10^6 Å porosities in THF. The graft copolymers and the poly(olefin sulfone)s were analyzed using the UV detector at 218 nm in conjunction with the differential refractive index (DRI) detector and PMMA GPC standards. The same instrument was used for the PDMS samples however a smaller column set was used due to their low molar mass range, typically less than 20000 g/mol. This column set had 100, 500, and 1000 Å porosities in toluene and was used with the DRI detector and PDMS standards synthesized in our laboratories.[56,57]

In addition, a very elegant investigation was performed by E. J. Siochi using GPC with differential viscosity and low-angle laser light scattering detectors for the analysis of the model branched PMMA-g-PMMA materials. The details can be found in her dissertation[58] and in a forth-coming manuscript.[59]

Differential Refractometry and Light Scattering

Classical molecular characterization, involving methods based on differential refractometry and light scattering, were solicited and kindly performed on several different samples of the PMMA-g-PDMS and PBS-g-PDMS copolymers at the Institute of Macromolecular Chemistry in Prague, Czechoslovakia by Professors Kratochvil and Stejskal

and their colleagues. This tedious work is presented here to unequivocally demonstrate the well-defined nature of the PMMA-g-PDMS copolymers prepared using anionic copolymerization methods.

The solvents used for these investigations were methyl ethyl ketone, tetralin (both from Fluka), toluene, dioxane, dimethylsulfoxide, tetrachloroethylene, and methanol (Lachema, Czechoslovakia). Refractive index increments of PMMA and PDMS (M_w = 7000) were determined with a Brice-Phoenix BP-2000-V differential refractometer at 25 °C for a wavelength of 546 nm. The refractive index increments, dn/dc, of the copolymer in various solvents were calculated according to the additivity rule:

$$(dn/dc)_C = (dn/dc)_A <X> + (dn/dc)_B (1 - <X>) , \qquad (3)$$

where A, B, and C refer to PMMA, PDMS, and the copolymer, respectively. <X> is the average copolymer composition expressed by the weight fraction of PMMA in the copolymer. For copolymer fractions, the differential refractometry was used to determine $(dn/dc)_C$ and to calculate their chemical composition, <X>, from equation 3. Methylethylketone was used as the solvent for this purpose.

The light scattering experiments were performed with a Sofica 42.000 (France) using a vertically polarized primary beam of wavelength 546 nm. Solutions were filtered through

sintered-glass filter G5 (VEB Jenaer Glasswerke, GDR) prior to measurement. Molar masses were evaluated from the light scattering data by the Zimm method.

Intrinsic Viscosity

Viscosity measurements were made with a Canon-Ubbelhode size 100 or size 50 viscometer in dichloromethane at 25 °C. The solution concentrations ranged from 0.2 to 0.5 g/dL.

Fractionation by Supercritical Fluid Extraction

The PMMA-g-PDMS copolymers prepared by both free radical and anionic copolymerization mechanisms were fractionated using sequential extractions with chlorodifluoromethane above its critical temperature and critical pressure (Tc = 96 °C; Pc = 5.02 MPa). The procedures were performed in the laboratories at Phasex Corporation by Dr. Val J. Krukonis and his colleagues. The graft copolymers were fractionated isothermally at 120 °C using an increasing pressure profile from 10.4 MPa to 27.6 MPa in an apparatus shown in Figure 1.10. Individual fractions were collected at ambient pressure in glass U-tubes positioned after the pressure let-down valve. Sample sizes of ca. 10 g were separated into fractions of

Figure 1.10 Supercritical fluid fractionation apparatus.

sufficient size for characterization. This was especially important since there was interest in the fractions that represented the extremes in composition and molar mass, which were only present in small amounts.

Fractionation by Demixing Solvents

The PMMA-g-PDMS copolymers prepared by free radical and anionic copolymerization techniques, were fractionated between the phases of demixing solvents of dimethyl sulfoxide (DMSO) and tetrachloroethylene (TCE). The procedure was performed in the laboratories of Professor Paval Kratochvil at the Institute of Macromolecular Chemistry in Prague, Czechoslovakia.[22] The method involves dissolving the parent graft copolymers in the above solvents at 60 °C in a cylindrical flask. After a homogeneous solution results at 60 °C, the flask is transferred to a 25 °C water bath. Three coexisting phases formed and at this time the upper and lower phases were removed via syringe. The copolymer present in the upper and lower phases were precipitated into methanol and dried. Another portion of DMSO and TCE were added to the middle phase and again the system was homogenized at 60 °C, followed by equilibration at 26 °C. This whole procedure was repeated at gradually increasing equilibration temperatures. Above 31 °C, only two phases would form. The copolymer poor phase

was removed and the copolymer rich phase was further fractionated by adding pure solvent of the kind that was removed. This procedure was continued and altogether, 14 to 20 fractions were collected depending on which sample was being fractionated. The recovery of the copolymer was greater than 99%. The chemical composition of these fractions were determined by differential refractometry. The weight average molar masses were determined by light scattering in methylethylketone and it was assumed that the apparent molar mass, <Map>, equals the weight average molar mass, <Mw>, which neglects the effect of chemical heterogeneity.[60]

Elemental Analysis

Elemental analysis was obtained on several different poly(olefin sulfone)s in order to obtain their average compositions. The experiments were performed at the Spang Microanalytical Laboratory (Star Route 1, Box 142, Eagle Harbor, Michigan 49951). This was an especially valuable technique to use to verify the composition of several of the PDMS graft copolymers since NMR can give false data on block and graft copolymers if micellularization occurred. Fortunately, this was not the case in the systems and solvents used in this work.

Differential Scanning Calorimetry (DSC)

DSC thermograms were obtained on the PBS-g-PDMS copolymers to study their microphase separation. The experiments were run on a SEIKO Instruments System I DSC 210. The PDMS neat oligomers were quenched to -160 °C and heated to 0 °C at 5 °C/min. The PBS-g-PDMS copolymers were analyzed as precipitated powders (5-7 mg). The samples were initially heated above the upper glass transition to 120 °C and held isothermally for 10 min followed by a quick quench to -160 °C. The samples were then heated to 120 °C at 5 °C/min to obtain information on the Tg of both components and the crystallization and melting behavior of PDMS. Glass transitions were determined as the midpoint of the change in heat capacity, the $\triangle$Tg was determined as the range in temperature where the DSC trace would deviate from the baseline to the temperature corresponding to the maximum of the physical aging peak. An attempt to measure the degree of phase miscibility (DPM) was made using the change in the heat capacity, $\triangle$Cp, associated with the glass transition. The $\triangle$Cp method developed by Pascault and Camberlin[61,62,63] was used to estimate the DPM as follows:

$$\text{DPM} = [1 - ((\triangle Cp''/w'') / \triangle Cp')] \times 100 \quad , \quad (4)$$

where where $\triangle$Cp' is the normalized value for PBS, $\triangle$Cp'' is the normalized value for the graft copolymers, and w'' is the weight fraction of PBS in the graft copolymer.

The percent crystallinity was determined by

$$\% \text{ crystalline} = \triangle Hm / \triangle Hm° \text{ x } 100 , \qquad (5)$$

where $\triangle Hm$ is the heat of fusion of the sample measured experimentally and $\triangle Hm°$ is the heat of fusion of a perfectly crystalline material. $\triangle Hm°$ is difficult to determine in macromolecules since perfectly crystalline substances are never obtained. The value of $\triangle Hm°$ for PDMS has been reported[64,65] to be 61.19 mJ/mg, which was obtained by using melting point depression data with added diluents.

Thermal Gravimetric Analysis (TGA)

TGA was performed on the various poly(olefin sulfone)s to obtain information about their thermal stabilities in air and in nitrogen using a Perkin Elmer System 2 instrument at a heating rate of 10 °C/min.

Water Contact Angle Analysis

Films of the PBS-g-PDMS copolymers were prepared for surface analysis by casting dilute chloroform solutions of the copolymers onto ferro-type metal plates in glass covered petri dishes and allowing the solvent to slowly evaporate (ca. 48 h). The polymer films on the metal substrate were placed in the goniometer (instrument) at room temperature and at atmospheric conditions. Water was added dropwise in

0.002 mL increments until an equilibrium contact angle was measured. The angle was referred to as the advancing contact angle. The drop was subsequently removed in similar increments and the contact angle was measured until an equilibrium contact angle was established. This contact angle was referred to as the receding contact angle. This procedure was repeated 3-4 times at various locations on the film in order to ensure reproducibility and a homogeneous film. All values were averages of several readings and the agreement was generally within $\pm 2°$.

X-ray Photoelectron Spectroscopy (XPS)

Films of the PBS-g-PDMS copolymers were prepared for surface analysis by casting dilute chloroform solutions of the copolymers onto ferro-type metal plates in glass covered petri dishes and allowing the solvent to slowly evaporate (ca. 48 h). Variable angle XPS was performed on a KRATOS XSAM 800 X-ray photoelectron spectrometer equipped with a hemispherical electron analyzer and a Mg X-ray source operated at 15 kV and 20 mA. A pressure of 10^{-8} torr was maintained in the sample chamber during spectra collection. The analyzer was operated in Fixed Retarding Ratio mode. Angle dependent analysis was performed by rotating the circular sample probe, thereby changing the angle between the sample plane and the analyzer. Angles ranging from 10°

to 90° were used. The PBS-g-PDMS copolymers were cooled using liquid nitrogen to ca. -120 °C to avoid degradation of the PBS during sample analysis.

Transmission Electron Microscopy (TEM)

TEM was performed by Mr. Greg York who was collaborating on the structure/property relationship aspect of this work. Films of the PBS-g-PDMS copolymers were prepared for TEM analysis by casting dilute chloroform solutions of the copolymers in glass vials and allowing the solvent to slowly evaporate (ca. 48 h). The films were sectioned on a Reichert-Jung ULTRACUT FC-4 ultramicrotome system at a temperature of about -110 °C. The liquid used in the boat was methanol and a diamond knife was employed. A Phillips EM 420 STEM operated at 100 kV with condenser and objective apertures of 50 and 30 micron respectively were utilized for the TEM analysis.

Scanning Electron Microscopy (SEM)

SEM analysis was performed to study the topogaraphy of various surfaces during evaluation of PBS-g-PDMS in microelectronic device applications. A Phillips IL 420 STEM was used in the SEM mode. Samples were first coated with gold to minimize charging effects.

Microlithographic Evaluation

Microlithographic evaluation of the PBS-g-PDMS copolymers was performed by the author and his coworkers at Bell Communications Research in Red Bank, New Jersey in the laboratories of Dr. Murrae J. Bowden and Dr. Antoni Gozdz.

Thin Film Preparation. The PBS-g-PDMS copolymers were dissolved in purified cyclopentanone to yield 5 wt% solutions. The graft copolymers having PDMS grafts of molar mass 20000 g/mol, were dissolved in chloroform because of the insoublity of these materials in the cyclic ketones. Pure novolac resin was used as the planarizing layer in a two-layer resist system on a silicon substrate. The novolac planarizing layer was a $1.2\,\mu$m thick film spun cast from 10 wt% ethoxyethylacetate and extensively crosslinked for 1 h at 200 °C. All solutions were filtered three times through $0.45\,\mu$m Teflon filters.

Oxygen Reactive Ion Etching. The investigations into the resistance of the title graft copolymers to oxygen reactive ion etching (RIE) were performed on ca. 2200 Å thick films that were spun cast onto silicon wafers from solution and dried at 110 °C for 15 min. The oxygen RIE measurements were performed using a Cooke Vacuum Products parallel-plate reactor at an RF frequency of 13.56 MHz, 15 mtorr oxygen, gas flow rate of 10 sccm, and a self-bias

of -350 V for various incremental time periods. The films of known initial film thickness were placed on the oxygen RIE chamber for various periods of time and their thickness as a function of time was monitored and measured using a Tencor Instruments surface profilometer.

Electron Beam Sensitivity. Sensitivity curves were established on the two-layer test samples. A PBS-g-PDMS film was spin coated onto a silicon wafer already having a 1.2 μm thick crosslinked novolac coating, followed by a 15 min drying step at 110 °C. The resulting PBS-g-PDMS resist layer was 1800 Å thick. Test patterns were exposed with a 25 kV electron beam (JEOL JBX II(U) Electron Beam Lithography System) with various dose (per area) levels ranging from 0.6 μC/cm^2 to 9.3 μC/cm^2 (microcoulombs per square centimeter) or, in terms of dose per gram, 6.9 Rad to 107.5 Rad. The patterns were dip developed with 5-methyl-2-hexanone for various time periods at room temperature. The remaining film thickness at each different area of exposure was then measured with the profilometer and the results were plotted as normalized film thickness vs log dose.

Pattern Transfer Experiments. High density lithographic pattern transfer experiments were carried out on the two-layer sensitivity test samples mentioned above. The test patterns exposed were 0.5 μm lines having various

pitches ranging from 1.5μm to 0.75μm. The samples were exposed at 4μC/cm^2 (46.2 Rad) and were dip developed in 5-methyl-2-hexanone for 30 s at room temperature followed by drying in a stream of dry nitrogen. The patterns developed in the PBS-g-PDMS top layer were transferred into the bottom planarizing layer by oxygen RIE for 13 min using the RIE system and procedure described above.

RESULTS AND DISCUSSION

INTRODUCTION

Multiphase polymeric systems are an important class of materials that have the ability to exhibit the physical properties of both components. The capacity to synthesize materials of this type is varied. The methodologies available to synthesize heterophase materials include step-growth polymerization processes, living anionic and cationic chain-growth systems, traditional "grafting from" free radical methods, and finally the macromonomer technique established by Rempp[66] and Milkovich.[1,67]

Many anionic polymerizations have the distinguishing characteristic of allowing one to establish the conditions necessary for instant initiation, continuous propagation without side reactions, and the lack of terminating reactions. Alternatively, other mechanisms, such as cationic, have a tendency towards deactivation. These parameters, in concert, allow the synthesis of high molar mass monodisperse block and graft copolymers with predictable molar masses and narrow molar mass distributions. There are many factors that determine the ability of a particular ion pair to give rise to these desired characteristics. These factors primarily include the nature of the growing polymer chain and its counterion, the nature and number of other ligands in the coordination

sphere, the nature of the reaction medium, reaction temperature, reaction pressure, and reactant concentrations.

All of these factors influence the integrity of the growing chain end and its lack of steric and electronic hinderance towards propagation. At first glance, the concept of the degree of association of ion pairs in a Weinstein[68] sense is appropriate to explain these phenomena; indeed this treatment will illustrate a number of features; however, the concept needs to be expanded to address not only the "tightness" and "looseness" of ion pairs but also the number of ion pairs that are actually associated to form aggregrates. In understanding the mechanisms of these reactions, one must not forget the possibly dominating role that penultimate and antepenultimate groups play in addition to the nature of the counterion.

These concepts will play a substantial part in several different facets of the living polymerization work presented here in which are orientated towards the synthesis heterophase materials. In the synthesis of PMMA-g-PMMAs, both anionic and GTP mechanisms were employed and resulted in the synthesis of perhaps the most well-defined graft homopolymers ever before made. Also, in the synthesis of PMMA-g-PDMSs, anionic polymerizations, resulting in living siloxanolates and enolates, led to the synthesis of very

well-defined graft copolymers that rival diblock copolymers in their uniformity of molecular characteristics.

The common theme in both of these systems is that living polymerization methods were utilized not only in the preparation of the macromonomers, which is relatively common, but also in the copolymerization step. This unique approach results in the formation of graft polymers having narrow molar mass distribution graft parts and backbone parts. These extremely well-defined materials are currently being used to investigate structure/property relationships, both in solution and in the bulk, in an unprecedented manner as a result of the synthetic control demonstrated using living copolymerization methods.

The results and discussion section will now follow. This section will attempt to address the subtleties involved in the preparation of several new materials including the PMMA-g-PMMA's of various degrees of branching, the poly(5-ethylidene-2-norbornene sulfone) homo- and copolymers, and the PBS-g-PDMS's of various compositions and architectures. In addition, details will be presented on the elucidation of the chemical composition distribution of graft copolymers prepared by the macromonomer method and its sensitivities regarding polymerization mechanism.

POLY(METHYL METHACRYLATE)-G-POLY(METHYLMETHACRYLATE)S

Polymer Science is a multidisciplinary subject. Advances in the understanding of the synthesis and properties of macromolecules involve a close interaction between scientists whose fields of interest and skill are traditionally labeled as organic chemistry, physical chemistry, solid state physics, materials engineering, and many others.

The concept for this particular investigation evolved from the need to determine the accuracy of an established analytical technique, the so-called "universal" calibration method utilized in gel-permeation chromatography (GPC).[69,70] This method involves the characterization of the molar mass and the molar mass distribution of macromolecules by taking advantage of the fact that the product of the intrinsic viscosity and the number average molar mass is equivelent to the hydrodynamic volume. In order to even consider this investigation, novel well-defined macromolecules needed to be synthesized; therefore, a multidisciplinary approach was taken.

It was proposed by the author to synthesize a series of model graft homopolymers and study their dilute solution properties using hyphenated state-of-the-art GPC instrumentation in conjunction with classical characterization techniques to reaffirm the applicability of the

universal calibration GPC method for polymers that exhibit long chain branching.

The model branched homopolymers were synthesized using the macromonmer technique and living anionic copolymerization methods. This system, having a narrow molar mass distribution for the graft and backbone components, coupled with compositional homogeneity, is an ideal branched polymer system to investigate the universal calibration GPC method, avoiding micellularization problems that often occur.

The hydroxyl functionalized PMMA oligomers were synthesized by Dr. Ann Marie Hellstern[53] using group transfer polymerization with a protected hydroxyl functional initiator based on 2-hydroxyethyl methacrylate. The synthesis of the protected GTP initiator is shown in Scheme 1.5. GTP is sensitive to protonic sources, and therefore, it was necessary to protect the hydroxyl group of HEMA as shown. The hydrosilylation of the protected HEMA utilized Wilkinson's catalyst which is highly selective for 1,4-hydrosilylations.[71]

Initiation of the group transfer polymerization of MMA using the protected initiator is shown in Scheme 1.6. GTP easily allows the synthesis of primary hydroxyl

Scheme 1.5 Synthesis of protected GTP initiator.

I. PROTECTION:

II. HYDROSILATION:

Scheme 1.6 Initiation, propagation, and termination in GTP.

INITIATION

${}^+$NBu$_4$ ${}^-$Benzoate

PROPAGATION

MMA

TERMINATION

Methanol

Scheme 1.7 Deprotection and formation of methacryloyloxy functionalized PMMA macromonomer.

$$H\left(\begin{matrix}CH_3 \\ | \\ C \\ | \\ C=O \\ | \\ OMe\end{matrix}-CH_2\right)_n\begin{matrix}CH_3 \\ | \\ C \\ | \\ CH_3\end{matrix}\begin{matrix}O \\ || \\ C\end{matrix}-O-CH_2CH_2-O-SiMe_3$$

HCl

$$H\left(\begin{matrix}CH_3 \\ | \\ C \\ | \\ C=O \\ | \\ OMe\end{matrix}-CH_2\right)_n\begin{matrix}CH_3 \\ | \\ C \\ | \\ CH_3\end{matrix}\begin{matrix}O \\ || \\ C\end{matrix}-O-CH_2CH_2-OH$$

**Methacryloyl Chloride
Triethylamine**

$$H\left(\begin{matrix}CH_3 \\ | \\ C \\ | \\ C=O \\ | \\ OMe\end{matrix}-CH_2\right)_n\begin{matrix}CH_3 \\ | \\ C \\ | \\ CH_3\end{matrix}\begin{matrix}O \\ || \\ C\end{matrix}-O-CH_2CH_2-O-\begin{matrix}C=O \\ | \\ C-CH_3 \\ || \\ H_2C\end{matrix}$$

functionalized PMMA after hydrolysis of the trimethylsilylprotecting group, shown in Scheme 1.7. Since it has been demonstrated that GTP is a living polymerization, polymers of controlled molar mass having a narrow molar mass distribution can easiiy be synthesized, as shown in Figure 1.1. The number average molar mass obtained by VPO was 7020 g/mol and shows very good correlation with the value of 6300 g/mol obtained by GPC. A molar mass distribution of 1.11 was calculated from the GPC trace using linear PMMA GPC standards. The resulting PMMA oligomers were reacted with methacryloyl chloride after hydrolysis to afford a methacryloyloxy functionalized PMMA macromonomer as outlined in Scheme 1.7.

The methacryloyloxy functionalized PMMA macromonomer was then statistically copolymerized with MMA, with various feed ratios, using anionic copolymerization methods to afford the grafted homopolymers, Scheme 1.8. The anionic copolymerization of the PMMA macromonomer with MMA is an approach for obtaining a near monodisperse graft polymer. The polymerizations were carried out in dilute solutions in order to maintain the desired low temperatures during the polymerization exotherm. The addition of aliquots of the DPHL initiator solution allowed for the titration of any protonic impurities that were present. When all of the

GPC OF HYDROXYL FUNCTIONALIZED PMMA

<Mn> = 6300 g/mol

MWD = 1.11

32 33 34 35 36 37 38

Figure 1.11 GPC trace of PMMA macromonomer.

Scheme 1.8   Synthesis of PMMA-g-PMMA.

CH₃ │ H₂C=C │ C=O │ O——PMMA

+

CH₃ │ H₂C=C │ C=O │ OMe

DPHL

THF

-78 C

PMMA BRANCHED HOMOPOLYMER

impurities have reacted with DPHL, the polymerization proceded with the accompanying exotherm. At these temperatures and concentrations, exotherms lasting as long as three minutes were observed. The polymerization exotherm was important to monitor since further addition of the DPHL initiator would have resulted in materials with bimodal molar mass distributions.

The achievement and maintenance of -78 °C in the reaction flasks where one is anionically polymerizing MMA should never be assumed. It requires that the flask is almost entirely submerged in the dry ice/isopropanol (IPA) bath and that one uses dry ice powder which results in a viscous IPA slurry. In addition, when all of the monomer is charged prior to initiation (or when the monomer is added too quickly to a DPHL solution) one can easily rise above -65 °C, the upper temperature limit previously reported[72] for avoiding deleterious side reactions, due to the polymerization exotherm. Therefore, it is necessary to work with dilute solutions in order to efficiently dissipate the heat evolved (or one should add the monomer slower when making linear poly(alkyl methacrylate)s).

One can easily estimate the impurity level inherent in the reactions when macromonomers are used, which can not be easily purified to high levels like conventional small

monomers can be by distillation, by sacrificing one of the reactions and adding smaller increments of the initiator. Once it is determined exactly how much initiator it took for the polymerization exotherm to be noticed, one can simply add this amount of initiator to the calculated amount of the initiator to achieve the desired molar mass polymer. This procedure is not unlike to the procedure used for the low-pressure polymerization reactors developed by Dr. James Hoover[73] and, as will be shown later, the PMMA-g-PMMA polymers were all of high molar mass, centered at 250,000 g/mol, and within 15% of one another.

Gel permeation chromatograms for the reaction products of a series of graft polymers are shown in Figure 1.12. The chromatograms are of the crude reaction products of three copolymerizations that had various amounts of the same molar mass PMMA macromonomer charged to them, which varied the initial feed ratios of the copolymerization. The raw chromatograms were obtained using a UV detector at 218 nm. It is clear that some of the macromonomer was not incorporated, as evidenced by the small peaks that come at 34 mL elution volume corresponding to the elution volume of the starting macromonomer. The apparent molar masses and apparent molar mass distributions, that is relative to linear PMMA GPC standards, of the major peak in the chromatograms, shows the materials to be of high molar mass

GPCs OF PMMA-g-PMMA (UNFRACTIONATED)

Figure 1.12 GPC traces of crude reaction product.

and relatively narrow molar mass distributions. In order to obtain the number average molar mass of the high molecular weight branched polymer by membrane osmometry and the weight average molar mass by light scattering, it was necessary to fractionate the low molar mass unincorporated oligomer from the high molar mass component. This was accomplished by dissolving the crude product in THF and slowly adding a nonsolvent, hexane, to the solution and selectively precipitating the high molar mass material. Figure 1.13 shows the chromatogram for one sample before and after the fractionation procedure. As one can see, the method was successful in removing the unincorporated macromonomer, as evidenced by the flat baseline at 48 mL elution volume for the fractionated material. Even more importantly, one can see that the chromatograms are virtually superimposable in the high molar mass region, indicating that the fractionation procedure did not effect the molar mass distribution of the branched polymer to any large extent.

Calculation of the Number of Grafts per Backbone. In order to calculate the number of grafts per macromolecule or backbone, a variety of information was needed. A sample calculation is given in Figure 1.14. This included the results from the GPC of the crude reaction product, the VPO data of the PMMA macromonomer, the MO data on the

CONCENTRATION CHROMATOGRAMS

Figure 1.13 GPC traces of fractionated and unfractionated PMMA-g-PMMA.

Assume that the amount of polymer precipitated from the copolymerization was 10 g, but, we charged 8 g monomer and 4 g of macromonomer, this leaves an 83% yield,

10 g product / (8 g MMA + 4 g macromonomer) = 0.83

Now, assuming that we get all of our macromonomer back, either free or incorporated, then 4 g of the 10 g yield is attributed to the macromonomer; however, from GPC we know that 5 wt% of the yield is actually free macromonomer,

0.05 x 10g = 0.5g free macromonomer

So that the amount of macromonomer that was incorporated was

(4 g charged macromer) - (0.5 g free macromer) = 3.5 g ,

which leaves

3.5 g / (10 g - 0.5 g) x 100 = 37 wt%

This means that 37 wt% of the graft polymer is made up of grafts. If the <Mn> of the graft polymer is 100,000 g/mol by membrane osmometry, then

0.37 x 100,000 g/mol = 37,000 g/mol

is attributed to the graft part of the copolymer. By VPO, we know that the <Mn> of the macromonomer was 7,000 g/mol, then

7,000 g/mol / 37,000 g/mol = 5.3 grafts/backbone.

Figure 1.14 Sample calculations for the number of grafts per backbone.

fractionated PMMA-g-PMMA series of polymers, as well as the knowledge of the overall synthetic yield of the copolymerization and the known feed ratio data. The only assumption made in this calculation was that the macromonomer charged during the synthesis was fully recovered in the product as either a graft on the branched PMMA or as a free, unincorporated species whose peak on the chromatogram was fully resolved from the peak of the high molar mass branched PMMA. The absolute molar mass and the cummulative mass distribution of the unextracted form of the copolymers obtained from the GPC experiments were used to calculate the percentage of unincorporated macromonomer present in the final synthetic yield of graft PMMA. Based on this information, the weight of unincorporated macromonomer was determined. This allowed for the determination of the weight fraction of the branched PMMA that was comprised of grafts. The final step involved taking the percentage of the <Mn> of the graft copolymer (obtained from MO on the fractionated branched PMMA) attributed to the graft parts and dividing by the <Mn> of the macromonomer (obtained from VPO on the neat PMMA macromonomer) to determine the average number of grafts per backbone.

The results, the average of three runs, are presented in Table 1.2, for the series of three PMMA-g-PMMA's with

Table 1.2 Molar mass and molar mass distribution data
for PMMA-g-PMMA.

Sample	<Mn> of Graft Polymer (kg/mol) [a]	<Mw> of Graft Polymer (kg/mol) [b]	Molar Mass Distribution (<Mw>/<Mn>)	Number of Grafts
A	281	295	1.05	2.2
B	215	233	1.08	7.4
C	249	266	1.07	14.1

[a] Determined by membrane osmometry

[b] Determined by light scattering

different levels of branching. As one can see, all of the branched PMMA's have their number average molar masses centered around 250000 g/mol (± 13%), indicating good control of the molar mass during the synthesis, given that the target molar mass was 200000 g/mol. The weight average molar masses are also listed along with their molar mass distributions. As one can see, the resultant graft homopolymers all have very narrow distributions and therefore lend themselves very nicely as model branched polymers for structure/property relationship investigations. The levels of branching, at essentially constant molar mass, ranged from 2 grafts per backbone to 14 grafts per backbone which works out to be 5 wt% up to 40 wt% of long chain branching.

Details of the dilute solution properties of these well-defined PMMA-g-PMMA copolymers can be found in a series of preprints[74,75] and in a forth-coming manuscript.[76]

POLY(METHYL METHACRYLATE)-G-POLY(DIMETHYLSILOXANE)S

Living polymerization methods allow the synthesis of polymers of controlled molar mass having a narrow molar mass distribution. Of particular interest to this study was poly(dimethylsiloxane) (PDMS) macromonomers synthesized through the anionic organolithium initiated ring-opening

polymerization of hexamethylcyclotrisiloxane or D_3. This investigation involved the functional termination of the living polymerization with a chlorosilane derivative of allyl methacrylate to afford methacryloyloxy functionalized PDMS macromonomers having molar masses ranging from 1000 g/mol to 20000 g/mol. These macromonomers were subsequently copolymerized with MMA to afford the title graft copolymers.

The desirable properties of PDMS include a very low glass transition temperature, biocompatibility, low surface energy, oxygen permeability, and resistance towards degradation by atomic oxygen and oxygen plasmas. A heterophase material therefore, consisting of microphase separated PDMS domains embedded in a PMMA matrix, such as the graft copolymers synthesized in this paper, should illustrate the desirable properties of both components.

Poly(dimethylsiloxane) Synthesis. The poly(dimethyl-siloxane) macromonomers were synthesized using the living ring-opening polymerization of D_3 as described in the Experimental Section. The polymerization was initiated by the addition of sec-butyllithium to a pure cyclohexane solution of D_3. This results in the initiation of the ring-opening polymerization without any further propagation reactions taking place. In a nonpolar medium, such as

cyclohexane, the living siloxanolate exists as a very tight ion-pair with the lithium counterion and that these ion-pairs exist as aggregates of three, or more likely, four ion-pairs.[77] Upon the addition of the polar solvent, THF, the polarity of the solution changes, which loosens the ion-pair and probably breaks up the ion-pair aggragates to some extent, allowing propagation to occur to afford high polymer of controlled molecular weight in a living manner as shown in Scheme 1.9[78,79,80,81,82,83]

To control the molar mass, it is necessary that the initiation reaction takes place instantaneously and faster than the propagation reactions. This criterion is artificially enforced under the experimental conditions illustrated above. It has been shown, in an excellent paper by Frye and coworkers[84] in 1970, that upon the addition of alkyllithiums, specifically n-butyllithium and t-butyllithium, to D3, rapid ring-opening reactions occur to yield lithium siloxanolates. These species are in turn completely consumed by additional alkyllithiums in an even faster series of alkylation reactions to yield the simple triorganosiloxanolate. These subsequent alkylation reactions of the alkyllithiums on the lithium siloxanolates are so much faster than the reactions of the alkylithiums on cyclic neutral species that there is no evidence of any lithium siloxanolates with more than one repeat unit of

Scheme 1.9 Synthesis of living siloxanolate.

$$CH_3-CH_2-\overset{\overset{\displaystyle CH_3}{|}}{CH}-Li$$

+

$$CH_3-CH_2-\overset{\overset{\displaystyle CH_3}{|}}{\underset{\underset{\displaystyle CH_3}{|}}{CH}}\!-\!\!\left(\!\overset{\overset{\displaystyle CH_3}{|}}{\underset{\underset{\displaystyle CH_3}{|}}{Si}}\!-\!O\!\right)_{\!\!X}\!\!\overset{\overset{\displaystyle CH_3}{|}}{\underset{\underset{\displaystyle CH_3}{|}}{Si}}\!-\!O \quad \ominus \quad \oplus \atop Li$$

≡ **D₃**

CYCLOHEXANE

2 HOURS

ROOM TEMP

(X = 2,1, or 0)

m D₃

THF (10% BY VOLUME)

24 HOURS

$$CH_3-CH_2-\overset{\overset{\displaystyle CH_3}{|}}{\underset{\underset{\displaystyle CH_3}{|}}{CH}}\!-\!\!\left(\!\overset{\overset{\displaystyle CH_3}{|}}{\underset{\underset{\displaystyle CH_3}{|}}{Si}}\!-\!O\!\right)_{\!\!3m}\!\!\overset{\overset{\displaystyle CH_3}{|}}{\underset{\underset{\displaystyle CH_3}{|}}{Si}}\!-\!O \quad \ominus \quad \oplus \atop Li$$

siloxane, in hydrocarbon solvents. This enhanced preference is presumably attributed to the nature of the association of the ion-pairs which gives rise to a locally higher concentration of lithium siloxanolates and organolithiums relative to organolithiums and the cyclic trimer. When ether is added to the hydrocarbon solution of these reactants, alkyllithiums were shown to be more reactive than the lithium siloxanolates towards D_3.

The living polymerization was terminated after 48 h according to Scheme 1.10. We have shown, by silicon-29 NMR[85], GPC, and end group analysis by FTIR[2], that even towards the end of the polymerization reaction, under the times and conditions used here, no cyclic formation and no broadening of the molar mass distribution had occured by 48 h. This allows for excellent control of the molar mass and functionality of PDMS oligomers and polymers. The terminating agent used for methacrloyloxy functionalized PDMS oligomers was 3-methacryloyloxypropyldimethylchloro-silane. This reagent is an adduct prepared from the hydrosilylation[86] of allyl methacrylate with dimethyl-chlorosilane using chloroplatinic acid as depicted in Scheme 1.11. The terminating agent was added directly to the polymerization reactions using airless techniques. Shortly after the addition, one could observe the formation

Scheme 1.10 Functional termination of living siloxanolate.

$$CH_3-CH_2-CH-\left(Si-O\right)_{3m}Si-O^{\ominus} \quad Li^{\oplus}$$

(with CH₃ substituents on the silicon atoms as drawn)

"LIVING SILOXANOLATE"

$$Cl-Si-\left(CH_2\right)_3-O-C-C=CH_2$$

(chlorodimethylsilyl propyl methacrylate structure with CH₃ groups on Si, C=O, and CH₃ on the vinyl carbon)

(reaction arrow pointing downward)

Final product structure:

$$H_2C=C(CH_3)-C(=O)-O-(CH_2)_3-Si(CH_3)_2-O-Si(CH_3)_2\cdots$$

$$R-\left(Si(CH_3)_2-O\right)_{3m}Si$$

Scheme 1.11   Synthesis of 3-methacryloyloxydimethyl-chlorosilane.

and precipitation of lithium chloride, indicating successful termination. The precipitation of lithium chloride is also a driving force towards the formation of highly functionalized PDMS macromonomers. After the described work-up, the methacryloyloxy functionalized PDMS macro-monomers were characterized by a variety of techniques which include GPC (using the UV detector in an isorefractive solvent and with the refractive index detector in a nonisorefractive solvent), VPO, UV spectroscopy, and NMR.

The target molar masses for the PDMS macromonomers used in the CCD investigations ranged from 5k g/mol to 20k g/mol. The number average molar masses and molar mass distributions were determined by GPC in toluene using the refractive index detector and PDMS GPC standards. The number average molar mass was also determined by performing an endgroup analysis using UV spectroscopy and by vapor phase osmometry as described in the Experimental Section - Part 1. As one can see in Table 1.3, a good correlation exists between the values determined by GPC, VPO, and UV spectroscopy and the target values are listed in the first column. A typical GPC trace for the methacryloyloxy functionalized PDMS macromonomers is shown in Figure 1.15.

Table 1.3 Number average molar masses and molar mass distributions of methacryloyloxy functionalized PMMA macromonomers.

Target Molar Mass (kg/mol)	GPC <Mn> (kg/mol)	Molar Mass Distribution	Vapor Phase Osmometry (kg/mol)	UV (kg/mol
5.0	7.5	1.15	5.6	4.7
10.0	10.5	1.15	9.8	8.8
20.0	22.8	1.07	----	----

GPC OF POLY(DIMETHYLSILOXANE)

MACROMONOMER

(MW = 20K, MWD = 1.07)

30   31   32   34   35

ELUTION VOLUME (mL)

Figure 1.15 GPC of methacryloyloxy functionalized PDMS.

The methacryloyloxy functionalized PDMS macromonomers described above were then used as a comonomer with MMA using two different copolymerization techniques, namely free radical and anionic methods. The copolymerizations yielding the PMMA-g-PDMS copolymers will be discussed next along with their molecular characterization and CCD evaluation.

Free Radical Copolymerization. PMMA-g-PDMS copolymers were prepared using a free radical copolymerization mechanism according to Scheme 1.12. Toluene was found to be a good solvent and did not show problems of significant chain transfer with methyl methacrylate. The homogeneous solution polymerizations were run at 20 w/v%. This concentration was determined adequate to obtain high molar mass (>100 kg/mol) polymers while still maintaining a homogeneous copolymerization. The parameters involved in determining if heterogeneity would occur include the molar mass of the macromonomer, the volume fractions of macromonomer and monomer, the specific system (X_{12} parameter), temperature, and the solvent. Phase separation could be most easily induced with the higher molar mass PDMS macromonomers.

The resultant graft copolymers always contained a certain amount of unincorporated PDMS macromonomer after precipitation in methanol. The free PDMS oligomer was conveniently removed by thorough extraction of the reaction product with either hexanes or isopropanol in a soxhlet extractor. Figure 1.16 shows two GPC traces of the PMMA-g-PDMS copolymers prepared using the free radical copolymerization mechanism. The trace on the left is the crude reaction product. The trace on the right is the graft copolymer after extraction showing the material being free

Scheme 1.12 Free radical copolymerization of MMA with methacryloyloxy functional PDMS macromonomer.

AIBN (0.1 WT% BASED ON MMA)

TOLUENE

64 °C

ca. 20 W/V% SOLUTION

Figure 1.16 GPC trace of PMMA-g-PDMS before and after
extraction of PDMS macromonomer.

of unincorporated PDMS oligomer. The UV detector was used to obtain these traces and therefore the signal from the free PDMS is due to the absorbance from the methacryloyloxy functional group.

One of the main interests in these materials was for their use in elucidating the chemical composition distribution of graft copolymers prepared by the macromonomer method. We first needed to establish that there was not a drift in the feed ratio as a function of conversion. This would lead to a broadening of the CCD due to conversional heterogeneities as described in the Results and Discussion Section - Part 1. It was therefore important to check if there was a significant drift in the chemical compostion of the graft copolymers as a function of conversion. The graph in Figure 1.17 shows the wt% PDMS incorporated in a copolymerization of MMA and a PDMS macromonomer with a molar mass of 5000 g/mol. As one can see, within experimental error, the composition remains constant as a function of conversion. This result allows us to attribute any broadening of the CCD to statistical heterogeneity. The contribution to the CCD of this system from conversional heterogeneity is therefore negligible. The chemical composition distribution (CCD) was even

COPOLYMER COMPOSITION VS CONVERSION

Figure 1.17 Chemical composition as a function of conversion.

measured for this system as a function of conversion and the results will be presented in the section dealing with CCD.

Anionic Copolymerization. The anionic copolymerization of the methacryloyloxy functionalized PDMS macromonomer with MMA is an approach for obtaining a monodisperse graft copolymer with a Poisson distribution of degrees of polymerization for the backbone component along with the graft component. The methacryloyloxy functionalized PDMS macromonomer was then statistically copolymerized with MMA, with various feed ratios, using anionic copolymerization methods to afford the graft copolymers, Scheme 1.13. The polymerizations were carried out in dilute solutions in order to maintain the desired low temperatures during the polymerization exotherm. The addition of aliquots of the DPHL initiator solution allowed for the titration of any protonic impurities that were present. When all of the impurities have reacted with DPHL, the polymerization would proceed with the accompanying exotherm. At these temperatures and concentrations, exotherms lasting as long as three minutes were observed. The polymerization exotherm was important to monitor since further addition of the DPHL initiator would have resulted in materials with bimodal molar mass distributions.

Scheme 1.13   Anionic copolymerization of methacryl-oyloxy functionalized PDMS macromonomer with MMA.

As was illustrated in Table 1.1 in the Literature Review Section - Part 1 dealing with the parameters that affect the ability of a macromonomer to copolymerize with small monomers, the most important item listed dealt with the nature of substitution on the unsaturated end group. This constraint is very mechanistic dependent. In other words, for the free radical copolymerization method to synthesize PMMA-g-PDMS, one could have used a styrenic functional PDMS macromonomer to copolymerize with MMA because free radically, styrene copolymerizes very well with MMA. In fact, styrene will copolymerize better with MMA than MMA polymerizes with itself. However, for anionic statistical copolymerizations of small monomers with macromonomers, such as the case we have here, it is necessary that when a lithium enolate forms from the anionic polymerization of MMA, that it can cross over to form an equally reactive chain end with the PDMS macromonomer, and visa versa. We could not have therefore statistically copolymerized a styrenic functionalized macromonomer with MMA.

The achievement and maintenance of -78 °C in the reaction flasks where one is anionically polymerizing MMA should never be assumed and the precautions listed in the Results and Discussion Section dealing with PMMA-g-PMMA synthesis should be consulted. If one maintains the desired

low temperatures, it is possible to synthesize graft copoymers with apparently narrow molar mass distributions, as shown in Figure 1.18, for an anionically copolymerized graft copolymer after extraction to remove free PDMS macromonomer.

Table 4 shows some typical data for the incorporation of the PDMS macromonomers into the copolymers using anionic copolymerization methods. The series presented all used the same molar mass PDMS macromonomer, namely 10 kg/mol, with initial feed ratios ranging from 10 wt% to 40 wt%. The results show that typically 50% of the PDMS macromonomer charged was incorporated. It must be noted, however, that these reactions were short stopped at ca. 85% conversion which corresponded to 3-5 min after the polymerization exotherm began. This was done to prevent blocks of grafts forming, which could theoretically form for a living polymerization that is becoming higher in PDMS concentration as a function of conversion.

Molecular Characterization. For a chemically heterogeneous copolymer, light scattering methods yield an apparent molar mass, M_{ap}, instead of the true weight average molar mass, M_w. The relationship between these two quantities was defined in the Literature Review Section and

GPC OF PMMA-G-PDMS

PREPARED ANIONICALLY

(GRAFT MW = 20K, PDMS = 16 wt%)

Figure 1.18   GPC trace for PMMA-g-PDMS prepared by anionic copolymerization methods.

Table 1.4 Summary of pdms macromonomer incorporation into PMMA-g-PDMS prepared using anionic copolymerization.

Sample	PDMS \<Mn>	wt% PDMS Charged	wt% PDMS Incorp.	Apparent \<Mn>	Apparent MWD
A	10k	10%	5%	113k	1.18
B	10k	20%	9%	158k	1.24
C	10k	30%	12%	180k	1.29
D	10k	40%	21%	114k	1.16

was shown to be:

$$M_{ap} = M_w + 2PR + QR^2 \qquad (6),$$

where R was defined as the difference of the refractive index increments for each components homopolymer divided by the refractive index increment for the copolymer. Equation 6 represents a parabolic function of the variable R, the value of which is mainly dependent upon the refractive index of the solvent. By determining the apparent molar mass, M_{ap}, in the seven solvents with different refractive indices (ranging from 1.37 to 1.53), all three parameters in equation 6, M_w, P, and Q, can be evaluated. The results, plotted as the parabolic function, are shown in Figure 1.19. In addition, when one performs the light scattering experiment in a solvent that has the same refractive index as PDMS, such as THF, only the PMMA component will result in the scattering of light. This allows the determination of the weight average molar mass of the backbone after the polymer is already prepared according to:

$$M_{w, PMMA} = \langle x \rangle \, M_{ap} \qquad , \qquad (7)$$

Alternatively, when the light scattering experiment was conducted in a solvent that was isorefractive with PMMA, such as toluene, the scattering was only due to the PDMS component. This allowed the evaluation of the weight average molar mass of the PDMS grafts while they are already

Figure 1.19 Determination of the weight average molar mass of the PMMA-g-PDMS copolymer by the parabolic fit of equation 7.

copolymerized according to the equation:

$$M_{w,PDMS} = (1 - <x>)M_{ap}, \qquad (8)$$

The molar mass distributions for the copolymer, the PMMA backbone, and the PDMS grafts could be calculated by combining the isorefractive light scattering data with the number average molar masses determined from membrane osmometry and the composition determination by NMR. The results are listed in Table 1.5, and as one can see, the PMMA-g-PDMS copolymers prepared using the living anionic copolymerization method have very narrow overall molar mass distributions. In addition, the molar mass distributions for the graft and backbone parts are very narrow, in accordance with the fact that living polymerization processes were used to synthesize both of these components. The molar mass distribution values for the PDMS grafts were 1.02 and 1.09, which correspond very well with the 1.07 value obtained on the neat PDMS oligomer before polymerization using GPC with PDMS GPC standards. A third point to note is that the results allow the determination of the average number of grafts per molecule, where the values range from ca. 2 grafts/molecule to ca. 7 grafts/molecule.

Chemical Composition Distribution. The chemical composition distribution (CCD) was determined for the PMMA-

Table 1.5 Molecular characteristics of anionically prepared PMMA-g-PDMS copolymers and of their individual parts.

	MW GRAFT = 20K WT% PDMS = 17	MW GRAFT = 20K WT% PDMS = 34
[1] <Mw> COPOLYMER	227 ± 14	414 ± 38
[2] <Mw> PMMA BACKBONE	200	288
[2] <Mw> PDMS GRAFT	34.2	154
[3] <Mn> COPOLYMER	203	406
[4] <Mn> PMMA BACKBONE	69.5	273
[4] <Mn> PDMS GRAFT	33.5	141
<Mw>/<Mn> COPOLYMER	1.11	1.02
<Mw>/<Mn> PMMA BACKBONE	1.18	1.05
<Mw>/<Mn> PDMS GRAFT	1.02	1.09
AVG. NUMBER OF GRAFTS PER BACKBONE	1.7	7.1
[1] CHEMICAL COMPOSITION (WT. FRACTION PMMA)	0.83	0.66

[1] DETERMINED BY LIGHT SCATTERING IN SEVERAL SOLVENTS
[2] DETERMINED BY ISOREFRACTIVE LIGHT SCATTERING
[3] DETERMINED BY MEMBRANE OSMOMETRY
[4] DETERMINED FROM <Mn> OF COPOLYMER AND COMPOSITION DATA

g-PDMS copolymers prepared by both the free radical and anionic copolymerization mechanism. The methods used to evaluate the CCD were SCFE fractionation and fractionation in demixing solvents. Each method was employed to obtain small fractions of the overall copolymer. These small fractions were then analyzed to determine their chemical composition by either ^{1}H NMR (for the SCFE fractionated materials) or by refractive index (for the materials fractionated in demixing solvents). The results were then plotted as cumulative weight fraction versus composition in order to evaluate the CCD.

In 1987, our coworkers[87] in Czechoslovakia outlined a theory of chemical composition distributions for graft copolymers prepared by the macromonomer technique, where the resulting copolymer had a Zimm-Schultz distribution of degrees of polymerization. Their predictions show that the distribution of chemical composition is a function of both the molar mass of the macromonomer and the number of grafts per backbone. As the number of grafts is increased at a constant weight percent macromonomer, which is achieved by lowering the molar mass of the starting macromonomer, the breadth of the CCD narrows, assuming that the incorporation of the macromonomer into the graft copolymer is random. This is demonstrated in Figure 1.20. The curves were all generated based on their theory for a graft copolymer formed

PW

$$20\,(1K) \rightarrow$$
$$2\,(10K) \rightarrow$$
$$1\,(20\,K) \rightarrow$$

COMPOSITION (WT% PMMA)

MW = 100,000 g/mol, 20 wt% PDMS, 80 wt% PMMA

IF MACROMER MW = 1,000 g/mol

$$\frac{20,000}{1,000} = 20 \quad \text{GRAFTS / BACKBONE}$$

IF MACROMER MW = 10,000 g/mol

$$\frac{20,000}{10,000} = 2 \quad \text{GRAFTS / BACKBONE}$$

IF MACROMER MW = 20,000 g/mol

$$\frac{20,000}{20,000} = 1 \quad \text{GRAFT / BACKBONE}$$

Figure 1.20 Theoretical CCD profiles for PMMA-g-PDMS copolymers with various graft molar masses at constant composition.

using monodisperse macromonomers with molar masses of 1k g/mol, 10k g/mol, and 20k g/mol and incorporating 20 wt% macromonomer at a constant degree of polymerization. Their results show that as you have more and more shorter grafts the CCD begins to sharpen relative to fewer longer grafts. In order to verify their theory, a series of graft copolymers were synthesized using free radical copolymerization methods. Under the conditions employed for the free radically copolymerized graft copolymers, the reactions typically yield materials of constant degree of polymerization, as shown in Table 1.6 for a similar series of copolymers. These materials all had the same molar mass PDMS macromonomer, 10k g/mol, but had varying amounts of siloxane incorporated. The isorefractive light scattering method was utilized to obtain the weight average molar mass of the PMMA backbone for the series, which centered around 225k g/mol. In addition, the apparent weight average molar mass, which is related to a combination of both the graft and backbone molar masses, increaseses at essentially constant degree of polymerization due to the effect of incorporating the high molar mass macromonomers. Similar copolymers were subsequently fractionated using SCFE methods and the compositions were determined by NMR. The results, plotted as the cumulative weight fraction versus weight fraction PMMA, are shown in Figure 1.21. The results show

Table 1.6 Molecular characterization of PMMA-g-PDMS copolymers prepared by free radical copolymerization.

Sample	Composition (% PDMS)	Mw,app (kg/mol)	Mw,backbone (kg/mol)
JMD-095-A	5%	229	218
JMD-095-B	14%	275	237
JMD-095-C	26%	297	220

PMMA-G-PDMS: 45, 28, 13 WT% PDMS

Figure 1.21 Experimentally determined CCD profiles for PMMA-g-PDMS copolymers with various graft molar masses at constant composition.

that as the number of grafts per molecule increases, i.e. as the wt% PDMS increases, the breadth of the CCD decreases. These experimentally evaluated CCDs correlate very well with those predicted by theory.

The CCD was also evaluated as a function of conversion during a free radical copolymerization of the methacryloyloxy functionalized PDMS macromonomer with MMA. This was done in order to verify that the observed CCD was a result of statistical heterogeneity and not conversional heterogeneity, as discussed in the Literature Review Section - Part 1. The sample chosen for this study was a free radical copolymerization of a 10k g/mol PDMS macromonomer with MMA. The initial feed ratio was approximately 32 wt% PDMS to 68 wt% MMA for a total of 20 wt% solids in toluene at 65 °C with 0.1 wt% AIBN. Large aliquots were withdrawn as a function of conversion and the product was precipitated and throughly extracted to remove unincorporated PDMS macromonomer. The graft copolymer was then fractionated with SCFE methods and the data was treated as described above. The results, Figure 1.22, show the observed CCD at 16 wt%, 60 wt%, and 100 wt% conversion. The CCDs are fairly constant as a function of conversion which illustrates that

CCD as a Function of Conversion

Figure 1.22 CCD as a function of conversion for a free radical copolymerization of methacryloyloxy functionalized PDMS macromonomer with MMA.

the observed CCD is primarily the result of statistical heterogeneity and not due to conversional heterogeneity.

Another one of our goals was to compare and contrast the experimentally determined CCD of the PMMA-g-PDMS copolymers prepared by both the free radical and the anionic copolymerization methods. Two PMMA-g-PDMS copolymers of comparable architecture, composition, and molar mass were synthesized. One utilized the free radical copolymerization process and the other utilized the anionic copolymerization process. Both of the copolymer samples were fractionated using the SCFE procedure. The results, again plotted as the cumulative weight fraction versus PMMA composition, are shown in Figure 1.23. As one can clearly see, the CCD for the anionically copolymerized graft copolymers was substantially more narrow than the CCD for the corresponding material copolymerized free radically. This observation is in agreement with the principles of living polymerizations.

The application of the SCFE fractionation technique for determining the CCD of a copolymer is a novel approach of polymer fractionation for this purpose. Most classical fractionation methods are laborious and time consuming, but the use of SCFE methods has afforded the routine

Figure 1.23 Experimentally determined CCD profiles for copolymers copolymerized free radically (top) and anionically (bottom).

fractionation of many of our materials. The ease and versatility of this technique has allowed the use of this method of fractionation as a tool to evaluate and follow the synthesis of many copolymers. The availability of this new method for routine polymer fractionation should encourage more research on fractionated polymers.

The elucidation of the distribution of composition in copolymers can be complex. The reason for this is that most fractionation methods are based on the solubility of the material and therefore the influence of the molar mass on the fractionation is not always clearly understood. We have set out to investigate the efficacy of two entirely different fractionation techniques in regards to their abilities to elucidate the CCD of our graft copolymers.

Two large batches of PMMA-g-PDMS copolymers were synthesized using the anionic copolymerization of a 20k g/mol PDMS macromonomer with various amounts of MMA. A portion of this material was fractionated using SCFE techniques and another portion was fractionated using the technique of demixing solvents, TCE and DMSO. The molecular characteristics of the graft copolymers can be found in Table 1.5.

The results of the different fractionation methods are shown in Figures 1.24 and 1.25 as a plot of the cumulative

PMMA-G-PDMS: 34 WT% PDMS, 20K GRAFTS

PMMA-G-PDMS: 34 WT% PDMS, 20K GRAFTS

Figure 1.24 CCD profiles for PMMA-g-PDMS copolymers of high PDMS content prepared anionically and fractionated by SCFE (top) and solvent demixing.

PMMA-G-PDMS: 17 WT% PDMS, 20K GRAFTS

PMMA-G-PDMS: 17 WT% PDMS, 20K GRAFTS

Figure 1.25 CCD profiles for PMMA-g-PDMS copolymers of low PDMS content prepared anionically and fractionated by SCFE (top) and solvent demixing.

weight fraction versus composition. As one can see, both techniques give comparable results; that is, the CCD for the PMMA-g-PDMS copolymers prepared by the anionic copolymerization method are relatively narrow regardless of the method used to fractionate the copolymers. The fact that the results parallel one another demonstrates the efficiency of both techniques. It must be noted that the method of fractionation based on the demixing solvents was capable of observing an unpronounced shoulder extending to the low PMMA region of the CCD shown in Figures 1.24 and 1.25. It is anticipated that if the initial fractions were smaller in size, that the SCFE method would also give similar results to those obtained by demixing solvents. Figure 1.25 demonstrates that even at low graft content the CCD is relatively narrow. This is significant, since the materials that would have the broadest CCD would be those materials that have the fewest grafts, as depicted in Figure 1.20.

POLY(OLEFIN SULFONE)S

Introduction

Our interest in poly(olefin sulfone)s grew out of our collaborations with Dr. Murrae Bowden at Bell Communications Research and his extreme interest in the fabrication of microelectronic devices. It had been well established that poly(olefin sulfone)s have excellent sensitivity towards e-beam irradiation in which the macromolecules undergo random chain scission as depicted in Scheme 1.14. However, poly(olefin sulfone)s also possess very high etch rates under plasma or reactive ion etch conditions. This is an undesirable feature in view of the industry trend toward dry post development processing.

Our approach has been to incorporate silicon into the poly(olefin sulfone)s. It was believed that the silicon would impart a greater resistance toward RIE processes while still maintaining the excellent sensitivity characteristics of the poly(olefin sulfone)s. In addition, we wanted to avoid the already established problems of silicon-containing resists, namely reduced sensitivity, which results from the high silicon content required for effective etch resistance, a lowering of the glass transition temperature, and extreme solubilities. To address these problems, we decided to use silicon in the form of grafted poly(dimethylsiloxane). The incorporation of PDMS, as opposed to molecularly dispersed

Scheme 1.14 Degradation process of poly(1-butene sulfone) with electron beam irradiation.

-SiR$_3$ moieties, would allow the formation of heterophase materials with enhanced surface domination due to the low PDMS surface free energy. Also, the multiphase materials will have very different solubility characteristics with respect to single phase materials, thus allowing a wider window of development conditions. Our initial efforts involved attempting to synthesize poly(olefin sulfone)s that contained functional groups that could be further utilized to graft on a properly functionalized PDMS oligomer. To this end, the details will be presented for the synthesis of several new poly(olefin sulfone)s based on the inexpensive diene, 5-ethylidene-2-norbornene. Another approach simultaneously pursued involved the use of an appropriately functionalized PDMS macromonomer to use as a comonomer during the polymerization to form the heterophase poly(olefin sulfone). This approach worked very well and therefore developed into the major focus of this effort.

Poly(5-ethylidene-2-norbornene sulfone)s

The apparently unprecedented synthesis of soluble poly(5-ethylidene-2-norbornene sulfone) (PENS) is interesting from many points of view. The alternating copolymerization of the bicyclodiene, which was purchased as a mixture of the endo and exo isomers, appears to have proceeded almost entirely through the cyclic olefin as

depicted in Scheme 1.15. The percentage of unreacted ethylidene groups was detected and quantified by ^{1}H NMR as shown in Figure 1.26. This mode of polymerization leaves a large percentage of ethylidene groups intact (5.3 ppm and 5.6 ppm) and potentially available for post reactions such as crosslinking and hydrosilylations, just to mention a few. The ratio of sulfur dioxide to olefin monomer was determined by elemental analysis for all of the poly(olefin sulfone)s that were synthesized. It can be seen in Table 1.7, there is good agreement between the experimentally observed values and the theoretically calculated values for other poly(olefin sulfone)s made under similar conditions, namely poly(norbornene sulfone) (PNS) and poly(1-hexene sulfone) (PHS). There is a discrepency, however, in the ratio of cyclic monomer to sulfur dioxide for PENS. A typical GPC trace for PENS is shown in Figure 1.27, which demonstrates some tailing of the molecular weight distribution towards the lower molecular weight region. All three of these observations, the less than 1:1 ratio of ethylidene groups to monomer, the slightly higher 1:1 ratio of sulfur dioxide to diene monomer, and the tailing of the molar mass distribution towards the lower molar mass region, suggest a certain amount of branching taking place through the ethylidene moiety. It was anticipated that the degree of branching was a function of temperature due to the

Scheme 1.15 Synthesis of poly(5-ethylidene-2-norbornene sulfone).

Mixture of endo and exo

CH₂Cl₂
-15 °C
5 W/V% SOLUTION

Figure 1.26 ^{1}H NMR of poly(5-ethylidene-2-norbornene sulfone)

Table 1.7 Elemental analyses of poly(norbornene sulfone), poly(1-hexene sulfone, and poly(5-ethylidene-2-norbornene sulfone).

Polymer	% Carbon		% Hydrogen		% Oxygen		% Sulfur	
	Theo.	Exp.	Theo.	Exp.	Theo.	Exp.	Theo.	Exp
PNS	53.3	53.1	6.3	6.4	20.2	20.3	20.2	20.0
PHS	48.7	48.8	8.1	8.3	21.6	21.6	21.6	21.5
PENS	58.7	55.6	6.5	6.3	17.4	19.3	17.4	19.0

Figure **1.27** GPC trace of poly(5-ethylidene-2-norbornene sulfone).

inevitable difference in the reactivity and ceiling temperature of the two different olefins present in this diene monomer. In order to investigate the influence of temperature on branching, two series of experiments were performed. The first one involved running the copolymerizations in solution with a 2:1 ratio of sulfur dioxide to diene monomer at various temperatures ranging from -30 °C to +20 °C. It was anticipated that a 2:1 ratio of sulfur dioxide to diene monomer would allow for enough sulfur dioxide to be present to obtain the maximum degree of branching possible. The other series of experiments involved running the copolymerizations at a 1:1 ratio of sulfur dioxide to diene monomer to gain insight into the importance of the monomer ratio at various temperatures. The results are presented in Table 1.8 and Table 1.9. As one can see in Table 1.8, the reported yields, calculated based on the formation of a 1:1 copolymer, increase as the temperature of the copolymerization increases and it surpasses the 100% mark at 20 °C. This clearly indicates a higher than 1:1 ratio of sulfur dioxide to diene monomer in the copolymer. Also, as the temperature rises, the intrinsic viscosities decrease as one would expect for free radical reactions, but it also could be due to an increase in branching. This would also lower the viscosity even if the molar masses were not decreasing. Membrane osmometry

Table 1.8 Temperature dependence study of the copolymerization of EN and sulfur dioxide (2:1).

Sample	Temp (°C)	Yield (1:1)	Intrinsic[a] Viscosity	Percent EN Intact (^{1}H NMR)	Ratio (SO_2:EN) (elemental analysis)
A	-30	0%	----	-----	-------
B	-20	95%	1.37	75%	1.22:1
C	0	99%	0.76	68%	1.23:1
D	20	110%	0.57	62%	1.15:1

[a] Determined in dichloromethane at 25 °C.

Table 1.9   Temperature dependence study of the copolymerization of EN and sulfur dioxide (1:1).

Sample	Temp (°C)	Yield (1:1)	Intrinsic[a] Viscosity	Percent EN Intact (^{1}H NMR)	Ratio (SO_2:EN) (elemental analysis)
F	-20	52%	0.84	74%	1.16:1
G	0	86%	0.75	66%	1.14:1

a   Determined in dichloromethane at 25 °C.

would have to be used to determine this however. The most striking pieces of data are listed in the last two columns of Table 1.8, the percent of the ethylidene moiety intact and the ratio of sulfur dioxide to diene monomer found in the copolymer by elemental analysis. The percent of the unreacted ethylidene moiety remaining in the copolymer decreases as the temperature of the copolymerizations rises. This indicates that branching through the ethylidene moiety is taking place and is a strong function of temperature. The ratio of sulfur dioxide to EN is constant at a level higher than 1:1 from 0 °C and below, 1.22:1. The ratio is lower than this at 20 °C, however, indicating perhaps a lower ceiling temperature for the type of linkage associated with the incorporation of a second sulfur dioxide per cyclic monomer unit.

Table 1.9 shows similar data but for a system where the initial feed ratio of sulfur dioxide to cyclic monomer was 1:1. As you can see, the overall yields also increase as a function of temperature. The intrinsic viscosity data shouldn't be compared to the above data where the initial feed ratio was 2:1 because the experiments were run at similar EN concentrations but different sulfur dioxide concentrations. The concentration would decrease the molar masses due to concentration effects alone. In addition, the molar masses also decrease with temperature and the same

arguments hold here as for the 2:1 study but the absolute numbers shouldn't be compared to that study since the sulfur dioxide concentration was also lowered. However, one can compare the relative amounts of the ethylidene moiety that remained intact during the copolymerizations for both the 2:1 study and the 1:1 study. It may be seen that the values are the same in both experiments at their given temperatures. Also, the relative amount of sulfur dioxide incorporated was at least 5% less for the 1:1 study relative to the 2:1 study. The last two results indicate that the degree of branching through the ethylidene moiety is a strong function of temperature, but, it is invariant to the ratio of sulfur dioxide to cyclic monomer, at least from a ratio of 1:1 to 2:1. The amount of sulfur dioxide incorporated into the polymer is a function of the feed ratio. This was expected since a very bright yellow green color formed when sulfur dioxide was added to 5-ethylidene-2-norbornene, indicating a charge transfer complex had formed at some ratio of cyclic monomer to sulfur dioxide. The exact ratio was not determined.

In order to rationalize all of the above findings, we postulate that several different structures must be present in addition to the expected structure depicted in Scheme 1.15. Figure 1.28 shows three possible chemical structures

Figure 1.28 Possible chemical structures present in poly(5-ethylidene-2-norbornene sulfone).

that could account for the above findings. Chemical structure A is the predominate expected structure as outlined in Scheme 1.15. Chemical structure B depicts a branching scenario through the ethylidene moiety. This type of structure could be consistent with the degree of branching being a function of temperature while holding the ratio of sulfur dioxide relative to cyclic monomer constant. Chemical structure C is speculative but would account for a greater than a 1:1 ratio of sulfur dioxide to cyclic monomer. In addition, it seems likely that this residue may be the reminants of the charge transfer complex that was known to form, but this should be investigated in more detail. Structure C is not without precedent since a similar structure was elucidated for the bicyclo-copolymerization of cis,cis-1,5-cyclooctadiene, where the sulfone moiety linked two bridgehead carbons.[88]

Terpolymerizations were also performed between sulfur dioxide, EN, and other olefins such as norbornene or 1-butene, as shown in Scheme 1.16. Even under these conditions at -20 °C, one could obtain terpolymers with the ethylidene moiety intact as shown in Table 1.10. When the very reactive norbornene comonomer was used, about 80% of the charged ethylidene moiety could be detected. When 1-butene was the comonomer, a greater amount of the ethylidene monomer was detected, illustrating the greater

Scheme 1.16 Terpolymerizations of sulfur dioxide, 5-ethylidene-2-norbornene, and other olefins.

Mixture of endo and exo

$+$ SO$_2$

CH_2Cl_2

-15 °C

5 W/V% SOLUTION

Table 1.10 Terpolymerization results using 5-ethylidene-2-norbornene as a comonomer.

Comonomer	Films	Percent Yield	% EN Charged	% EN[a] Incorporated	Intrinsic Visc.[b]
Norbornene	Clear	83%	5%	4%	2.23
Norbornene	Clear	95%	20%	17%	1.14
1-Butene	Clear	46%	5%	7%	0.43
1-Butene	Clear	79%	20%	22%	0.41

[a] Determined by ^{1}H NMR.

[b] Measured at 25 °C in dichloromethane.

reactivity of the strained cyclic over the ¯-olefin.

This concludes the results with 5-ethylidene-2-
norbornene monomer. The initial idea for using this diene
in conjunction with other monomers was a good one; however,
the macromonomer approach gave excellent results and the
focus of the research was switched to this route for making
heterophase poly(olefin sulfone)s.

Poly(1-butene sulfone)-g-Poly(dimethyl-siloxane)s

Graft Copolymer Synthesis. Poly(olefin sulfone)s have been known since 1898[89] and still generate significant interest almost a hundred years later. Poly(1-butene sulfone) (PBS) has been the focus of some of the most active research efforts and therefore was chosen, in addition to its well documented utilization in microelectronics, for this study. PBS homopolymer is routinely synthesized as shown in Scheme 1.17 or in the presence of excess sulfur dioxide as the polymerization solvent. The initiator, t-butyl hydroperoxide, under goes rapid decomposition in the presence of sulfur dioxide, well below its thermal decomposition temperature, due to a redox process illustrated in Scheme 1.18. The various radical species shown were detected by electron spin resonance spectroscopy[90] and are all assumed to participate in the various polymerization steps. The ¯-olefins are not able to homopolymerize under these free radical conditions due to the inherent stability of the would be allylic radicals; however, in the presence of sulfur dioxide, they form very nice 1:1 alternating copolymers as shown. We now wanted to utilize the above chemistry and add a third monomer, namely an appropriately functionalized PDMS macromonomer, in hopes of synthesizing multiphase graft copolymers.

Scheme 1.17 Synthesis of poly(1-butene sulfone).

CH₂=CH
|
CH₂
|
CH₃

+

SO₂

CH₃
|
H₃C—C—O—O—H
|
CH₃

│
↓

CH₂Cl₂
-20 °C
20 W/V% SOLUTION

O
‖
————(CH₂———CH————S)ₙ————
| ‖
CH₂   O
|
CH₃

Scheme 1.18 Decomposition of t-butylhydroperoxide.

$$CH_3-\overset{\overset{\displaystyle CH_3}{|}}{\underset{\underset{\displaystyle CH_3}{|}}{C}}-O-O-H \;+\; SO_2 \longrightarrow CH_3-\overset{\overset{\displaystyle CH_3}{|}}{\underset{\underset{\displaystyle CH_3}{|}}{C}}-O^\bullet \;+\; HO-SO_2^\bullet$$

$$CH_3-\overset{\overset{\displaystyle CH_3}{|}}{\underset{\underset{\displaystyle CH_3}{|}}{C}}-O-O-H \;+\; SO_2 \longrightarrow HO^\bullet \;+\; CH_3-\overset{\overset{\displaystyle CH_3}{|}}{\underset{\underset{\displaystyle CH_3}{|}}{C}}-O-SO_2^\bullet$$

$$HO^\bullet \;+\; SO_2 \longrightarrow HO-SO_2^\bullet$$

The parameters that affect the ability or efficiency of a macromonomer to copolymerize with other monomers are numerous as delineated in the Literature Review Section – Part 1. The most important is the nature of the substitution at the polymerizable end group of the macromonomer. In order to incorporate the PDMS macromonomers into a poly(1-olefin sulfone) copolymer in a statistical fashion, it was necessary to design the macromonomer to have an end group that closely emulates the olefin monomer, 1-butene. Therefore, a normal 1-alkene end group was chosen based on 5-hexenyldimethylchlorosilane.

The preparation of the 5-hexenyl functionalized PDMS macromonomers of high functionality, controlled molar mass, and possessing a narrow molar mass distribution was the first step in preparing well-defined graft copolymers. The synthesis of the macromonomers is outlined in Scheme 1.19. The living polymerization of D_3 for the synthesis of hexenyl functionalized PDMS macromonomers is similar to that described for the synthesis of methacryloyloxy functionalized PDMS macromonomers outlined in the Results and Discussion Section for the PMMA-g-PDMS copolymers and therfore will not be repeated here. The difference in the synthesis lies in the functional termination of the

Scheme 1.19 Synthesis of controlled molar mass PDMS living siloxanolates.

I. INITIATION AND PROPAGATION:

$$CH_3-CH_2-\overset{\overset{\displaystyle CH_3}{|}}{CH}-Li \quad + \quad D_3$$

CYCLOHEXANE | ROOM TEMP

2 HOURS

$$CH_3-CH_2-\overset{\overset{\displaystyle CH_3}{|}}{CH}\left(\overset{\overset{\displaystyle CH_3}{|}}{\underset{\underset{\displaystyle CH_3}{|}}{Si}}-O\right)_{\overline{X}}\overset{\overset{\displaystyle CH_3}{|}}{\underset{\underset{\displaystyle CH_3}{|}}{Si}}-O \quad \ominus \quad \oplus \quad Li$$

$$(X = 2,1, \text{ or } 0)$$

$$m \, D_3 \quad | \quad \text{THF (10\% BY VOLUME)}$$

24 HOURS

$$CH_3-CH_2-\overset{\overset{\displaystyle CH_3}{|}}{CH}\left(\overset{\overset{\displaystyle CH_3}{|}}{\underset{\underset{\displaystyle CH_3}{|}}{Si}}-O\right)_{\overline{3m}}\overset{\overset{\displaystyle CH_3}{|}}{\underset{\underset{\displaystyle CH_3}{|}}{Si}}-O \quad \ominus \quad \oplus \quad Li$$

Scheme 1.20 Termination of living PDMS siloxanolate to afford an hexenyl functionalized PDMS macromonomer.

II. FUNCTIONAL TERMINATION:

$$CH_3-CH_2-CH+Si-O)_{3m}Si-O \quad \ominus \quad Li \oplus$$

with pendant CH_3 groups and Si–O backbone

"LIVING SILOXANOLATE"

$$Cl-Si+(CH_2)_4-CH=CH_2$$
with CH_3 groups on Si

$$H_2C=CH-(CH_2)_4-Si(CH_3)_2-O-Si...$$

$$R+Si-O)_{3m}Si_{,,,}CH_3$$

polymerization as shown in Sceme 1.20. A chlorosilane derivative based on 5-hexene was used to afford the hexenyl functionalized PDMS macromonomers of controlled molar mass. The molar mass of the polymer was regulated by the ratio of the grams of D_3 monomer to the moles of initiator with target values of 1k g/mol, 5k g/mol, 10k g/mol, and 20k g/mol. The molar mass and the molar mass distribution of the PDMS macromonomers were investigated using GPC with PDMS standards, Figure 1.29. The PDMS macromonomers were analyzed using ^{1}H NMR as shown in Figure 1.30. The region between 5.7 ppm and 5.9 ppm was amplified and on can observe the typical splitting pattern for a terminal aliphatic olefin. In addition, the number average molar mass and the functionality of the macromonomers were determined using quantitative ^{29}Si NMR. As can be seen in Figure 1.31, there are three different types of silicon atoms present in PDMS macromonomers. The technique can differentiate between the silicon next to the initiating sec-butyl fragment, the silicon next to the terminating 5-hexenyl fragment, and the silicon in the repeating dimethylsiloxane unit. The ratio of the integration of the repeating silicon atoms to that of an end group will result in the number average molar mass. Also, the ratio of the integrations of each of the terminal silicons results in a direct determination of the percent

Figure 1.29   GPC trace for hexenyl functionalized PDMS
macromonomer.

^{1}H NMR OF HEXENYL TERMINATED PDMS

Figure 1.30 ^{1}H NMR of hexenyl functionalized PDMS macromonomer.

Figure 1.31 Quantitative silicon-29 NMR of hexenyl functionalized PDMS macromonomer.

Table 1.11   Summary of the molecular characterization
of hexenyl functionalized PDMS macromonomers using GPC and
quantitative silicon-29 NMR.

Target <Mn> (kg/mol)	Percent[a] Functionality	<Mn>[a] (kg/mol)	<Mn>[b] (kg/mol)	Molar Mass Distribution
1.0	100%	9.4	-----	----
5.0	100%	5.62	4.10	1.08
10.0	100%	9.85	7.20	1.05
20.0	94%	24.6	17.50	1.03

[a]   Measured using the quantitative silicon-29 NMR
method.

[b]   Measured using GPC with PDMS standards.

functionality of the PDMS macromonomers. A summary of the GPC and ^{29}Si NMR data is given in Table 1.11 along with the target molar masses for the macromonomers. A good correlation exists between the target values and the resultant values.

Terpolymerizations of the 5-hexenyl functionalized PDMS macromonomer with 1-butene and sulfur dioxide were carried out in which the number average molar masses of the macromonomers and the composition of the graft copolymers were both varied. A low pressure polymerization reactor was utilized for the terpolymerizations in order to maintain the desired temperature to ± 2 °C.[91] The free radical polymerizations, shown in Scheme 1.21, were performed in dilute solutions, ca. 20 w/v% solids. This concentration was determined to be the highest percent solids one could use with the 20k g/mol PDMS macromonomer without macrophase separation during the course of the polymerization reaction. It was desired to use higher concentrations inorder to achieve higher overall molar masses, but macrophase separation became a problem. Higher molar mass materials would have performed even better in the lithographic application, which will be addressed later.

Scheme 1.21 Free radical polymerization to form PBS-g-PDMS copolymers of various compositions and architectures.

When these polymerizations were first undertaken, the graft polymers were precipitated into methanol. The result was that the polymers were no longer soluble and had become lightly crosslinked as evidenced by significant swelling in chloroform and dichloromethane. It was believed that upon workup of the graft polymers in the presence of unincorporated sulfur dioxide, the PDMS grafts under went a redistribution reaction since the sulfur dioxide could hydrolyze in wet methanol resulting in the formation of sulfurous acid which can oxidize to sulfuric acid. In an effort to avoid the deleterious side reactions in the presence of excess sulfur dioxide, the graft polymers were precipitated into methanol containing 2 v/v% triethylamine. It is suggested that the triethylamine scavenges any acid that is formed before it can react with the PDMS segments. This modified precedure results in soluble graft polymers after precipitation.

Once the polymers were precipitated, the unincorporated PDMS macromonomer was removed using extensive extractions with hexanes in a soxhlet extractor. Solvent cast films of these materials were all cloudy before extraction and clear after extraction. A typical ^{1}H NMR is shown in Figure 1.32. The compositions were determined, equation 9, by ratioing the integration of the silicon

Figure 1.32 ¹H NMR of PBS-g-PDMS.

methyl signal at 0.1 ppm to the methylene and methine signals for the PBS component as follows:

$$\% \ PDMS = \frac{[(PDMS \ / \ 6) \ \times \ M_{0,PDMS}]}{\{[(PDMS \ / \ 6) \ \times \ M_{0,PDMS}] \ + \ [(PBS \ / \ 3) \ \times \ M_{0,PBS}]\}} \ (9),$$

where $M_{0,PDMS}$ is the molecular weight of the PDMS repeat unit, $M_{0,PBS}$ is the molecular weight of the PBS repeat unit, and PDMS and PBS refer to the integrations of the respective signals which were then normalized.

Compositions are presented in Table 1.12 along with the corresponding initial feed ratios. As one can see, approximately two-thirds of the PDMS charged was actually incorporated into the graft copolymer. At the onset, this may seem like a rather low percentage for incorporation of the PDMS macromonomer relative to the formation of the PMMA-g-PDMS copolymers; however, one must realize that the PBS-g-PDMS system has two components that have very different solubility parameters relative to the PMMA-g-PDMS system. It was indicated in the Literature Review Section - Part 1, that when the macromonomer is chemically different from the backbone material, there is a tendancy towards deactivation of the macromonomer reactivity. For this case, a PDMS macromonomer and PBS, the materials are extremely different in regards of their solubility parameter difference of at least 2.7 [(cal/cm^3)]. Therefore, this system would

Table **1.12** Summary of PBS-g-PDMS synthesis illustrating macromonomer feed ratios and percent incorporation.

Sample	wt% PDMS Charged	wt% PDMS Incorporated	Series Designation
026-A	9	6	
026-B	9	6	6 wt%
026-C	9	6	PDMS
026-D	9	7	
			Low <Mn>
017-A	29	23 (21)	
017-B	29	20 (20)	20 wt%
017-C	29	20 (23)	PDMS
017-D	29	17 (19)	
031-A	9	5	
031-B	9	5	5 wt%
031-C	9	5	PDMS
031-D	9	6	
			High <Mn>
029-A	29	19	
029-B	29	17	17 wt%
029-C	29	17	PDMS
029-D	29	15	

probably be considered an extreme case and the results seem reasonable in light of the above arguments. This explanation for the low efficiency of PDMS incorporation appears to be correct in view of the outstanding percent functionality values and the apparently similar nature, and hence reactivity, of the hexenyl functional group to 1-butene. The compositions listed were determined by ^{1}H NMR as described earlier. The four values listed in parenthesis for the low molar mass 20 wt% PDMS series were obtained by differential refractometry in methyl ethyl ketone. The values obtained by the different methods correlate very well with one another. This gives credibility to the data obtained by NMR which must always be looked at carefully due to micellularization problems that often occur with block and graft copolymers.

Analysis of the PBS-g-PDMS copolymers by GPC was difficult to obtain in THF (PBS is insoluble in toluene). This was due to the UV absorption of PBS being below the THF UV cutoff value of 210 nm, the relative insensitivity of our differential refractive index detector for PBS copolymers (PDMS is isorefractive THF), and the potentially broad molar mass distribution of at least the high molar mass series due to the multiple initiator charge during the synthesis.

The molar masses were, however, investigated using intrinsic viscosity data which was supplemented in a few cases with apparent weight average molar masses and PBS backbone weight average molar masses obtained for the graft copolymers using light scattering techniques. The values are listed in Table 1.13. The low molar mass series of graft copolymers have very low intrinsic viscosities ranging from 0.06 to 0.18 dL/g. However, the corresponding apparent weight average molar masses range from 68k g/mol to 41k g/mol which decrease as the graft molar mass increases. In addition, the weight average molar mass for the PBS component obtained by isorefractive light scattering in THF, show the values for the PBS backbone also decreasing as the molar mass of the macromonomer increases. These relationships may be related to the phase behavior during the synthesis, which may begin to show signs of phase separation which are not able to be detected by the eye or unusual chain conformations and associations in solution either during the analysis or during the synthesis.

Table 1.13 Intrinsic viscosity light scattering data on the PBS-g-PDMS copolymers.

Sample	Composition wt% PDMS	Intrinsic Viscosity	$M_{w,app}$ (kg/mol)	$M_{w,backbone}$ (kg/mol)
026-A		0.06		
026-B	6 wt%	0.12		
026-C	PDMS	0.14		
026-D		0.17		
017-A		0.04	68	54
017-B	20 wt%	0.09	50	40
017-C	PDMS	0.18	47	37
017-D		0.14	41	32
031-A		0.16		
031-B	5 wt%	----		
031-C	PDMS	----		
031-D		----		
029-A		0.29		
029-B	17 wt%	0.24		
029-C	PDMS	0.28		
029-D		0.28		

Bulk and Surface Characterization

DSC thermograms were obtained on the four different molar mass PDMS macromonomers and on the low and high molar mass series of PBS-g-PDMS copolymers containing ca. 20 wt% PDMS using the four different molar mass macromonomers.

DSC methods are valuable for investigating microphase separation in block and graft copolymers.[92] Glass transition temperature measurements are often representative of the degree of phase separation in multi-component systems. The parameters that were investigated in this study include measurement of the glass transition temperature of the corresponding homopolymers relative to the graft copolymers and any deviations or shifts were quantified. In addition, the breadth of the glass transition temperatures and the change in heat capacities were measured and compared to the corresponding homopolymers as described in the experimental section. Another potential measure of microphase separation includes quantifying melting and crystallization transitions if one of the components can crystallize. In the PBS-g-PDMS system, PDMS is a component that can crystallize in its neat form at certain molar masses and in multicomponent systems.

The advantage of the macromonomer method as far as thermal analysis is concerned is that one can measure the

thermal properties of the identical macromonomer that is used to make the graft copolymer in its neat form. This allows for comparisons to be made on the same properties of the macromonomer component after its incorporated. The first DSC experiments involved thoroughly characterizing the four different molar mass PDMS macromonomers. Two different time-temperature profiles were used. The first profile is depicted in Figure 1.33 for a PDMS macromonomer having a molar mass of 20k g/mol. The x-axis in this figure is time and the temperature is plotted on the far left y-axis. The experimental conditions involved rapidly cooling the sample to a certain crystallization temperature, such as -72 °C, isothermally allowing the material to crystallize for 30 min, followed by a slow heat to measure the melting transition. In Figure 1.33, the crystallization exotherm was detected shortly after reaching the crystallization temperature. During the isothermal 30 min delay, the baseline was reestablished and the sample was heated to record the melting endotherm. The other DSC time-temperature profile involved quenching the sample to -150 °C at ca. -50 °C/min, then slowly heating the sample. The slow heat is shown in Figure 1.34 for a quenched PDMS sample with a molar mass of 20k g/mol. A comparison of the two thermograms shows that there are large differences due to their different thermal histories. An expanded region of

Figure 1.33 DSC experiment for isothermal crystallization studies.

Figure 1.34 is shown in Figure 1.35. There exists a large cold crystallization exotherm beginning immediately after reaching the glass transition temperature followed by several rather well-defined endothermic transitions prior to the larger melting transitions usually associated with PDMS.[93] These smaller transitions <u>may</u> be due to lamellae thickening or reorganization of metastable crystals during heating since it was observed that there was a heating rate dependence for these transitions. This preliminary data are presented here in hopes of enticing further investigations into this phenomenon. The percent crystallinity of the neat PDMS macromonomers was calculated as described in the Experimental Section - Part 1.

When the same two time-temperature profile DSC experiments were performed on the PBS-g-PDMS copolymers, only weak PDMS melting transitions were observed for the isothermal crystallization experiments. The values indicated that less than 1% of the PDMS component had crystallized in the copolymer whereas the neat materials measured 30% to 50% crystallinity under similar conditions. This indirectly demonstrates the constraints that are placed on the system when oligomers are incorporated into multicomponent materials. However, larger and more quantifiable melting endotherms were measured when the

Figure 1.34 DSC thermogram of a quenched 20k g/mol PDMS macromonomer.

Name: JMD076F2.4   Sample: JMD076F
Date: 89/05/17 00:05 Weight: 7.500 mg
Comment: Nitrogen purge Reference:
               QUENCHED TO-150   aluminum (0.000
               HEAT 5 C/MIN   Sampling: 0.1 sec

Figure 1.35 An expanded view of the minor endothermic transitions prior to the large PDMS melting transition.

samples were quick quenched then heated as described as the second time-temperature profile experiment for the neat PDMS oligomers. For this reason, only the data obtained for the quick quench experiments are presented.

A summary of the results is shown in Table 1.14. The PDMS macromonomers exhibited multiple melting endotherms and crystallization exotherms, as seen by others, depending on their mode of cooling. The lowest molar mass PDMS macromonomer, 1k g/mol, was not able to crystallize under the conditions utilized, but the oligomers with molar masses greater than 5k g/mol did crystallize. The Tg's of the PDMS macromonomers increased as the molecular weight increased, reflecting the dependence of glass transition on molar mass in this low molar mass region.

The DSC investigations of the high molar mass PBS-g-PDMS copolymers with ca. 17 wt% PDMS have focused on the results of the second heating cycle. The DSC results for the PBS-g-PDMS copolymers showed no detectable PDMS Tg regardless of the molar mass of the PDMS graft.

Single melting endotherms were observed for the PDMS component in all of the graft copolymers except for the 1k g/mol PDMS graft, which was observed not to crystallize even in its neat form. A shift in the Tm of the PDMS component to lower temperatures with increasing graft molar

Table 1.14 Summary of DSC investigations on PDMS macromonomers and PBS-g-PDMS copolymers.

<u>Sample</u> (g/mol)	<u>PDMS Tg</u> (C°)	<u>PDMS Tm</u> (C°)	<u>PDMS Tc</u> (C°)
1000	-135		
5000	-130		
10000	-129	-49/-35	-88
20000	-126	-50/-35	-97

<u>Sample</u>	PDMS <u>Tg</u> (C°)	PDMS <u>Tm</u> (C°)	PDMS <u>% x-tal</u>	<u>DPM</u>	PBS <u>Tg</u> (C°)	PBS <u>Δ Tg</u> (C°)
17 wt%, 1K	-----	-----	-----	29	80	20
17 wt%, 5K	-----	- 60	13	20	86	17
17 wt%, 10K	-----	- 48	15	-6	91	12
17 wt%, 20K	-----	- 42	11	-25	92	12
PBS Control	NA	NA	NA	NA	92	12

mass was observed. The percent crystallinity of the PDMS component, shown in Table 1.14, did not appear to be a function of the graft molar mass. This may be due to a shift in morphology and will be discussed later in the section dealing with TEM. In addition, a parallel shift in the Tg and the $\triangle$Tg of the PBS component was observed. The PBS Tg increases and the $\triangle$Tg decreases with a corresponding increase in the molar mass of the PDMS macromonomers and begins to approach the values observed for pure PBS. This possibly indicates a decrease in the degree of phase mixing between the two components with increasing graft molar mass. In addition, the degree of phase miscibility (DPM), as calculated in the Experimental Section, shows a very large trend towards the system becoming better phase separated with increasing PDMS molar mass. The absolute values for DPM, however, are significantly off scale as demonstrated by having a DPM less than zero!

The reason the above data only possibly indicates a change in the phase mixing is due to the topology of graft copolymers. The degree of polymerization for the backbone component of any graft copolymer, in this case PBS, must not just be considered as that value representing the total degree of polymerization for the copolymer as far as the glass temperature transitions are concerned. A more appropriate value should be the degree of polymerization

associated with the molar mass between branch points. This is the segment of the backbone that is in the PBS domain and experiences the influence of the critical molar mass for chain entanglements on its ability to undergo a glass transition. This reflects the nature of the morphology which places the branch points at the interface of the different phases. This places restrictions on these segments that may alter their ability to entangle, causing them to act independently of one another as detected in the glass transition phenomenon. A theoretical analysis on the effect of the number of junction points in graft copolymers coupled with experimental evaluation is encouraged. The approach would initially be similar to that demonstrated for the effect of molar mass on the glass transition temperature of polymers with linear and cyclic topologies of equivalent molar mass. Small angle X-ray scattering experiments would prove useful in determining the level of phase mixing by measuring the degree of phase separation through an invariant analysis.[94] This method compares the normalized electron densities of the two components and measures their their contrast which can be related to the degree of phase separation as a function of graft molar mass at constant composition. This could then be compared with the DSC results to determine if the system is actually becoming more miscible with a decrease in graft molar mass or if the

relative degree of miscibility is fairly constant and the trend of the DSC data on the PBS glass transition is reflective of the critical molar mass for chain entanglements.

The driving force for phase separation in the bulk is the difference in solubility parameters between the two components. Thus, the large disparity between the solubility parameter of the PDMS, 7.3 $(cal/cc)^{1/2}$, and that of PBS, > 10 $(cal/cc)^{1/2}$, suggests the reason for this system to be as phase separated as it is. An interesting comparison can be made between the PBS-g-PDMS copolymers and the PMMA-g-PDMS copolymers presented earlier. The solubility parameter for PMMA is 9.1 $(cal/cc)^{1/2}$. At least a full unit less than that for PBS and hence probably exhibiting a higher degree of phase mixing than for the PBS-g-PDMS system at equivelent degrees of polymerization, composition, and architecture. This may be demonstrated by the fact that PMMA-g-PDMS copolymers having the same weight percent PDMS and the same molar mass macromonomer as listed for the PBS-g-PDMS copolymers in Table 1.14, did not have any PDMS crystallization under similar thermal treatments.[2]

Another possible reason behind not observing PDMS crystallization in the PMMA system may be also related to their differences in morphology, but in a different way.

The crystallization phenomenon, according to Ehrenfest[95], is a first order thermodynamic transition that is accompanied by a discontinuous decline in the volume of the system. This decrease in volume may be accompanied by a corresponding increase in surface area, especially for a sperical morphology, which is thermodynamically disfavored. This may also account for the fact that at comparable compositions and architectures, the PDMS in the PMMA system did not crystallize whereas it did in the PBS system since the PBS system had a bicontinuous morphology and the PMMA system had a discrete morphology.[96]

The microphase separation of the title graft copolymers was also investigated by TEM on solvent cast films. The films were slow cast, taking greater than ca. 48 h, from chloroform in order to reach their quasi-equilibrium morphologies. Our preliminary work reported here is on films that were not annealed above room temperature. The TEM analysis demonstrated that the morphology of the PBS-g-PDMS system changes significantly as a function of copolymer composition and architecture and even more dramatic differences were observed as a function of overall molar mass at constant compositions and architectures. Both the low and high molar mass graft copolymers having ca. 5 wt% PDMS exhibited discrete spherical morphologies having sperical PDMS domains embedded

in the PBS matrix, shown in the top portions of Figure 1.36 and Figure 1.37. The domain sizes increased with a corresponding increase in the molar mass of the PDMS graft at constant compositions. TEM analysis showed that the low molar mass copolymers having ca. 20 wt% PDMS exhibited continuous morphologies, bottom portion of Figure 1.36. The low molar mass, high siloxane PBS-g-PDMS copolymer prepared using the 5k g/mol PDMS macromonomer showed a disordered bicontinuous morphology whereas the low molar mass graft copolymers containing the 10k g/mol and 20k g/mol PDMS grafts showed ordered cylindrical or lamallae morphologies with regions of disorder. The high molar mass, high siloxane graft containing copolymers all had bicontinuous disordered morphologies, bottom portion of Figure 1.37. The high siloxane containing low and high molar mass graft copolymers at equivelent compositions and architectures had very different morphologies for the samples having the 10k g/mol and the 20k g/mol grafts. The differences in the observed morphologies by TEM analysis for these graft copolymers can be attributed to the number of branch or junction points per molecule. The lower molar mass graft copolymers have fewer junction per molecule then do the high molar mass graft copolymers as depicted in Figure 1.38. These junction points need to be placed at the interphase

Figure 1.36 TEM analysis of the low degree of polymerization PBS-g-PDMS copolymers having 5 wt% and 20 wt% PDMS with 5k g/mol, 10k g/mol, and 20k g/mol PDMS grafts.

Figure 1.37 TEM analysis of the high degree of polymerization PBS-g-PDMS copolymers having 5 wt% and 17 wt% PDMS with 5k g/mol, 10k g/mol, and 20k g/mol PDMS grafts.

High Degree of Polymerization Four Junction Points per Molecule

Low Degree of Polymerization One Junction Point per Molecule

Domain A   Domain B   Domain A

Figure 1.38 Illustration of the number of branch points per molecule as a function of the degree of polymerization.

region between the PBS rich phases and the PDMS rich phases. This entropically disfavored constraint allows more degrees of freedom for the lower molar mass graft copolymers to assume their lowest energy conformations since they have fewer branch points relative to their higher molar mass counterparts.

An interesting side note relates the degree of polymerization to the chemical composition distribution (CCD). In the Literature Review Section - Part 1, the theoretical CCD was shown to dramatically increase as the degree of polymerization decreased. Intuitively, one would suspect that as the CCD increased, the degree of long range morphological order would decrease due to the non-uniformities of the system. The decrease in order with a corresponding decrease in the degree of polymerization is exactly opposite for the same trend in order with degree of polymerization when considering the number of junction points per macromolecule. These parameters, the CCD and the number of junction points per macromolecule, geometrically oppose one another as a function of degree of polymerization as far as polymer morphology is concerned. The TEMs for the PBS-g-PDMS copolymers of similar compositions and graft lengthes but different degrees of polymerization suggest that the number of junction points per molecule is the

dominant constraint and that the role of the CCD is relatively weak. However, it was pointed out that the materials having a low degree of polymerization for the 20 wt% PDMS had highly ordered regions and regions of disordered. Perhaps the CCD is playing a role in this regard. Of course, all of these arguments assume that the observed morpholgies are the equilibrium morphologies and that the kinetics for phase separation and ordering were the same and not a function of the degree of polymerization. This is probably a bad assumption, but this interesting dichotomy of influences should be addressed with a more appropriate system and a more directed study.

All of the graft copolymers analyzed by TEM showed a much higher volume fraction of the PDMS component than anticipated for the weight percent PDMS incorporated, as determined by NMR and differential refractometry. A possible reason for this, aside from the problems associated with the projection of a three dimensional object on a two dimensional surface, may be preferential swelling of a given domain by the solvent used to cast these films. In order to verify this, work needs to be done on analyzing films cast from different solvents and films that were annealed to thermally induce their equilibrium morphologies.

Because PDMS has a low surface energy relative to PBS and exists in a microphase separated system, it was anticipated that the PDMS component would tend to dominate the air/solid interface of the copolymers. Advancing and receding water contact angles were measured to verify these expectations and the results are listed in Table 1.15 for the low molar mass series of graft copolymers. Water contact angle measurements indicated a change in the surface composition of the films as a function of copolymer composition and architecture. The graft copolymers prepared using the higher molar mass PDMS macromonomers, which phase separate to a higher degree, exhibit higher advancing water contact angles due to the presence of a more complete overlayer of the PDMS at the surface. This agrees with several of our earlier results with other systems[97].

In order to quantify the water contact angle results, angular dependent XPS was performed at angles of 15°, 30°, and 90° on the solvent cast samples. Angular dependent XPS depth profiling indicated that the surface had a gradient of composition and that the surface composition was observed to be a function of copolymer composition and architecture. The higher angles of analysis penetrate deeper into the surface and will reflect the composition average of approximately the top 60 Å at 90°, about 15 Å at 30°, and a 10° angle will sample about the top 10 Å of the surface.

Table 1.15 Advancing and receding water contact measurements for the low molar mass PBS-g-PDMS copolymers.

SAMPLE	ADVANCING	RECEDING
PBS	73	48
PDMS (X-linked)	112	60
6 wt%, 1K	96	49
6 wt%, 5K	102	55
6 wt%, 10K	104	63
6 wt%, 20K	106	63
20 wt%, 1K	99	47
20 wt%, 5K	106	64
20 wt%, 10K	108	64
20 wt%, 20K	109	65

Figure 1.39 Angular dependent X-ray photoelectron spectroscopy results showing preferential PDMS surface segregation as a function of PDMS molar mass at constant composition (5 wt% PDMS).

The data is presented as a plot of the detected composition versus the sine of the escape or sampling angle and is shown in Figure 1.39. Important trends in composition as a function of graft molar mass and depth are observed. It is evident that the copolymers, already established as having well phase separated bulk morphologies, also have significant surface segregation which increases as the graft molar mass increases. The composition at the very top surface was found to be greater than an order of magnitude higher than the average bulk composition determined by NMR and differential refractometry. This enhancement will play a dramatic role in the lithographic performance of these material as will be demonstrated in the next section.

It is interesting to note that during the XPS analysis at room temperature, the sulfur 2p peak was observed to split after a certain amount of time into two peaks that did not show baseline resolution. It was concluded that under the environment of the analysis, the PBS-g-PDMS copolymers were degrading. Whether this degradation was cause directly by the impinging X-rays or whether this was caused by the generated electrons after excitation by the X-rays is unclear; however, the degradation was eliminated by cooling the sample probe with liquid nitrogen and allowing the

sample to come to thermal equilibrium, ca. 1 h, prior to analysis.

Microlithographic Evaluation

The samples investigated for their applicability as e-beam resists were the high molar mass PBS-g-PDMS copolymers having 5 wt% and 17 wt% PDMS with the four different molar mass PDMS macromonomers. The first step taken to evaluate the materials as resists involved transferring the copolymers onto a silicon wafer for the different analyses. Several different solvents were tried for the spin coating of the polymers onto silicon. It was desired to have a solvent with a fairly high boiling point, ca. 100 °C to 130 °C. A solvent with too low of a boiling point tends to evaporate quickly leaving a partial skin on the pool of dissolved polymer as you transfer the solution onto the wafer. When the wafer is spun, the skin breaks up and causes major defects in the thin films when observed under a light microscope. However, a solvent with too high a boiling point is difficult to completely remove during the drying step. Cyclopentanone proved to be a good solvent for all of the graft copolymers except the two that contained the 20k g/mol PDMS grafts with 5 wt% and 17 wt% PDMS. Solutions of these two graft copolymers in cyclopentanone were cloudy indicating micelle formation. Chloroform was used as the solvent for spinning instead of cyclopentanone for these two copolymers. The copolymer solutions gave excellent pin hole free films when spin coated onto silicon.

The log(film thickness) as a function of log(spinning rate), Figure 1.40, was found to be linear as expected. This allowed for predictable control of the film thickness at constant concentration by varying the spinning rate. The film thickness was measured by scratching the surface and measuring the depth of the scratch with a profilometer as shown in Figure 1.41.

The resistance towards degradation and weight loss of the graft copolymers was measured as described in the Experimental Section - Part 1. The investigations were performed on spin coated films all of approximately the same thickness of 2200 Å. The films were exposed to increasing increments of time in the oxygen RIE chamber. The results were plotted as normalized film thickness versus the time exposed to the oxygen RIE. Figures 1.42 and 1.43 show the results for the two different PDMS compositions as a function of the PDMS molar mass as it increased from 1k g/mol to 20k g/mol. The 5 wt% PDMS series does not have much resistance to the oxygen RIE, regardless of the copolymer architecture; however, the 17 wt% PDMS series exhibits superior resistance to the oxygen RIE. Figure 1.44 is a plot of normalized film thickness versus time for two graft copolymers having the same molar mass PDMS macromonomer, 10k g/mol, but having different

SPINNING RATE VERSUS FILM THICKNESS

Figure 1.40 Spinning rate versus film thickness for 5 wt% solution of PBS-g-PDMS in cyclopentanone.

Figure 1.41 Typical profilometer printout showing depth of scratch in a thin film to be ca. 6440 Å.

Figure 1.42 Oxygen RIE resistance for PBS-g-PDMS with 5 wt% PDMS as a function of graft molar mass.

Figure 1.43 Oxygen RIE resistance for PBS-g-PDMS with 17 wt% PDMS as a function of graft molar mass.

Figure 1.44 Oxygen RIE resistance for PBS-g-PDMS copolymer as a function of PDMS composition at constant graft molar mass, 10k g/mol.

compositions, 5 wt% and 17 wt% PDMS respectively. As is evident, the initial etching rate is higher than the equilibrium etch rate which was obtained after 3 or 4 minutes of etching. The higher initial etch rate is due to the fact that a certain amount of time is needed to build up the protective silica layer. The rate of film loss during the first 30 s of oxygen RIE decreases slightly with increasing molar mass of the PDMS graft, although the stationary etching rate seams to be independent of this parameter. The etching rates were found to be several times lower than those found previously for PMMA-g-PDMS copolymers having a comparable PDMS content.[39] The oxygen RIE resistance of the graft copolymers is significantly better than pure PBS and also better than lithographic grade novolac resin. It has been reported that to avoid line width erosion during RIE, it is necessary to have an etch ratio greater than 10:1 between the resist and the planarizing layers.[98] The etch rate for novolac resin is ca. 10^3 Å/min[99] and the PBS-g-PDMS copolymer with 17 wt% PDMS using 10k g/mol macromonomers has an equilibrium etch rate of 30 Å/min. This corresponds to an etch rate ratio of ca. 33:1, well within the regime for quality pattern transfer in two-layer lithography.

As stated earlier, the graft copolymers yielded excellent thin films when spun from solution. SEM analysis

of the as spun films were featureless up to 100K magnification. SEM analyses were also obtained on the originally 2200 Å thick films after 13 min of exposure to the oxygen RIE and are shown in Figures 1.45 to 1.49. Figure 1.45 is an SEM of a novolac control showing a featureless surface. Figure 1.46 is a similar SEM for the graft copolymer with 5 wt% PDMS and 1k g/mol grafts after the oxygen RIE exposure. This is the material that degraded extensively as measured by normalized film thickness versus time shown in Figure 1.44. It is clear that a significant amount of degradation took place as evidenced by the large craters and a significant degree of pitting. Figure 1.47 shows the SEM for the graft copolymer having the same composition as the material shown in Figure 1.46 but contains the higher molar mass PDMS grafts, 10k g/mol. Much less pitting is observed than the previous material having the same composition. This reflects the difference in PDMS surface composition as the molar mass of the grafts increases. Figures 1.48 and 1.49 show the SEMs for the 17 wt% PDMS containing PBS graft copolymers having 1k g/mol and 10k g/mol grafts, respectively, after a 13 min exposure to the oxygen RIE. The observed surfaces were essentially featureless at 100K magnification, which supports the film thickness versus time data presented in Figure 1.44.

Backscatter Image   Secondary Electron Image

Secondary Electron Image

Figure 1.45   SEM of novolac control.

Secondary Electron Image

Secondary Electron Image

Figure 1.46 SEM of PBS-g-PDMS copolymer having 5 wt%
PDMS and 1k g/mol grafts.

Backscatter Image · Secondary Electron Image

Secondary Electron Image

Figure 1.47 SEM analysis of PBS-g-PDMS copolymers having 5 wt% PDMS and 10k g/mol grafts.

Backscatter Image   Secondary Electron Image

Secondary Electron Image

Figure 1.48   SEM analysis of PBS-g-PDMS copolymers having 17 wt% PDMS and 1k g/mol grafts.

Backscatter Image   Secondary Electron Image

Secondary Electron Image

Figure 1.49 SEM of PBS-g-PDMS copolymer having 17 wt% PDMS and 10k g/mol grafts.

Angular dependent XPS (ADXPS) was also performed on the PBS-g-PDMS copolymers after exposure to the oxygen RIE. The ADXPS results for the extremely pitted material having only 5 wt% PDMS and 1000 g/mol grafts detected elemental silicon at 90°. We believe that the observation of elemental silicon only at 90° is due to sampling of the silicon wafer itself, which occurs since the silicon wafer is exposed as a result of the craters. At 30° and 10°, the bottom of the craters can not be sampled due to the angle, as shown in Figure 1.50, and therefore elemental silicon wasn't observed. More importantly, the silicon 2p electrons measured at all angles for the oxygen RIE exposed samples had a binding energy of 103.3 eV. However, the binding energy for the Si 2p electrons for PDMS is 102.4 eV. The value of 103.3 is similar to that measured for crystalline silicon dioxide which is 103.2 eV. This result confirms that the mechanism for protection of the graft copolymers upon exposure to the oxygen RIE is the oxidative transformation of PDMS to silicon dioxide.

It has been previously reported that organic polymers require at least 8-12 wt% silicon to impart sufficient resistance to oxygen RIE.[100] The resistance is believed to result from the formation of a silicon dioxide overlayer, whose presence was also confirmed in this study, that acts as a barrier to the oxygen RIE process and protects the

Silicon Wafer Sampling at 90°

30°

Figure 1.50 Geometric consequences during the ADXPS analysis for the observation of elemental silicon.

underlying organic substrate. The 17 wt% PDMS series of graft copolymer corresponds to only 6.4 wt% silicon. The high resistance of the 17 wt% graft copolymers to oxygen RIE, even though they contain less than 8 wt% silicon, may be directly related to two factors. First, the reported value of 8 to 12 wt% silicon was based on single phase polymers containing trialkyl silicon moieties, not for siloxane units that containing silicon already bonded to two oxygens. Second, it was demonstrated on slow solvent cast films that the surface of the copolymers was rich in the PDMS component. The silicon concentration at the solid/gas interface actually approaches 30 wt% (or 80 wt% PDMS) according to the ADXPS data. Since the protective mechanism is a surface phenomenon, perhaps the materials are actually above a critical threshold of silicon concentration where it is most important, at the top few nanometers of the surface.

The PBS-g-PDMS copolymer containing 17 wt% PDMS and having 10k g/mol grafts was selected for preliminary lithographic sensitivity evaluation. The evaluation of the sensitivity of the copolymers was carried out as described in the Experimental Section - Part 1. The procedure, outlined in Figure 1.51, involved exposing a bilayer test pattern containing a 1.2 μm highly cross linked novolac planarizing layer covered with a 1800 Å layer of the graft

PROCESS FOR MEASURING SENSITIVITY

a) Resist is spin coated onto silicon wafer previously coated
   with planarizing polyimide layer.

b) Wafer is divided into many sections with each section
   being exposed to various levels of e-beam irradiation.

c) After exposure, the image is developed with a solvent
   for the low molecular weight PBS-g-PDMS, which leaves
   the high molecular weight copolymer, producing the image.

d) After development, the thickness of the remaining
   PBS-g-PDMS is measured with a profilometer and the
   results are plotted versus log (exposure dose)

Figure 1.51 Procedure for measuring lithographic
sensitivity and contrast of positive electron beam resists.

copolymer. Different regions of the sample were exposed to different dose levels of e-beam irradiation. Approximately ten test patterns were generated by the computer controlled exposure tool which allowed for various different development solvents to be used and evaluated. At this point, the silicon wafer was cleaved obtaining a section that contained one pattern over the entire range of dose levels. The section was then dip developed in a solvent for a certain amount of time. The section of the resist that was exposed to e-beam had a lower molecular weight than the unexposed sections and therefore would dissolve faster, and hence the image was developed. The pattern was analyzed in a profilometer which measured the film thickness in the exposed regions relative to the unexposed regions. This would generate a series of depths that varied according to the dose level and was different for each different developing procedure used. The data was handled as shown in Figure 1.52. The ideal developing solvent would result in zero percent thinning and quantitative removal of the exposed area at low dose levels with a sharp break (high contrast). The first developing procedure chosen was a 60 s dip development in 2-methoxyethanol. The sensitivity curve is shown in Figure 1.53. As one can see, the break point in the curve is not smooth which results in nonselective

Figure 1.52 Data manipulation for the preparation of sensitivity curve graphs.

Figure 1.53 Sensitivity curve for PBS-g-PDMS, 17 wt% PDMS and 10000 g/mol grafts for 30 s dip development in 2-methoxyethanol.

removal of the resist layer. To demonstrate the impact that a poor developing solvent has on the resultant image, the pattern was transferred through the planarizing layer by oxygen RIE and the result is shown in Figure 1.54. The walls of this pattern are very jagged which indicates a significant amount of swelling had occurred. In addition, the solvent was not able to quantitatively clean out the exposed area which resulted in incomplete removal of the planarizing layer during RIE. Another developing solvent tried was isoamyl acetate and the sensitivity curve is shown in Figure 1.55. As you can see, a significant degree of thinning occurred which eliminated this solvent. Thinning occurs in the direction normal to the surface and also in the side walls; This broadens the image, resulting in a poor pattern. Finally a good developing solvent was found. 5-Methyl-2-hexanone (5M2H) was used as a developing solvent by dip development for a sustained 30 s and also by an intermittent procedure. The intermittent procedure involved dip developing the sample for 5 s, air drying it, dipping again for 10 s, air drying, and dipping again for 15 s. The resultant sensitivity curves are shown sensitivity of 4.5 $\mu C/cm^2$ and a contrast of 1.2 with minor thinning. The continuous 30 s dip development in 5M2H showed that the sample had a sensitivity of 8.8 $\mu C/cm^2$ and a contrast of

Figure 1.54 Developed and oxygen RIE transferred pattern demonstrating ineffective development procedure.

Figure 1.55 Sensitivity curve for PBS-g-PDMS, 17 wt% PDMS and 10k g/mol grafts, for 30 s dip development in isoamylacetate.

Figure 1.56 Sensitivity curves for PBS-g-PDMS, 17 wt% PDMS and 10k g/mol grafts, dip developed in 5-methyl-2-hexanone for a continuous 30 s and for an intermittent 30 s.

1.7, but thinned more than the intermittent procedure. The preliminary lithographic sensitivity and contrast data for the PBS-g-PDMS copolymer indicates that its lithographic properties are similar to those of PBS. The fact that the sensitivity was comparable with PBS is a little surprising in view of the lower molar mass of the graft copolymers relative to PBS as normally used in lithography. The graft copolymers are not as soluble as the poly(alkenyltrimethyl-silane sulfone)s[101]; therefore, their limited solubility facilitates a wider choice of developing solvents.

The lithographic potential of the PBS-g-PDMS copolymers was demonstrated by transferring a high density periodic lithographic pattern through the resist to the novolac substrate, Figures 1.57 and 1.58. The pattern was exposed on an 1800 Å thick PBS-g-PDMS layer using a 4 C/cm^2 exposure dose followed by a 30 s dip development in 5M2H and the developed pattern was transferred by an oxygen RIE for 13 minutes. The SEMs show that good resolution was obtained for 0.5μm lines with a 1.0μm and a 1.5μm pitch. In addition, no undercutting of the surface occurred resulting in well defined wall shapes. It must be kept in mind thatthe entire lithographic evaluation was preliminary and was not optimized in the slightest. In fact, the most

Figure 1.57 Oxygen RIE transfer of pattern from a bilayer resist setup with 0.5μm lines with a 1.0μm and a 1.5μm pitch.

Figure 1.58 Side view of oxygen RIE transfer of pattern from a bilayer resist setup with 0.5μm lines with a 1.0μm pitch.

rigorous conditions were used, 13 min of RIE, and the material still performed quite excellently.

CONCLUSIONS

The strong working relationships developed and sustained between the author and other scientists which include physical chemists, materials science engineers, chemical engineers, surface chemists, spectroscopists, and other synthetic chemists have resulted in a number of significant conclusions. Without the interdisciplinary approach, many of these conclusions would not have been drawn. Specific conclusions are as follows:

(1) GTP is a well established technique that allowed for the synthesis of hydroxyl functionalized PMMA of controlled molar mass having a narrow molar mass distribution.

(2) The conversion of the primary hydroxyl functional PMMA oligomer to a methacryloyloxy functionalized PMMA macromonomer allowed for the synthesis of PMMA-g-PMMA systems using living anionic copolymerization methods. The materials had not only narrow molar mass distributions for their graft parts but also for their backbone parts.

(3) The anionic ring opening polymerization of D_3 is a living polymerization that does not show any signs of the presence of equilibration reactions. In addition, it allows for the synthesis of highly functionalized PDMS macromonomers having controlled molar masses and narrow molar mass distributions.

(4) The free radical copolymerization of the methacryloyloxy functionalized PDMS macromonomer with MMA results in graft copolymers that have broad composition distributions that correlate well with theory.

(5) The anionic copolymerization of the methacryloyloxy functionalized PDMS macromonomer with MMA results in very well-defined graft copolymers that have very narrow molar distributions for both the graft parts and the backbone parts. In addition, the composition distributions

for the anionically copolymerized PMMA-g-PDMS copolymers are relatively narrow compared to their free radically copolymerized analogues, in keeping with the principles of of living polymerizations.

(6) The copolymerization of 5-ethylidene-2-norbornene with sulfur dioxide produces soluble poly(5-ethylidene-2-norbornene sulfone)s possessing a slightly higher than a 1:1 alternating stoichiometry (SO_2 to nonomer) and a majority of unreacted ethylidene groups left intact. The degree of branching was shown to be a strong function of temperature with increasing branching with a concomitant increase in temperature.

(7) The terpolymerization of hexenyl functionalized PDMS macromonomers with butene and sulfur dioxide results in PBS-g-PDMS copolymers. The PBS-g-PDMS copolymers were found to be a multiphase material whose degree of microphase separation and surface domination by PDMS was found to be a function of the wt% PDMS and of the graft molar mass at equivelent compositions.

(8) The PBS-g-PDMS copolymers were found to be very resistant to oxygen RIE processes at a lower wt% silicon than is typically seen. This is due to two reasons. First, the enhanced surface domination by PDMS results in an actually higher level of silicon at the top few nanometers of the surface. Second, the silicon present in PDMS is already bound to two oxygens and the previously reported values for the minimum amount of silicon was for molecular dispersed silicon in the form of trialkylsilyl moieties.

(9) The PBS-g-PDMS copolymers proved to be excellent lithographic resists as demonstrated by the transfer of a high density lithographic pattern having excellent resolution at least down to 0.5 um, the limit of testing!

FUTURE WORK

As one might suspect from such a diverse selection of polymeric systems, many interesting directions for future investigations have arisen and should be explored. It is the anticipation of the author that few of these will be pursued by the author at The University of North Carolina at Chapel Hill in collaboration with the Falculty at Virginia Tech. Some interesting areas include the following.

(1) It has recently been observed that the dynamic maechanical spectrum of the PMMA-g-PMMA materials showed a reproducable bimodal loss dispersion peak in the region of the expected glass transition temperature which seemed to be a function of the weight fraction of the grafts incorporated. It was never originally considered, but the backbone of the branched system was made by an anionic polymerization mechanism and should have a stereochemical microstructure of about 78% syndiotactic. The grafts on the other hand were made by GTP using tetrabutylammonium benzoate as the catalyst in THF and should be about 48% syndiotactic. It is well known that predominately syndiotactic PMMA will form a stereocomplex with predominately isotactic PMMA. It may be possible that in the bulk state, the PMMA-g-PMMA materials due to their different microstructures are forming a small degree of association that breaks up upon heating. This may be an inherent toughening mechanism for this system an should be explored in greater detail for verification and exploitation.

(2) The methacryloyloxy functionalized alkyl methacrylate macromonomers, of which t-butyl methacrylate could be used, should be incorporated into other systems to give industrially interesting materials exhibiting elastomeric multiphase properties.

(3) The CCD and its influence on polymer morphology and physical properties should be further explored. It is anticipated that the CCD plays an as important role in polymer properties as does the molar mass distribution.

(4)   The CCD should be further investigated for the PMMA-g-PDMS materials copolymerized using group transfer polymerzation.

(5)   The charge transfer complex formed between sulfur dioxide and 5-ethylidene-2-norbornene should be investigated as to its role in forming the resultant copolymer.   In addition, the deep UV sensitivity of this material may be interesting to investigate in light of the recent investigations by Japanese researchers using the poly(styrene sulfone)s as UV resists.

(6)   Post reactions should be further explored on the unreacted ethylidene moiety present in the poly(olefin sulfone)s derived from 5-ethylidene-2-norbornene.

(7)   The general concept of imparting resistance to various reactive ion etching plasmas into radiation sensitive materials should be further explored.

(8)   A fundamental study should be performed on the influence that the degree of polymerization has on the morphological charateristics of graft copolymers.   It was pointed out in the Results and Discussions Section - Part 1 that the expected influence that the CCD and the number of junction points per molecule have on polymer morphology are divergent with one another.   A series of graft copolymers could be synthesized having identical compositions and graft molar masses but different degrees of polymerization.   The various series of materials could be characterized by light scattering to obtain their P and Q parameters, which reflect their CCDs.   In addition, their morphological charateristics could be evaluated by SAXS for equilibrium morphologies obtained by thermal methods, void of solvent influences.

(9)   A technologically important issue that is starting to gain attention is the determination of the limit in dimensions for microphase separated domains before they begin to affect the the limits of lithographic pattern definition.

PART 2

INVESTIGATIONS OF ALUMINUM PORPHYRINS AS INITIATORS IN

LIVING POLYMERIZATIONS

LITERATURE REVIEW

INTRODUCTION

Detailed knowledge of the reaction mechanisms involved in various living polymerizations is a continuing goal of macromolecular chemistry. Information and insight into these processes is essential in order to scientifically attempt to control and modify the resultant polymers as well as to optimize the polymerization process itself.[102,103,104,105,106] One such living polymerization system that has generated significant academic as well as industrial interest is the (5,10,15,20-tetraphenylporphinato)aluminum initiators reported by Inoue.[107]

This section of the dissertation, Part 2, deals with investigations of the aluminum porphyrin polymerization system. It begins with a literature review, focussing primarily on work reported from the laboratories of Professor Inoue, on the use of aluminum porphyrins as initiators and catalysts for the living polymerizations of alkylene oxides, lactones, and methacrylates and the alternating living copolymerizations of alkylene oxides and cyclic anhydrides to form polyesters and of alkylene oxides and carbon dioxide to form aliphatic polycarbonates. This will be followed by a brief literature review of aluminum-27

NMR and its utility for the analysis of organoaluminum compounds.

Following the Literature Review Section, the details of the experimental investigations will be presented followed by the Results and Discussion Section. The research has followed two different paths. One involved the attempted synthesis of novel polymeric materials using a monomer that would result in a semicrystalline polymer. The other involved the initial studies into mechanistic investigations using aluminum-27 nuclear magnetic resonance spectroscopy. This will be succeeded by some preliminary conclusions and list of areas for future consideration. The Literature Review - Part 2 will now follow.

LIVING POLYMERIZATIONS USING ALUMINUM PORPHYRINS

In 1981, Aida and Inoue[108] reported the living polymerization of epoxides with metalloporphyrins derived from diethylaluminum chloride (DEAC) and (5,10,15,20-tetraphenyl)porphine (TPPH$_2$). They found that the initiator, (5,10,15,20-tetraphenylporphinato)aluminum chloride (TPPAl-Cl), would polymerize ethylene oxide, propylene oxide, and 1,2-butene oxide to produce living polymers having narrow molar mass distributions. They synthesized di- and triblock copolymers using sequential additions of different monomers after quantitative conversion of the preceding monomer yielding polymers of controlled molar mass having narrow molar mass distributions.

Since that initial report, Inoue and coworkers have continued to extend the applicability of the aluminum porphyrin initiator system to other monomers. In 1982,[109] they disclosed that TPPAl-Cl could be used to also incorporate a certain percentage of carbon dioxide into the system with propylene oxide to form aliphatic carbonate linkages; however, they only managed to incorporate 22 mol% of carbon dioxide, resulting in less than a 1:1 alternating copolymer structure. A key observation was that the polymers all had narrow molar mass distributions. It was several years later that they reported the successful

formation of an exactly alternating 1:1 copolymer with carbon dioxide. This will be discussed later.

In 1984, TPPAl-Cl was used to polymerize 4-membered lactones[110], specifically ß-propiolactone and ß-butyro-lactone, in a living manner. This allowed for the preparation of polyester-polyether block copolymers of controlled molar mass having a narrow molar mass distribution. In 1987,[111] Inoue and coworkers extended this concept to the living polymerization of six membered $\hat{\delta}$-valerolactone. In addition, some very interesting kinetic data were obtained. It was shown that TPPAl-Cl was not an active initiator/catalyst for for the polymerization of Ł-valerolactone. However, a modified version of the initiator, TPPAl-OR, did bring about the living polymerization of ζ-lactone. The most remarkable observation was that upon the addition of TPPAl-Cl to the polymerization system initiated with TPPAl-OR, an acceleration was observed, as shown in Figure 2.1, without losing the living character. The molar mass of the polymers was independent of the amount of added TPPAl-Cl and only depended on the ratio of monomer to TPPAl-OR. In addition, it was determined that the rate of the reaction was first order with respect to TPPAl-OR, first order with respect to TPPAl-Cl, and first order with respect to monomer, thus third order overall. When TPPAl-Cl was absent from the

system, the reaction was found to be second order with respect to TPPAl-OR and first order with respect to monomer. Further, they spectroscopically confirmed the coordination of δ-valerolactone to TPPAl-Cl using strong proton NMR shifts for the free monomer relative to the coordinated monomer. Supported by these findings, they proposed that two aluminum porphyrin molecules participated in the propagation step as shown in Scheme 2.1. Based on these results, they also suggested that this process applies for the polymerization of epoxides, too. But they gave no experimental evidence to support their claim.

The versatility of the aluminum porphyrin system was extended in 1985[112] and 1987[113] when Inoue and coworkers showed that protic reagents, such as alcohols, carboxylicacids, hydrogen chloride and water, acted as chain transfer agents. They showed that these protic reagents lowered the molar mass of the resultant polymers but did not terminate the polymerization, as they would for conventional anionic polymerization processes. This led Inoue to coin the phrase "immortal" polymerization for a living polymerization process that could withstand the presence of acidic hydrogens. McGrath and coworkers[114] extended this idea to bisphenolic compounds to synthesize secondary dihydroxyl functional polymers using chain transfer agents based on bisphenol-A. In addition, primary dihydroxyl

Figure **2.1** Time-Conversion Curve ⌐or the Polymerization of δ-valerolactone with TPPAl-OMe in the Absence of TPPAl-Cl (open circles) and in the Presence of TPPAl-Cl (closed circles) at 50 °C Without Solvent.[115]

Scheme 2.1 Proposed Polymerization Mechanism Showing
Participation by Two Aluminum Porphyrin Molecules.[115]

functional PPO and dinitro functional PPO were prepared using benzyl alcohol and nitrophenol chain transfer agents, respectively, followed by coupling of the polymer molecules with diacid chlorides. The dinitrophenyl and the derived diaminophenyl PPO oligomers were also demonstrated to display remarkably enhanced thermooxidative stability, relative to commercially available PPO.[116]

In 1985,[117] Inoue reported that they were able to incorporate equimolar amounts of carbon dioxide or cyclic anhydrides with epoxides to form exactly alternating 1:1 copolymers yielding aliphatic polycarbonates or polyesters, respectively. These polymers were shown to have controlled molar masses and narrow molar mass distributions. This was achieved by adding a stoichiometric amount of a quaternary organic salt, such as tetrabutylammonium bromide or tetraphenylphosphonium bromide, to the aluminum porphyrin initiator system. They showed that this was the first example of a catalytic reaction to occur simultaneously on both sides of a metalloporphyrin plane. The anion of the quaternary organic salt was said to be activated as a nucleophile by the aluminum porphyrin. They determined the structure of the active growing species to be a novel six-coordinate aluminum porphyrin carrying one reactive axial ligand on both sides respectively of its square planar N_4Al

skeleton. The synthetic utility of this technique was exploited to synthesize well-defined polyesters and block copolyesters[118] and well-defined aliphatic polycarbonates and block copolycarbonates.[119]

One of the most interesting extensions of the aluminum porphyrin system has been to the synthesis of poly(alkyl methacrylate)s.[120] Inoue and coworkers demonstrated that TPPAl-Me polymerized methyl methacrylate in a living manner when the system was irradiated by visible light. They synthesized block copolymers of methyl methacrylate and butyl methacrylate. Using proton NMR with t-butyl methacrylate, they showed that the active chain end consisted of an aluminum-enolate bond. The aluminum-enolate structure was not only shown with α,β-unsaturated esters but also with α,β-unsaturated ketones.[121] In fact, the (porphinato)aluminum enolates, formed by hydrogen abstraction from a ketone by (porphinato)aluminum diethylamide, TPPAl-Et, or (porphinato)aluminum thiolate, were all found to be in the Z geometric isomer form by proton NMR. They also showed that the (porphinato)aluminum enolates rapidly exchanged, similar to the (porphinato)-aluminum alkoxides and phenates.

It is probably safe to say that no other living polymerization method has been demonstrated to have the

versatility that the aluminum porphyrin system possesses. It is this reason alone that we are interested in understanding this system in greater detail. The next section will describe the usefulness of aluminum-27 nuclear magnetic spectroscopy and how it can be employed to study aluminum porphyrins.

ALUMINUM-27 NUCLEAR MAGNETIC RESONANCE

Aluminum-27 is a very favorable nucleus for NMR investigations.[122] This is due to its high natural abundance and its favorable ratio of line width to spectral range. The drawback of aluminum-27 NMR is that line widths can vary from 3 Hz to several thousand Hz. This negative aspect is counterbalanced by two very significant and extremely useful pieces of information obtainable from ^{27}Al NMR spectra.

The first important aspect of aluminum-27 NMR spectra of organoaluminum compounds is the correlation that has been established by many workers in the field[122,123] between the δ-value (ppm), or chemical shift, and the coordination number of the aluminum atom. The δ-values (ppm) and the coordination number for many organoaluminum compounds have been compiled by Benn and coworkers and are listed in Table 2.1 along with some additional entries. The δ-values in the 250+ ppm range have been attributed to a tricoordinated aluminum atom. The tetracoordinated aluminum atom δ-values have been established to be in the 140-180 ppm region. In the dimeric complexes of pentacoordinate aluminum atoms, the δ-values lie in the 110 - 120 ppm range; however, in the pentacoordinate adducts of aluminumtri-chloride and aluminumtribromide, the δ-value is between 35 ppm and 63 ppm. Hexacoordinate organoaluminum compounds

Table 2.1 Summary of organoaluminum compounds: correlation of chemical shift values. line width (Hz) and coordination number (C.N.).

COMPOUND	∂ (^{27}Al, PPM)	$W_{1/2}$	C. N.
1. iPr$_3$Al	256	5900	3
2. iBu$_3$Al	276	6300	3
3. tBu$_3$Al	255	6100	3
4. Et$_3$Al	154	2550	4
5. nBu$_3$Al	152	7800	4
6. Et$_2$AlH	157	4500	4
7. Et$_2$AlCl	167	3300	4
8. Et$_2$AlNEt$_2$	160	1220	4
9. Et$_2$AlOEt	151	2450	4
10. Et$_2$AlO(CH$_2$)$_3$OEt	150	7200	4
11. Me$_2$AlO(CH$_2$)$_2$OMe	121	1830	5
12. Et$_2$AlO(CH$_2$)$_2$OEt	126	6000	5
13. Et$_2$AlO(CH$_2$)$_2$NEt$_2$	112	7200	5
14. Cl$_3$Al...2PEt$_3$	59	—	5
15. Cl$_3$Al...2Me$_2$PPh	59	—	5
16. Cl$_3$Al...2THF	63	240-500	5
17. Br$_3$Al...2THF	49	500	5
18. Al(H$_2$0)$_6$$^{3+}$	0	2.5-40	6
19. (acac)$_3$Al	0	100	6
20. Al(EtOH)$_6$$^{3+}$	0	70	6
21. Al(DMSO)$_6$$^{3+}$	1.8	5.5	6

have δ-values in the range of -40 to +20 ppm and this is the region that has been termed the octahedral region of the spectrum.[124] In general, inspection of Table 2.1 shows that aluminum-27 chemical shifts can be catagorized according to the degree of substitution about the aluminum atom.

The other important information obtained from aluminum-27 NMR spectra of organoaluminum compounds has to do with their molecular symmetries. Aluminum-27 has a high spin number of 5/2 which results in a nuclear quadrupolar moment that strongly interacts with the electric field gradients that originate in an asymmetric arrangement of the ligands around the aluminum(III) cation.[125] The very broad aluminum-27 NMR line widths are a result of the relaxations of the quadrupole moment. An important consequence of this is that the highly symmetric aluminum bonding configurations, such as those compounds belonging to the O_h and T_d Schoenflies point groups, have much sharper aluminum-27 NMR line widths. Conversely, a necessary correlation to this statement is that any breakdown in the symmetry of the compound shouls result in broadening of the aluminum-27 NMR line widths. This broadening should take place without a dramatic change in the chemical shift, as outlined earlier and substantiated by the values in Table 2.1.

EXPERIMENTAL

PURIFICATION

This section describes in detail the purification of the many reagents used throughout this work involving the study of aluminum porphyrins. Particular emphasis was placed not only on the purification of the reagents but also in their subsequent handling under anaerobic conditions when necessary; for example, use of syringe techniques, cannulas, and inert manipulations in a glove box for air sensitive reagents.

Nitrogen

Prepurified nitrogen was purified as described in the Experimental Section - Part 2.

Glassware

The glassware was rigorously cleaned and dried as explained in the Experimental Section - Part 2.

Reagents

Dichloromethane and Chloroform-d. Dichloromethane (Mallinckrodt, Analytical Grade) was washed with concentrated sulfuric acid, aqueous sodium bicarbonate, and

with distilled water until the aqueous layer was neutral to litmus paper. The solvent was then dried with magnesium sulfate, refluxed over calcium hydride for 48 h under nitrogen then fractionally distilled and the middle fraction was collected. The solvents were subsequently stored in dark bottles under nitrogen for only short periods of time (2-3 days) and handled using airless syringe techniques.

(5,10,15,20 - Tetraphenyl)porphine (TPPH$_2$). TPPH$_2$ (Aldrich) was recrystallized twice from chloroform/methanol. Typically, 350 mL of distilled chloroform was added to ca. 15 g of TPPH$_2$ in a 500 mL Erhlemeyer flask and the solution was brought to reflux. About 50 mL of distilled methanol was added and the solution was brought back to reflux and concentrated by evaporation of ca. 20 mL of solvent. The solution was slowly allowed to cool to room temperature then stored for two days at -20 °C. The purified TPPH$_2$ was filtered and washed three times with hexanes and dried under reduced pressure at 50 °C.

Alkyl Aluminiums. Triethylaluminum (TEA), trimethylaluminum (TMA), and diethylaluminum chloride (DEAC) were kindly supplied by Dr. Tom Hanlon from Ethyl Corporation. For the polymerization studies, the alkylaluminums were used as received, usually 1.9 M in heptane. For the mechanistic studies, however, TEA and TMA

were further purified. Triethylaluminum was vacuum distilled immediately prior to use and handled under inert conditions. Trimethylaluminum was fractionally distilled under nitrogen immediately prior to use. The extremely pyrophoric trialkylaluminums were handled and transferred in a glove box for the mechanistic studies using microliter gas tight syringes. For the polymerization studies, the alkylaluminums were handled using the usual syringe techniques.

Monomers. Propylene oxide (PO) (DOW Chemical Company) and isobutylene oxide (iBO) (ARCO Chemical Company) were kindly provided and stored over 4 Å molecular sieves prior to use. The monomers were generally stirred for ca. 12 h over calcium hydride (1 g/100 mL) and a small amount of potassium hydroxide (0.1 g/100 mL). They were then fractionally distilled under prepurified nitrogen and the middle fraction was collected. The monomers were always distilled immediately prior to use and were handled using anaerobic techniques.

Miscellaneous Reagents. Acetic acid (Aldrich) (20 mL) was refluxed and distilled from acetic anhydride (1 mL) and KMnO4 (0.5 g). Trifluoroacetic acid (Aldrich) and pivalic acid (Aldrich) were used as received and handled under nitrogen. Tetraethylammonium acetate was obtained by the

.

dehydration of the commercial tetrahydrate complex (Aldrich) by azeotropic distillation with previously distilled benzene using a Dean-Stark trap for 24 h. Nitrophenol was recrystallized from chloroform immediately prior to use .

Initiators and Catalysts

Pentacoordinate Aluminum Porphyrins. (5,10,15,20-Tetraphenylporphinato)ethylaluminum (TPPAl-Et), (5,10,15,20-tetraphenylporphinato)aluminum chloride (TPPAl-Cl) and (5,10,15,20-tetraphenylporphinato)methylaluminum (TPPAl-Me) were prepared by dissolving 1.0 mmol $TPPH_2$ in purified dichloromethane (0.0325 M) under 6-8 psig (42-56 kPa) nitrogen atmosphere at 25 °C in a previously dried round bottom flask fitted with a septum and a stir bar. After dissolution, 1.0 mmol of TEA, DEAC, or TMA was added in a glove box (for polymerization studies, the alkyl aluminums were handled using only gas tight syringes) and allowed to react for 12 h to yield TPPAl-Et, TPPAl-Cl, and TPPAl-Me, respectively.

(5,10,15,20-Tetraphenylporphinato)aluminum carboxylates were prepared by adding 1.0 mmol of the corresponding acid to TPPAl-Me. Acetic acid and trifluoroacetic acid were added neat and pivalic acid was added as a solution in chloroform (0.963 M) to form $TPPAl-OOCCH_3$, $TPPAL-OOCCF_3$, and $TPPAl-OOCCMe_3$.

Hexacoordinate Aluminum Porphyrin. The hexacoordinate (5,10,15,20-tetraphenylporphinato)aluminum pivalate adduct with a quaternary ammonium salt was prepared by adding 1.0 mmol of purified tetraethylammonium acetate (0.403 M in

chloroform) to 1.0 mmol of TPPALOOCCMe$_3$ in dichloromethane
and allowed to react for 12 h.

Polymer Synthesis

Poly(propylene oxide). Coordinated anionic
polymerizations of PO were carried out in rigorously cleaned
and flame dried one-neck round bottom flasks equipped with a
Teflon coated magnetic stirring bar and a rubber septum
secured with copper wire under a 6-8 psig (42-56 kPa)
prepurified nitrogen atmosphere. The initiators used were
either TPPAl-Cl or TPPAl-Et. Typically, the initiator was
synthesized in situ by weighing a calculated amount of TPPH$_2$
into the dried reaction flask, resealing with a three-way
stop cock fitted with a septum and purging with dry
nitrogen, followed by dissolution in purified
dichloromethane (3 w/v%). A stoichiometric amount of either
TEA or DEAC was added and allowed to react for 5 h. If it
was desired to measure the molar mass by end group analysis,
an aromatic chain transfer agent was added at this point to
TPPAL-Et, such as nitrophenol, and allowed to react for 2 h.
Usually the ratio of nitrophenol to TPPAl-Et was either 1:1
or 2:1. Once the desired initiator was formed, purified PO
monomer was added via syringe at room temperature and an
exotherm would immediately follow. After an appropriate
time, the volatile fractions were vacuum stripped and the

percent conversion was measured gravimetricly by knowing the initial tare. The polymer was isolated by adding a large excess of methanol to coordinate to the initiator, followed by stripping the volatile fraction again, redissolving in hexanes and filtering the precipitated initiator.

Poly(isobutylene oxide). Polymerization of iBO was marginally successful under appropriate conditions. A modified Fisher-Porter bottle, similar to the one described in Appendix A, was utilized. The TPPAl-Et initiator was made directly in the reactor (a 20% excess of TEA was used instead of the usual stoichiometric amount) and the volatiles were stripped to leave the crystalline purple initiator. The initiator was then dissolved in neat purified iBO and the reactor was brought to 60 °C under ca. 25 psig. After 8 days, the reactor was cooled to room temperature and methanol was added to the slurry. The product was isolated by filtration (38% yield).

NMR Experiments

The above aluminum porphyrin compounds were isolated for analysis by stripping the solvent under vacuum at 25 °C. The dried powders were then transferred from the round bottom flasks to small test tubes in a glove box, followed by dissolution in purified chloroform-d under nitrogen (2

w/v%). Each solution was transferred to a previously dried 10 mm NMR tube (Wilmad) via cannula and sealed under vacuum at -78 °C.

Proton and carbon-13 NMR measurements were recorded on a Bruker WP 200 spectrometer operating at 200.135 and 50.324 MHz, respectively. Occasionally, proton NMR measurements were measured on a Bruker WP 270 spectrometer operating at 270.132 MHz The carbon-13 spectra were obtained using either an inverse gated decoupling pulse sequence or, to aid in making signal assignments, using a Distortionless Enhanced by Polarization Transfer pulse sequence commonly known as a DEPT experiment. In general, this experiment allows one to edit or separate CH, CH_2, and CH_3 subspectra for unambiguous signal assignments.

Aluminum-27 NMR spectra were recorded on a Bruker WP 200 spectrometer operating at 52.15 MHz. The NMR experiments were made using a 10 mm multinuclear broad band probe. For the aluminum-27 NMR experiments, a 36000 Hz sweep width was used with a 45° pulse width of 10 s. A total of 2000 transients were collected and the background aluminum signal at approximately 67 ppm was eliminated by subtracting the FID of the spectra recorded for an empty NMR tube from the FID of the sample to be analyzed. The FIDs were transformed using an exponential multiplication and a

line broadening of 10 Hz. The chemical shifts (aluminum-27, ppm) for all of the aluminum-27 NMR spectra were reported relative to an external standard comprised of a saturated aluminum acetylacetonate solution in benzene-d_6.

Gel Permeation Chromatography (GPC)

The apparent molar mass and apparent molar mass distributions for PPO were analyzed by GPC. The instrument was a Waters 150-C17 GPC equipped with Ultra Styragel columns of 500, 103, 104, 105, and 106 porosities in THF. The PPO made by TPPAl-Cl was analyzed using the refractive index detector and the PPO made using the nitrophenol modified initiator also used the UV detector at 254 nm.

Differential Scanning Calorimetry

DSC thermograms were obtained on PiBO at ARCO Chemical. The measurements were run on a DuPont Model 2100 Thermal Analysis system at 20°C/min. The sample analyzed was in powder form and only the first heating scan was obtained.

RESULTS AND DISCUSSION

Introduction

The aluminum porphyrin initiator system has been well established in our laboratories as a very versatile method for the preparation of well-defined macromolecules having controlled molar masses and architectures, narrow molar mass distributions, enhanced thermal stabilities, and desired end-group functionalities.[116,126,114] As described in detail in the Literature Review Section - Part 2, the aluminum porphyrin initiators have been shown to polymerize a wide variety of monomers ranging from alkylene oxides and lactones to methacrylates. It is the inherent versatility of this initiator that intrigues us to continue investigating in this area. To this end, our goals have been two-fold. First, we wanted to continue to synthesize novel polymeric materials with controlled molecular characteristics and useful properties. In this regard, we have focussed a portion of our efforts towards the polymerization and attempted block copolymerization of iBO. Poly(isobutylene oxide) has virtually the same temperature-modulus profile as isotactic poly(propylene), i. e. Tg -20 °C and Tm 170 °C. It was therefore desired to synthesize novel di- and triblock copolymers of a low Tg polymer, such as PPO, with PiBO in an effort to make elastomeric materials.

Our second goal was to try to further understand the mechanism of polymerization with the aluminum porphyrins. It has been possible to obtain informative aluminum-27 NMR spectra in an effort to elucidate the mechanism of the aluminum porphyrin initiator system. Aluminum-27 NMR has the unique ability to focus on the active site, the aluminum atom itself, which compliments earlier carbon-13 NMR results[117] and should lead to a further understanding of the mechanism. One precedent for this method of analysis was established as long ago as 1964 when workers in the field began to investigate Ziegler-Natta type polymerization catalysts formed from alkyl aluminums and various titanium compounds.[127] Fortunately, NMR instrumentation has come a long way since that time and is now even more appropriate.

Unfortunately, in all of the reported uses of aluminum-27 NMR to investigate organoaluminum compounds, no one has investigated aluminum compounds where the aluminum atom is centered in an aromatic ring system, where ring current effects can effectively shield the aluminum nucleus. In order to successfully use the reported NMR data and its correlation with symmetry and coordination number, we made several different aluminum porphyrin compounds. These were used to establish where the chemical shift values would be relative to the reported values for this previously uninvestigated class of organoaluminum compounds. In

addition, we were interested in the electronic and steric effects that a fith ligand would have on the aluminum atom. Indirectly, these results may lead us in the right direction to effectively modify the catalyst to increase polymerization rates, to impart stereoselectivity during the process, and to define the limits for living polymerization conditions.

Polymer Synthesis and Characterization

Initiator Synthesis. TPPH$_2$ was first synthesized over fifty years ago by Rothemund[128] who caused benzaldehyde and pyrrole in pyridine to react in a sealed bomb at 150 °C for 24 h. Adler and Longo[129] modified the harsh Rothemund procedure by allowing benzaldehyde and pyrrole to react for 30 min in refluxing proprionic acid (141 °C) open to the air. The TPPH$_2$ used in these experiments was purchased from Aldrich and recrystallized.

The recrystallization procedure for TPPH$_2$, described in the Experimental Section - Part 2, was utilized to attempt to remove the 2-3% of $\alpha,\beta,\gamma,\delta$-tetraphenylchlorin. Figures 2.2 and 2.3 show the endothermic melting transitions by DSC for TPPH$_2$ as received from Aldrich (T$_m$ = 454 °C) and after recrystallization (T$_m$ = 456 °C). It is evident that a small percent of an impurity still remains.

The first step of the synthesis of the initiator used for the synthesis of aromatic nitro terminated PPO is shown in Scheme 2.2. A 1:1 stoichiometric equivelent of triethylaluminum (TEA) was added to TPPH$_2$. Upon addition of TEA, two moles of ethane evolved as the initiator, TPPAl-Et, was generated. The ^{1}H NMR spectra for TPPH$_2$ and TPPAl-Et are shown in Figure 2.4 and Figure 2.5, respectively. The unusually large upfield shift observed for the internal

amine protons can be attributed to the strong shielding environment that these protons are found due to the significant aromatic ring currents of the porphyrin macrocycle. Figure 2.5 shows the disappearance of the amine protons at -1.45 ppm and the appearance of the methyl and methylene protons shifted up field to -3.5 ppm and -6.4 ppm. The power gated and DEPT ^{13}C NMR spectra for TPPH$_2$ are shown in Figure 2.6. There are seven different carbons present in TPPH2; however, the lower ^{13}C NMR shows only five carbon signals and one broad carbon signal. Using the DEPT experiment to eliminate quaternary carbons, we have made the assignments as shown. Upon the formation of TPPAl-Et, the broad ^{13}C NMR signal for carbons f and g become resolved, shown in Figure 2.7, due to the large electronic influence imparted by the aluminum atom. The initiator was then modified by adding either a 1:1 ratio or a 2:1 ratio of nitrophenol to TPPAl-Et to form TPPAl-O-Ar-NO$_2$ as shown in Scheme 2.3.

Poly(propylene oxide). The polymerization involved the addition of purified PO to the TPPAl-O-Ar-NO2 initiator already formed in the polymerization flask as shown in Scheme 2.4. As was described in the Experimental Section - Part 2, the initiation step involves insertion of the firstmonomer unit between the aluminum-phenate bond to form an aluminum-alkoxide bond. Propagation involves the

Figure 2.2 DSC thermogram of as received $TPPH_2$.

Figure 2.3 DSC thermogram of once recrystallized TPPH$_2$.

Scheme 2.2 Synthesis of TPPAl-Et.

Al (Et)$_3$ +

2 ethane

TPPH2.001
DATE 12-6-89

SF   200.132
SY   80.1300000
O1   2530.000
SI   32768
TD   16384
SW   4504.505
HZ/PT   .275

PW   15.0
PD   1.000
AQ   1.819
RG   4
NS   32
TE   297

FW   5700
O2   3200.000
DP   63L PO

LB   .300
GB   0.0
CX   20.00
CY   5.0
F1   12.180P
F2   -10.304P
HZ/CM 224.992
PPM/CM 1.124
SR   2345.18

Figure 2.4 ^{1}H NMR of TPPH2.

TPPALET IN CDCL3

Figure 2.5 ^{1}H NMR of TPPAl-Et.

Figure 2.6 ^{13}C NMR spectra for TPPH$_2$.

Figure 2.7 ^{13}C NMR spectra of TPPH$_2$ and TPPAl-Et.

Scheme 2.3 Synthesis of modified initiator.

Scheme 2.4 Synthesis of PPO using TPPAl-O-Ar-NO$_2$.

$$\text{Al—O-Ar-NO}_2 \quad + \quad \underset{\text{H}_2\text{C} \quad \text{CH(CH}_3)}{\overset{\text{O}}{\triangle}}$$

25 °C

$$\text{Al—O—CH—CH}_2\text{—O-Ar-NO}_2$$
$$\underset{\text{CH}_3}{|}$$

$$\underset{\text{H}_2\text{C} \quad \text{CH(CH}_3)}{\overset{\text{O}}{\triangle}}$$

25 °C

$$\text{Al—O—CH—CH}_2\text{—(—O—CH—CH}_2\text{—)}_n\text{—O - Ar - NO}_2$$
$$\underset{\text{CH}_3}{|} \qquad\qquad\qquad \underset{\text{CH}_3}{|}$$

CH$_3$OH

$$\text{Al—O—CH}_3 \qquad \text{H—(—O—CH—CH}_2\text{—)}_n\text{—O - Ar - NO}_2$$
$$\underset{\text{CH}_3}{|}$$

Figure 2.8 ^{1}H NMR of functionalized PPO.

Scheme 2.5 Side reactions present during metal alkoxide initiated polymerization of propylene oxide.

$$HO\text{-}(CH_2\underset{\underset{CH_3}{|}}{CH}\text{-}O^-)\ K^+\ +\ \overset{O}{\underset{}{\triangle}}CH_3$$

$$\downarrow$$

$$HO\text{-}(CH_2\underset{\underset{CH_3}{|}}{CH}\text{-}O)\text{-}H\ +\ K^+\ {}^-CH_2\text{-}\overset{O}{\underset{}{\triangle}}$$

$$\downarrow$$

$$CH_2\text{=}CH\cdot CH_2\text{-}O^-\ K^+$$

$$\downarrow$$

$$CH_2\text{=}CH\cdot CH_2\text{-}O\text{-}(CH_2\underset{\underset{CH_3}{|}}{CH}\text{-}O)_n H$$

continual insertion of PO into the aluminum-alkoxide bond to afford high polymer of controlled molar mass. The resultant polymer has an aromatic nitro group on one end and a secondary hydroxyl group on the other end. A ^{1}H NMR is shown in Figure 2.8 which demonstrates the aromatic nitro end group and the absence of any unsaturation which is common for metal hydroxide catalysts as shown in Scheme 2.5.

In addition, by end group analysis, the number average molar mass was determined to be 2.6k g/mol which was good considering that the target value was 2.5k g/mol. A typical GPC trace is shown in Figure 2.9. The observed narrow molar mass distribution illustrates the living nature of the process.

Poly(isobutylene oxide). The polymerization of iBO involved the use of higher temperatures and pressures due to the sterically hindered nature of the monomer and the crystallinity of the polymer. The TPPAl-Et form of the initiator was used, as shown in Scheme 2.6, due to its higher initial reactivity over TPPAl-Cl. Only limited success has been achieved with the polymerization of this monomer and only under certain conditions. A modified Fisher-Porter bottle similar to that presented in Appendix A was utilized for the reaction, but it was not fitted with an

Figure 2.9   GPC trace of functionalized PPO made by
TPPAl-O-Ar-NO$_2$.

Scheme 2.6 Synthesis of poly(isobutylene oxide) by metalloporphyrin.

overhead stirrer or a heating/cooling coil. The TPPAl-Et form of the initiator was made directly in the reactor by dissolving the $TPPH_2$ in purified dichloromethane. A 20 mol% excess of TEA was added and the reaction was allowed to stir for 12 h, followed by stripping the volatile fraction (solvent and excess TEA) for 2 h at 60 °C under vacuum. The cyclic monomer, iBO, was added via syringe directly to the solid initiator to form a homogeneous solution. The reaction was stirred with a magnetic stirring bar and the reactor was heated by submerging the bottle into an oil bath at 60 °C. The polymerization was allowed to procede for 8 days at 60 °C. There was no evidence at 60 °C after eight days of an increase in viscosity, although it was difficult to see since the reactions are very dark. Upon cooling the sample to room temperature, however, a free flowing slurry formed which seemed to be small precipitates in the low viscosity monomer. The precipitates were removed by filtration and a 38% yield was calculated based on the weight of the precipitated fraction. The initial ratio of monomer to initiator for the bulk polymerization would have yielded a polymer of 20k g/mol had the reaction gone to 100% conversion. The 38% yield corresponds to a molar mass of 7.6k g/mol assuming a living polymerization without any chain transfer. The precipitate was insoluble in all

solvents tried at room temperature but showed marginal solubility in xylenes and diglyme at temperatures greater than 110 °C. The DSC thermogram is shown in Figure 2.10. The sample shows two endothermic peaks, one at 132 °C and one at 155 °C. The lower than expected melting point is probably due to the low molar mass of the polymer, since high molar mass PiBO has a melting point of 170 °C.

Attempted Block Copolymerization of PO and iBO. It was desired to make block copolymers of PO and iBO for several reasons. The materials would have certainly showed multiphase characteristics leading to elastomeric properties at certain compostions. In addition, it was envisioned that one may be able to impart solubility to the PiBO if there was a long enough segment of PPO covalently bound to it. With these things in mind, several nonsuccessful experiments were tried. First, PPO was polymerized with TPPAl-Cl in solution, followed by the addition of iBO monomer after 3 days. The results showed no additional reaction after the PO conversion. A second experiment involved stripping the solvent after the polymerization of PO in order to have a bulk polymerization for the iBO segment. But again, no conversion of iBO was observed as shown by the ^{1}H NMR in Figure 2.11. The spectrum was obtained on the reaction product after 3 days at 50 °C and shows only PPO.

Figure 2.10 DSC thermogram of poly(isobutylene oxide).

Figure 2.11 ^{1}H NMR of product from attempted block copolymerization of PO and iBO.

The above results are very preliminary and a concentrated effort should be given to the synthesis of iBO homo- and block copolymers using the aluminum porphyrin catalyst. The limited success is encouraging, however, and probably more results could have been obtained if high temperature bulk and solution polymerizations were used more extensively.

Multinuclear Magnetic Resonance Spectroscopy

Multinuclear (^{1}H, ^{13}C, and ^{27}Al) magnetic resonance experiments were conducted at various temperatures on several different aluminum porphyrins. The aluminum porphyrin compounds investigated can be divided into two classes: pentacoordinate and hexacoordinate. The four different pentacoordinate aluminum porphyrin compounds are identical except for the fifth ligand.

For these detailed NMR experiments, TMA was used instead of TEA because of the difficulty in distilling TEA with out having any ß-hydride elimination occurring that would result in the formation of ethylene and higher branched alkyl chains. The presence of which is clearly shown in the ^{1}H NMR spectrum of the "purified" TEA shown in Figure 2.12. The higher than C_2 aluminum alkyls are known to give signals around 0.9 ppm and 1.3 ppm,[130] which are clearly evident. The expanded region shows a certain amount of ethylene (5.3 ppm), aluminum hydride (3.8 ppm), and aluminum ethoxide (3.6 ppm).

The pentacoordinate compounds were synthesized according to Scheme 2.7, where the first step was identical in all cases to form TPPAl-Me. The second step involved quantitative removal of the alkyl group bound to the

TEA IN CDCL3/5MM

Figure 2.12   ^{1}H NMR of distilled triethylaluminum.

Scheme 2.7 Synthesis of pentacoordinate aluminum porphyrins.

aluminum with a carboxylate group derived from the corresponding acid to generate a mole of methane.

All of the aluminum-27 NMR spectra shown are baseline corrected as described in the Experimental Section - Part 2 to remove the broad signal inherent in the probe used in the Bruker WP 200 at this frequency. Representative spectra are shown in Figure 2.13. The bottom trace is the result from an NMR tube containing $TPPH_2$ dissolved in the lock solvent, void of any added aluminum reagents. The top spectrum is the result for TPPAl-Et dissolved in the lock solvent under identical conditions. Figure 2.14 is the baseline corrected aluminum-27 NMR spectrum showing removal of the probe signal and removal of the baseline roll.

The variable temperature aluminum-27 NMR spectra for TPPAl-Et are shown in Figure 2.15. The one on the left was at 25 °C, the middle spectrum was at 60 °C and the the spectrum on the right was recorded after cooling the sample back down to 25 °C. Initially at room temperature there seem to be two different aluminum NMR signals in a ratio of approximately 95:5. Upon heating the solution to 60 °C, the broad signal at 43 ppm seems to decline whereas the sharp signal at 20 ppm seems to grown in intensity; but, upon cooling back down to 25 °C, the signal remains essentially

Figure 2.13 ^{27}Al NMR spectra showing background signal and baseline roll.

TPPALET IN CDCL3/BASLINESUBTRACTED

Figure 2.14 Baseline corrected ^{27}Al NMR spectra for TPPAl-Et.

Figure 2.15 Variable temperature ^{27}Al NMR spectra for TPPAl-Et.

the same as it was at 60 °C. The reason for this apparent transformation in the aluminum-27 NMR signal with temperature is unclear at this point.

The ^{1}H NMR spectra for the aluminum porphyrin carboxylates are shown in Figures 2.15 - 2.17 for TPPAl-OOCR where R = -CH$_3$, -CF$_3$, and -CMe$_3$, respectively. The acetate protons are found upfield at -1.5 ppm due to the shielded environment. The spectrum for the trifluoroacetate adduct shows no upfield signal due to the quantitative removal of the aluminum alkyl group. The pivalate protons are found at -1.1 ppm, somewhat downfield from where the acetate protons are found.

The room temperature aluminum-27 NMR spectra for the pentacoordinate aluminum porphyrin carboxylates are shown in Figure 2.19. The first spectrum is for TPPAl-OOCCF$_3$ and the middle spectrum is for TPPAl-OOCCH$_3$. These two compounds are an interesting pair in that they exhibit comparable steric interactions between the fifth ligand and the aromatic porphyrin ring, but should have very different electronic properties due to the large differences in acidity of the corresponding acids. The third spectrum is for TPPAl-OOCCMe$_3$, which is very similar electronically toTPPAl-OOCCH$_3$, but very different sterically. As one can see in the aluminum-27 NMR summary table, Table 2.2, the two

TPPAL00CCH3 IN CDCL3 - 5 MM

BRUKER
TPPALAC.005
DATE 14-9-89

SF   270.133
SY   120.1300000
O1   3500.000
SI   32768
TD   16384
SW   5952.381
HZ/PT   .363

PW   4.0
RD   0.0
AQ   1.376
RG   100
NS   32
TE   297

FW   7500
O2   0.0
DP   63L PO

LB   .300
GB   0.0
CX   20.00
CY   0.0
F1   12.504P
F2   -9.401P
HZ/CM   295.857
PPM/CM   1.095
SR   3065.03

Figure 2.16 ^{1}H NMR of TPPAl-OOCCH$_3$.

TPPALOOCCF3 IN CDCL3 - 5 MM

BRUKER

TPPALAF.005
DATE 14-9-89

SF   270.132
SY 120.1300000
01   3500.000
SI   32768
TD   16384
SW   5952.381
HZ/PT   .363

PW   4.0
RD   0.0
AQ   1.376
RG   80
NS   32
TE   297

FW   7500
02   0.0
DP   63L PO

LB   .300
GB   0.0
CX   20.00
CY   0.0
F1   12.504P
F2   -9.401P
HZ/CM 295.857
PPM/CM   1.095
SR   3065.03

Figure 2.17 ^{1}H NMR of TPPAl-OOCCF$_3$.

TPPALOOOO(CH3)3 IN CDCL3/10MM

BRUKER

TPPALAO.001
DATE 12-6-89

SF   200.132
SY   80.1300010
O1   2530.000
SI   32768
TD   16384
SW   4504.505
HZ/PT   .275

PW   15.0
RD   1.000
AQ   1.819
RG   1
NS   32
TE   297

FW   5700
O2   3200.000
DP   63L PO

LB   .500
GB   .000
CX   20.00
CY   0.0
F1   12.1776
F2   -10.3060
HZ/CM 224.960
PPM/CM 1.124
SR   2345.19

Figure 2.18 ^{1}H NMR of TPPAl-OOCCMe$_3$.

Figure 2.19 ^{27}Al NMR spectra for the pentacoordinate aluminum porphyrin carboxylates.

Table 2.2   Summary of Aluminum-27 NMR Investigations.

SAMPLE		Temp = 25 °C δ (^{27}Al, PPM)	$W_{1/2}$ (Hz)	Temp = 60 °C δ (^{27}Al, PPM)	$W_{1/2}$ (Hz)
Al(NO)$_3$ (D$_2$O)		----	8		
Al(AcAc)$_3$ (sat'd C$_6$D$_6$)		0	180	0	140
Al(CH$_2$CH$_3$)$_3$		155	2500		
TPPAl - CH$_2$CH$_3$	Broad	43	2200	34	2200
	Sharp	20	210	19	300
TPPAl - OOCCF$_3$		12	2680	12	1600
TPPAl - OOCCH$_3$		12	2500	11	890
TPPAl - OOCC(CH$_3$)$_3$		12	1110	13	620

HEXACOORDINATE SALT:

Temp = -60 °C δ (^{27}Al, PPM)	$W_{1/2}$ (Hz)	Temp = 25 °C δ (^{27}Al, PPM)	$W_{1/2}$ (Hz)	Temp = +60 °C δ (^{27}Al, PPM)	$W_{1/2}$ (Hz)
- 22	1960	-12	890	- 7	530

compounds that are sterically very similar and electronically very different (TPPAl-OOCCH$_3$ and TPPAl-OOCCF$_3$) give rise to similar aluminum-27 NMR signals, both in regards to chemical shift and line width. The two compounds that are similar electronically and very different sterically (TPPAl-OOCCH$_3$ and TPPAl-OOCCMe$_3$) have equivalent chemical shift values. In addition, these two compounds give rise to line widths that are different by more than a factor of two at room temperature. Since the line width is reportedly related to the symmetry of the electric field gradient about the aluminum nucleus, we conclude that TPPAl-OOCCMe$_3$ possesses a more symmetric field gradient than TPPAl-OOCCH3, perhaps due to conformational differences.

The hexacoordinate aluminum porphyrin was synthesized by reacting a stoichiometric amount of TPPAl-OOCCMe$_3$ with purified tetraethylammonium acetate as shown in Scheme 2.8. The aluminum-27 NMR analysis of the hexacoordinate aluminum porphyrin at -60 °C, 25 °C, and 60 °C is shown in Figure 2.20 and is summarized in Table 2.2. It was observed that not only did the line width change as a function of temperature, as expected for a quadrupolar nucleus, but so did the chemical shift change. It is important to note that the hexacoordinate aluminum porphyrin has a much greater

Scheme **2.8**   Synthesis   of   hexacoordinate   aluminum
porphyrin.

+ $(CH_3)_3CCOOH$

ETHANE ↑

$(CH_3)_3CCOO$—Al

$(CH_3CH_2)_4N^+ CH_3COO^-$

$(CH_3)_3CCOO$—Al—$OOCCH_3$

$(CH_3—CH_2)_4N^+$

Figure 2.20 Variable temperature ^{27}Al NMR of hexacoordinate aluminum porphyrin.

chemical shift vs temperature slope than does the also hexacoordinate NMR standard, which is nearly zero. This shift in the aluminum-27 NMR signals may be related to the rapid exchanges of the two different carboxylate groups at elevated temperature and their subsequent decrease in exchange rate at low temperature.

Figure 2.21 shows the expanded ^{1}H NMR aromatic region for the hexacoordinate aluminum porphyrin as a function of temperature. The ß-pyrrole protons are found downfield at 8.5 to 8.8 ppm. The spectrum obtained at high temperature shows up to six different ß-pyrrole signals. At room temperature and then at -60 °C, the ß-pyrrole signals change in intensity to the point at -60 °C, only four ß-pyrrole signals are observed. The strong function of temperature on the ß-pyrrole signals of the hexacoordinate aluminum porphyrins was also observed by Inoue and coworkers.[28] It can be related to the dynamic equilibrium that exists between the two different carboxylate groups present and the various combinations that can exist as shown in Figure 2.22.

T = -60 C   T = 25 C   T = -60 C

Figure 2.21 Expanded ^{1}H NMR expanded region for the hexacoordinate aluminum porphyrin as a function of temperature.

Figure 2.22 Possible ligand combinations for the hexacoordinate aluminum porphyrin.

CONCLUSIONS

The aluminum porphyrin living polymerization initiator has been shown to be a more complex system then initially perceived. The initiator has proven itself in the hands of the author to be useful for the synthesis of controlled molar mass PPO having a narrow molar mass distribution with defined end groups. The initiator has also been shown to polymerize isobutylene oxide, to some extent, under more rigorous conditions than is used for PO or EO. However, the applicability of this initiator to make block copolymers of isobutylene oxide and propylene oxide seems real, but elusive as of yet.

Aluminum-27 NMR has proven to be a unique tool to probe this initiator system. It has allowed us to begin to probe the conformational characteristics of the aluminum porphyrins. It has also generated more questions than answers at this point. From the aluminum-27 NMR experiments, it was observed that the chemical shift in aluminum porphyrin complexes is also mainly determined through coordination, whereas electronic and steric factors have little or no effect. But, both pentacoordinate and hexacoordinate aluminum porphyrin complexes have chemical shift values that are far upfield from the pentacoordinate and hexacoordinate complexes reported in the literature.

SUGGESTED FUTURE STUDIES

The research presented here concerning the aluminum porphyrin initiator system has at least laid the groundwork for many future directions to be followed. These include:

(1) The polymerization of isobutylene oxide using more rigorous conditions which include higher temperatures and pressures. In addition, one should establish whether less reactive, stronger Lewis acid porphyrins, such as TPPAl-Cl, can polymerize iBO. If they do not, they should be added to activate the monomer towards propagation.

(2) Along this line, one should investigate other non-metalloporphyrin type Lewis acids that could aid in the polymerization using aluminum porphyrins. These could include chiral Lewis acids for use in PO polymerization.

(3) In light of the industrial interest in primary hydroxyl functionalized PPO, triphenylsilanol or diphenylmethylsilanol could be utilized as chain transfer agents to yield primary functionalized PPO after coupling and hydrolysis.

(4) Using aluminum-27 NMR, the aluminum porphyrins that represent models for the active chain ends during polymerization, such as TPPAl-OEt (EO), TPPAl-OiPr (PO), TPPAl-OtBu (iBO), and TPPAl-enolate (MMA), should be investigated.

(5) The aluminum-27 NMR technique should then be used to study the polymerization itself to gain insight into the nature of the process. This may lead to a logical approach to modify either the process or the reagents in order to expand the practicality of the system.

(6) It was observed that the addition of an acid to TPPAl-Me resulted in quantitative formation of TPPAl-OOCR. Also, it was observed that the hexacoordinate aluminum porphyrin formed quantitatively when a stoichiometric amount of quaternary salt was added to the aluminum porphyrin carboxylates. Taking advantage of the quantitative nature of these reactions, one could form novel polymers containing the metalloporphyrin moiety in the polymer main chain.

303

APPENDIX A - Polymerization Reactor Design

The anionic synthesis of block copolymers and related materials have traditionally been performed using high vacuum rack techniques. In 1986, Hoover and McGrath[131] reported their design for a laboratory scale, low pressure reactor for living polymerization studies. They recognized the need to synthesize large batches of samples in order to study structure/property relationships in an efficient manner. These reactors, built and utilized in Professor McGrath's laboratories, have capacities of approximately 800 mL. They serve their intended purpose excellently.

In working with the synthesis of the poly(1-olefin sulfone)s and with the synthesis of semicrystalline polymers using the aluminum porphyrin catalysts, it was necessary to run these reactions in a vessel other than normal round bottom glassware for several reasons. First, the highly exothermic synthesis of the poly(olefin sulfone)s, specifically poly(norbornene sulfone), often lead to temperature jumps of 50 °C when using only an external cooling bath. This temperature jump obviously coincided with a pressure increase which would sometimes result in expulsion of wired on septa. Secondly, the aluminum porphyrin system often involved running the reactions above the boiling points of the monomers, PO and iBO, which would also generate significant pressure. For these reasons, it

was desired to employ a reactor system similar to the one developed by Hoover, but having the ability to conveniently remove the reactor head and with a capacity on the order of 200 mL. In addition, it was desired to have all of these requirements at 20% of the cost. To this end, a reactor was designed based on the commericially available Fisher-Porter bottles (Lab Crest Scientific Glass Company, Warminster, PA, (215)674-6614). The Fisher-Porter bottles (Model No. 110122 003 and 110122 0006) come with a threaded cap that allows for the addition of reagents using several different accessories. The objective was to use the same method of sealing the cap but to have a modified cap that contained: (1) a stirring assembly, (2) an inlet and outlet for a heating and cooling coil, (3) a septum port, (4) a nitrogen inlet, (5) a vacuum inlet, (6) a temperature controller, (8) a pressure gauge, (9) a vent, and (10) an automatic pressure relief valve. With these requirements in mind, Mr. Herb Rettke made the appropriate drawings and the reactor caps out of 316 stainless steel. A schematic drawing, not drawn to scale, is shown in Figure A.1. The reactor cap has all of the desired inlet and outlet ports that were mentioned above. They were assembled using standard items that can be found in a Swagelok catalogue. The stirring assembly was a Parr A1120HC Magnetic Drive which utilized a swivel blade stirring assembly (C443V632 U01) purchase from Lab Crest.

The technical drafts are shown in Figures A.2 to A.7 and are self explanatory.

STIRRER

PRESSURE
GAUGE

TO VACUUM

N_2

VENT

LIQUID
NITROGEN

COOLING
COIL

THERMOCOUPLE

FISHER-
PORTER
BOTTLE

STIRRER
BLADES

Figure A.1. Schematic drawing of low pressure laboratory reactor.

(attachment nut not shown)

Figure A.2. Drawing of reactor vessel opening.

Figure A.3. Reactor head overall dimensions.

Figure A.4. Reactor head top view.

Figure A.5. Reactor head side view.

Figure A.6. Reactor head bottom view.

Figure A.7. Reactor stirring assembly hub.

APPENDIX B - Pulse Width Calibration for Aluminum-27 NMR

Before beginning to use aluminum-27 nuclear magnetic resonance spectroscopy for detailed mechanistic investigations, it was necessary to determine the 90° pulse width of aluminum for the Bruker WP 200 found in the Department of Chemistry at Virginia Tech. This was done by taking a known aluminum compound and varying the pulse width systematically. The starting place for this search begain by obtaining a single scan spectra with a less than a 45° pulse width. This spectrum is used to determine the phase correction required for a positive absorption signal. Repeating the experiment with increasing pulse widths allows the null point corresponding to a 180° flip angle to be detected. The predetermined phase correction results in the signal appearing inverted once the 180° flip angle is exceeded which allows for the determination of the null value.

The first pulse width used was 39 s resulting in somewhere close to a 170° flip angle. The free induction decay or FID was transformed and plotted without additional phase correction. The pulse width was incrementally increased by $0.2 \, \mu$s and this process was continually repeated until it was observed that the signal went through the null value, an exact 180° flip angle, and began to go negative (a flip angle greater than 180° and less than

270°). The individual spectra were plotted next to one another to allow for a line to be drawn to exactly determine the 180° pulse width as shown in Figure B.1. From this value the 90° pulse width was calculated (half the 180° pulse width).

Once the 90° pulse width was determined, this value was used to obtain a single scan spectrum of a known aluminum standard whose width at half height was compared to its literature value. Figure B.2 shows a single scan spectrum of 1.5M aluminum(III)nitrate ($Al(NO_3)_3$) in D_2O. The resultant line width, measured at half height, is about 8 Hz. This value is in excellent agreement with the literature value of 8 Hz.[132]

The spectral reference used in the aluminum-27 NMR investigations was a saturated solution of aluminum(III)-acetylacetonate ($Al(AcAc)_3$) in C_6D_6. This was an external reference whose chemical shift value was set to 0.0 ppm, Figure B.3. This resulted in a spectral reference (SR) value of 292.13 (SR value reported as the last parameter in Spectrometer Parameter List). The temperature dependence of the external spectral reference was investigated by determining the chemical shift value at 60 °C using the same SR value of 292.13. The result, Figure B.4, showed that the hexacoordinate aluminum standard's spectral reference was

Aluminum-27 NMR: Pulse Width Calibration

| 39.4 | 39.6 | 39.8 | 40.0 | 40.2 | 40.4 | 40.6 | 40.8 | 41.0 | 41.2 | 41.4 |

180° = 40.2 μs

90° = 20.1 μs

Figure B.1   Pulse width calibration.   The signal
passes through a null when the flip angle is π, 2π ...

AL(NO3)3 IN D2O 1.5M/90 DEG

Figure B.2 Single scan spectrum of 1.5M Al(NO$_3$)$_3$ in D$_2$O.

27-AL-STANDARD/AL(ACAC) SAT. IN C6D6

Figure B.3 Aluminum-27 NMR of Al(AcAc)$_3$, the external reference used for aluminum-27 NMR.

AL(ACAC)3 IN BENZENE AT 60C - 10 MM

BRUKER

BLKOLD.222
DATE 14-9-99

SF   52.149
SY   52.1480000
O1   3000.000
SI   4096
TD   4096
SW   35714.286
HZ/PT   17.439

PW   10.0
RD   0.0
AQ   .057
RG   228
NS   2000
TE   297

FW   44700
O2   3250.000
DP   5H P0

LB   10.000
GB   0.0
CX   20.00
CY   0.0
F1   490.906P
F2   -193.620P
HZ/CM 1.78463
PPM/CM 34.226
SR   292.13

$$
\begin{array}{cccccccccccccccc}
450 & 400 & 350 & 300 & 250 & 200 & 150 & 100 & 50 & 0 & -50 & -100 & -150
\end{array}
$$

PPM

Figure B.4   Aluminum-27 NMR of Al(AcAc)$_3$ at 60 °C.

invariant to temperature, unlike the chemical shift values for the hexacoordinate aluminum porphyrin compounds reported in the Results and Discussion Section - Part 2.

REFERENCES

1 Milkovich, R.; Chiang, M. US Patent 3 786 116, 1974.

2 Smith, S. D. Ph.D. Dissertation, Virginia Polytechnic Institute and State University, 1987, pp. 3-58.

3 Gillman, K. F.; Senogles, E.; J. Polym. Sci., Polym. Lett. **1967**, 5, 377.

4 Yamashita, Y.; Tsukahara, Y. Polym. Bull. **1981**, 5, 335.

5 Nakashima, T.; Takakura, K.; Komoto, Y. J. Biomed. Mat. Res. 1977, 11, 787.

6 Cacioli, P.; Hawthorne, D.; Laslett, R.; Rizzardo, E.; Solomon, D. J. Macromol. Sci., Chem. **1986**, A23(7), 839.

7 Schulz, G. O.; Milkovich, R. J. Appl. Polym. Sci. **1982**, 27, 4773.

8 Serre, B.; Worsfold, D. J. Polymer **1987**, 28, 881.

9 Schulz, G.; Milkovich, R. J. Polm. Sci., Polym. Chem. Ed. **1984**, 22,1633.

10 Rempp, P.; Franta, E. Adv. Polym. Sci. **1984**, 58,1.

11 Cameron, G. G.; Chisholm, M. S. Polymer **1985**, 26, 437.

12 Ito, K.; Matsuda,, Y.; Shintani, T.; Kitano, T.; Yamashita, Y. Polym. J. **1983**, 15, 443.

13 Kennedy, J. P.; Lo, C. Y. Polym. Bull. **1982**, 8, 63.

14 Ito, K.; Tsuchida, H.; Kitano, T Polym. Bull. **1986**, 15, 425.

15 Gnanou, G. Presentation at The Ralph Milkovich Symposium at the Akron Heterophase Polymer Symposium at the Institute of Polymer Science, University of Akron, Akron, OH, June 20, 1988.

16 Glockner, G.; van den Berg, J. H. M.; Meijerink, N. L. J.; Scholte, T. G.; Koningsveld, R. Macromolecules **1984**, 17, 962.

17 Stejskal, J.; Kratochvil, P.; Jenkins, A. D. Macromolecules **1987**, 20, 181.

18 Stejskal, J.; Kratochvil, P. Macromolecules **1989**, 22, 429.

19 Stejskal, J.; Kratochvil, P. Polymer J. **1982**, 14, 603.

20 Elias, G. Macromolecules, Vol. 1; Plenum: New York, 1984; pp. 42-45; 317-319.

21 Inagaki, H.; Tanaka, T. Pure Appl. Chem. **1982**, 54, 309.

22 Stejskal, J.; Strakova, D.; Kratochvil, P.; Smith, S. D.; McGrath, J. E. Macromolecules **1989**, 22, 861,

23 DeSimone, J. M.; Smith, S. D.; Hellstern, A. M.; Ward, T. C.; Krukonis, V. J.; McGrath, J. E. Polym. Prepr. (Am. Chem. Soc. Div. Polym. Chem.) **1988**, 29, 361.

24 DeSimone, J. M.; Hellstern, A. M.; Siochi, E. J.; Smith, S. D.; Ward, T. C.; Galagher, P.; Krukonis, V. J.; McGrath, J. E. Makromol. Chem. accepted for publication, January, 1990.

25 Bushuk, W.; Benoit, H. Can J. Chem. **1958**, 36, 1616.

26 Dumelow, T.; Holding, S. R.; Maisey, L. J.; Dawkins, J. V. Polymer **1986**, 27, 1170.

27 Soane, D. S.; Martynenko, Z. Polymers in Microelectronics: Fundamentals and Applications; Elesevier: Amsterdam; 1989; pp 77 - 143.

28 Siegle, W. T. Director, Advanced Technology Center, International Business Machines Corporation, East Fishkill, New York, personal communication, 1989.

29 Mucha, J. A.; Hess, D. W. In Introduction to Microlithography; Thompson, L. F.; Willson, C. G.; Bowden, M. J., Eds.; <u>American Chemical Society Symposium Series No. 219;</u> American Chemical Society: Washington, D. C., 1983; pp 215 - 285.

30 Thompson, L. F.; Bowden, M. J. <u>The Lithographic Process;</u> ACS Symposium Series 219; American Chemical Society: Washington, D. C.; 1983.

31 Ito, H,; Willson, C. G. <u>Org. Coatings and Appl. Polym. Sci. Proc.</u> **1983**, <u>48</u>, 60.

32 Slemp, W. S.; Santos-Mason, B.; Sykes, G. F.; Witte, W. G. <u>AIAA-85-0421, AIAA 23rd Aerospace Meeting,</u> January, **1985**.

33 Visentine, J. T.; Lejer, L. J.; Kuminecz, J. F.; Spiker, I. K. <u>AIAA-85-0415, AIAA 23rd Aerospace Meeting,</u> January, **1985**.

34 Johnson, B. <u>Ph.D. Dissertation,</u> Virginia Polytechnic Institute and State University, 1983.

35 Arnold, C. A.; Chen, D,; Chen, Y. P.; Graybeal, J. D.; Bott, R. H.; Yoon, T.; McGrath, B. E.; McGrath, J. E. <u>PMSE Prepr. (Am. Chem. Soc. Div. Polym. Mat. Sci. Eng.)</u> **1988**, <u>59</u>, 934.

36 Taylor, G. N.; Wolf, T. M. <u>Polym. Eng. Sci.</u> **1980**, <u>20</u>,1087.

37 Gozdz, A. S.; Carnazza, C.; Bowden, M. J. <u>Proc. SPIE,</u> **1986**, <u>631</u>,2.

38 Ito, S.; Ono, H.; Kim, S. J., Matsuda, M. <u>IUPAC Abstracts,</u> **1986**, p 542.

39 Bowden, M. J.; Gozdz, A. S.; Klausner, C.; Mcgrath, J. E.; Smith, S. D. In <u>Polymers for High Technology: Electronics and Photonics;</u> Bowden, M. J.; Turner, R. S., Ed.,; ACS Symposium Series No. 346.; American Chemical Society: Washington, D. C., 1987; pp 122 - 137.

40 Suzukie, M.;Saigo, H.; Gokan, H.; Ohnishi, Y.; <u>J. Electrochem. Soc.</u> **1983**, <u>130</u>, 1962.

41 MacDonald, S. A.; Steinman, A. S.; Ito, H.; Hatzakis, M.; Lee, W.; Hiraoka, H.; Willson, C. G. Int. Symp. Electron, Ion, Photon Beams, Los Angeles, CA, 1983.

42 Miller, R. D.; Hofer, D. C.; Willson, C. G. Polym. Prepr. (Am. Chem. Soc. Div. Polym. Chem.) **1984**, 25, 307

43 Wilkins, Jr., C. W.; Reichmanis, E.; Wolf, T. M.; Smith, B. C. J. Vac. Sci. Technol. **1985**, 3, 306.

44 Saotome, Y. Goken, H.; Saigo, K.; Suzuki, M.; Ohnishi, Y. J. Electrochem. Soc., Solid State Sci. Technol. **1985**, 132, 909.

45 Hayashi, N.; Ueno, T.; Shiraishi, H.; Nishida, T.; Toriumi, M. Nonogaki, S. PMSE Prepr. (Am. Chem. Soc. Div. Polym. Mat. Sci. Eng.) **1986**, 55, 611.

46 Hartney, M. A.; Novembre, A. E. Proc SPIE Conf., "Advances in Resist Technology and Processing II," **1985**, 539, 90.

47 Szwarc, M. In Carbanions, Living Polymers and Electron Transfer Processes; Interscience: New York, 1968; p. 12.

48 Long, T. E. Ph.D. Dissertation, Virginia Polytechnic Institute and State University, 1987.

49 Perrin, D. D.; Armarego, W. L. F. Purification of Laboratory Chemicals; Pergamon: Oxford, 1988; p. 131.

50 Allen, R.D.; Long, T.E.; McGrath, J.E. Polym. Bull. **1986**, 15, 127.

51 Winkle, M.R.; Lanisinger, J.M.; Ronald, R.C. J. Chem. Soc. Chem. Comm. **1980**, 87.

52 Spach, G.; Monteiro, H.; Levy, M.; Szwarc, M. Trans. Faraday Soc. **1962**, 58, 1809.

53 Hellstern, A. M. Ph.D Dissertation, Virginia Polytechnic Institute and State University, 1989.

54 Greene, T. W. Protective Groups in Organic Synthesis; John Wiley and Sons: New York, 1981; Chapter 2.

55 Derome, A. E. Modern NMR Techniques for Chemistry Research; Pergammon: Oxford, 1987.

56 Elsbernd, C. S.; Hellstern, A. M.; Siochi, E. J.; DeSimone, J. M. unpublished results.

57 Elsbernd, C. S. Ph.D. Dissertation, Virginia Polytechnic Institute and State University, 1987.

58 Siochi, E. J. Ph.D Dissertation, Virginia Polytechnic Institute and State University, 1989.

59 Siochi, E. J.; DeSimone, J. M.; Hellstern, A. M.; McGrath, J. E.; Ward, T. C. submitted to Macromolecules, December, **1989**.

60 Podesva, J.; Stejskal, J.; Kratochvil, P. Macromolecules **1987**, 20, 2195.

61 Pascault, J. P.; Camberlin, Y. J. Polym. Sci. Polym. Chem. Ed., **1983**, 21, 415.

62 Pascault, J. P.; Camberlin, Y. J. Polym. Sci. Polym. Phys. Ed. **1984**, 22, 1835.

63 Pascault, J. P.; Camberlin, Y. Polym. Comm. **1986**, 27, 230.

64 Lebdev, B. V.; Mukhina, N. N.; Kulagina, T. G. Polym. Sci. USSR (Engl. Trans.) **1979**, 20, 1458.

65 Wang, B.; Krause, S. Macromolecules **1987**, 20, 2201.

66 Rempp, P.; Loucheux, M. L. Bull. Soc. Ch. Fr. **1958**, 1497.

67 Milkovich, R. M. In Anionic Polymerization; McGrath, J. E., Ed.; ACS Symposium Series 166; American Chemical Society: Washington, D. C., 1981; pp 41-59.

68 Winstein, S.; Clippinger, E.; Fainberg, A. H.; Heck, R.; Robinson, G. C. J. Am. Chem. Soc. **1956**, 78, 328.

69 Benoit, H.; Grubisic, Z.; Rempp, P.; Decker, D.; Zillioux, J. G. J. Chim. Phys. **1966**, 63, 1507.

70 Grubisic, Z.; Rempp, P.; Benoit, H. J. Polym. Sci. **1967**, 5, 753.

71 Ojima, I.; Kumagal, M.; Nagai, Y. J. Orgmat. Chem. **1976**, 111, 43.

72 Rempp, P.; Volkov, W.; Parrod, J.; Sadron, C. Bull. Soc. Chim. France **1960**, 1919.

73 Hoover, J. M. Ph.D. Dissertation, Virginia Polytechnic Institute and State University, 1987.

74 DeSimone, J. M.; Siochi, E. J.; Hellstern, A. M.; Ward, T. C.; McGrath, J. E. Polym. Prepr. (Am. Chem. Soc. Div. Polym. Chem.) **1989**, 30(1), 137.

75 Siochi, E. J.; DeSimone, J. M.; Hellstern, A. M.; McGrath, J. E.; Ward, T. C. Polym. Prepr. (Am. Chem. Soc. Div. Polym. Chem.) **1989**, 30(1), 140.

76 Siochi, E. J.; DeSimone, J. M.; Hellstern, A. M.; McGrath, J. E.; Ward, T. C. submitted to Macromolecules, December, **1989**.

77 Wilczek, L.; Kennedy, J. P. Polymer J. **1987**, 19(5), 531.

78 Lee, C. L.; Frye, C. L.; Johannson, O. K. Polym. Prepr. (Am. Chem. Soc. Div. Polym. Chem.) **1969**, 10(2), 361.

79 Bostick, E. E. U.S. Patent 3 337 496, 1967.

80 Fessler, W.; Juliano, P. C. Ind. Eng. Chem. Prod. Res. Dev. **1972**, 11(4), 407.

81 Saam, J. C.; Gordon, D. J.; Lindsey, S. Macromolecules **1970**, 35, 1308.

82 Yamashita, Y. J. Appl. Polym. Sci, Appl. Polym. Symp. **1981**, 36, 193.

83 Kawakami, K.; Yamashita, Y. In Ring Opening Polymerization; McGrath, J. E., Ed.; ACS Symposium Series 286; American Chemical Society: Washington, D. C.; 1985.

84 Frye, C. L.; Salinger, R. M.; Fearon, F. W. G.; Klosowski, J. M.; DeYoung, T. J. Org. Chem. **1970**, 35(5), 1308.

85 Riffle, J. S.; Sinai-Zingde, G.; DeSimone, J. M.; Hellstern, A. M.; Chen, D. H.; Yilgor, I. Polym. Prepr. (Am. Chem. Soc. Div. Polym. Chem.) **1988**, 29(2), 93.

86 Speir, J. L. In Advances in Organometallic Chemistry; Academic: New York; 1979; pp. 407-447.

87 Stejskal, J.; Kratochvil, P. Macromolecules **1987**, 20, 2624.

88 Frazer, A. H.; O'Neil, W. P. J. Am. Chem. Soc. **1963**, 85, 2613.

89 Solonia, W. J. Russ. Phys. Chem. Soc. **1898**, 30, 826.

90 Flockhart, B. D.; Ivin, K. J.; Pink, R. C.; Sharma, B. D. J. Chem. Soc., Comm. **1971**, D, 339.

91 See Appendix A.

92 Turi, E. A. Thermal Characterization of Polymeric Materials; Academic: New York; 1981.

93 Lee, C. L.; Johannson, O. K.; Flaningam, O. L.; Hahn, P. Polym. Prepr. (Am. Chem. Soc. Div. Polym. Chem.) **1969**, 10, 1311.

94 Alexander, L. E. X-ray Diffraction Methods in Polymer Science; Wiley: New York; 1969.

95 Ehrenfest, P. Proc. Acad. Sci., Amsterdam **1933**, 36, 153.

96 Wilkes, G. L. Personal Communication, 1990.

97 Smith, S. D.; DeSimone, J. M.; York, G. A.; Dwight, D. W.; Wilkes, G. L.; McGrath, J. E. Polym. Prepr. (Am. Chem. Soc. Div. Polym. Chem.) **1987**, 28, 150.

98 Tarascon, R. G.; Shugard, A.; Reichmanis, E. Proc. SPIE, Adv. Resist Technol. Process. III **1986**, 631, 40.

99 Gozdz, A. S. Personal Communication.

100 Reichmanis, E.; Smolinsky, G.; Wilkins, Jr., C. Solid State Technol. **1985**, 28, 130.

101 Gozdz, A. S.; Lin, P. S. D. Proc. SPIE Electron Beam, X-ray, and Ion-Beam Technology: Submicrometer Lithographies VII **1988**, 923, 172.

102 Odian, G. Principles of Polymerization, Second Edition, Wiley Interscience: New York, 1981.

103 Wiles, D. M. in Structure and Mechanisms in Vinyl Polymerizations; Tsumta, T; Driscoll, K. F., Eds.; Marcel Dekker: New York, 1969; Chapter 8.

104 Aida, T.; Inoue, S. In Ring Opening Polymerization, Saegusa, T.; Ivin, K., Eds.; Elsevier: New York; 1981.

105 Fayt, R.; Forte, R.; Jacobs, C.; Jerome, R.; Ouhadi, T.; Teyssie, Ph.; Varshney, S. K. Macromolecules 1987, 20(6), 1443.

106 Erusalimski, B. L. Mechanisms of Ionic Polymerization: Current Problems; Macromolecular Compounds Series; Koton, M. M., Series Ed.; Academy of Sciences of the USSR; Leningrad, 1986; English Edition-Consultants Bureau (Plenum): New York, 1986.

107 Aida, T.; Inoue, S. U.S. Patent 4,654,417, 1987.

108 Aida, T.; Inoue, S. Macromolecules 1981, 14(5), 1162.

109 Aida, T.; Inoue, S. Macromolecules 1982, 15, 682.

110 Yasuda, T.; Aida, T.; Inoue, S. Macromolecules 1984, 17, 2217.

111 Shimasaki, K.; Aida, T.; Inoue, S. Macromolecules 1987, 20, 3076.

112 Asano, S.; Aida, T.; Inoue, S. Macromolecules 1985, 18, 2057.

113 Endo, M.; Aida, T.; Inoue, S. Macromolecules 1987, 20, 2982.

114 Yoo, Y.; Kilic, S.; McGrath, J. E. Polym. Prepr. (Am. Chem. Soc, Div. Polym. Chem.) 1987, 28(2), 358.

115 Aida, T. Ph.D. Dissertation, University of Tokyo, 1984.

116 Yoo, Y. Ph.D. Dissertation, Virginia Polytechnic Institute and State University, 1988.

117   Aida, T.; Inoue, S. J. Am. Chem. Soc. **1985**, <u>107</u>, 1358.

118   Aida, T.; Sanuki, K.; Inoue, S. <u>Macromolecules</u>, **1985**, <u>18</u>, 1049.

119   Aida, T.; Ishikawa, M.; Inoue, S. <u>Macromolecules</u> **1986**, <u>19</u>, 8.

120   Kuroki, M.; Aida, T.; Inoue, S. <u>J. Am. Chem. Soc.</u> **1987**, <u>109</u>, 4737.

121   Arai, T.; Murayama, H.; Inoue, S. <u>J. Org. Chem.</u> **1989**, <u>54</u>, 414.

122   Delpuech, J. J. In <u>NMR of Newly Accessable Nuclei, Vol. 2</u>; Laxzlo, P., Ed.; Academic: New York, 1983; Chapter 6.

123   Denn, R.; Rufinska, A.; Lehmkuhl, H.; Janssen, E.; Kruger, C. <u>Angew. Chem., Int. Ed. Engl.</u> **1983**, <u>22(10)</u>, 779.

124   Akitt, J. W.; Mann, B. E. <u>J. Magn. Res., Comm.</u> **1981**, <u>44</u>, 584.

125   Delpuech, J. J.; Kaddar, M.; Peguy, A. A.; Rubini, P. R. <u>J. Am. Chem. Soc.</u> **1975**, <u>97(12)</u>, 3373.

126   Yoo, Y.; McGrath, J. E. <u>Polym. Prepr. (Am. Chem. Soc. Div. Polym. Chem.)</u> **1987**, <u>28(2)</u>, 360.

127   DiCarlo, E. N.; Swift, H. E. <u>J. Phys. Chem.</u> **1964**, <u>68</u>, 551.

128   Rothemund, P. <u>J. Am. Chem. Soc.</u> **1936**, <u>58</u>, 625.

129   Adler, A. D.; Longo, F. R.; Finarelli, J. D.; Goldmacher, J.; Assour, J.; Korsakoff, L. <u>J. Org. Chem.</u> **1967**, <u>32</u>, 476.

130   Simerall, L. (Ethyl Corporation) Personal Communication.

131   Hoover, J. M.; McGrath, J. E. <u>Polym. Prepr. (Am. Chem. Soc. Div. Polym. Chem.)</u> **1986**, <u>27(2)</u>, 150.

132   Brevard, C.; Granger, P. <u>Handbook of High Resolution Multinuclear NMR</u>; Wiley: New York; 1981.

VITA

Joseph M. DeSimone, son of Arlene and Philip DeSimone, was born on May 16, 1964 in Norristown, PA. He graduated from Perkiomen Valley High School in June of 1982 and began his undergraduate studies as a chemistry major with a minor in computer science at Ursinus College in Collegeville, PA. In his junior year he was exposed to a polymer chemistry course taught by Professor Ray Schultz which convinced him to pursue this area of chemistry as a career. His senior year of college was primarily focussed on an undergraduate research project in synthetic polymer chemistry. In May, 1986, he graduated with a Bachelor of Science Degree in Chemistry and married Suzanne Griffith a month later. During the summer of 1986, he worked at Pennwalt Corporation in the area of emulsion copolymerization. In the fall of 1986, he entered graduate school in the Department of Chemistry at Virginia Polytechnic Institute and State University and began his doctoral research with Professor James E. McGrath. His graduate research efforts were broadly defined but centered around the synthesis of well-defined single and multiphase polymers using living polymerization methods.

Joseph accepted an Assistant Professorship position in the Department of Chemistry at The University of North Carolina at Chapel Hill after finishing his Ph.D. requirements in March, 1990 at VPI&SU.